Aus der Poliklinik für Kieferorthopädie

Klinikum der Ludwig-Maximilians-Universität München

Dissertation

zum Erwerb des Doctor of Philosophy (Ph.D.) an der

Medizinischen Fakultät der

Ludwig-Maximilians-Universität München

Effect of hydrogen peroxide-induced oxidative stress on simulated orthodontic tooth movement in a cell culture model

vorgelegt von: Seyedeh Samira Hosseini

aus:

Ghazvin / Iran

Jahr: 2026

Mit Genehmigung der Medizinischen Fakultät der
Ludwig-Maximilians-Universität München

Erstes Gutachten von:	Priv. Doz. Dr. Uwe Baumert
Zweites Gutachten von:	Prof. Dr. Dr. Matthias Folwaczny
Drittes Gutachten von:	Priv. Doz. Dr. Christof Högg
Viertes Gutachtes:	Prof. Dr. Gabriele Sabbioni

Dekan: **Prof. Dr. med. Thomas Gudermann**

Datum der Verteidigung:

26.01.2026

Affidavit

Affidavit

Hosseini, Samira

Surname, first name

Street

Zip code, town, country

I hereby declare, that the submitted thesis entitled:

“Effect of hydrogen peroxide-induced oxidative stress on simulated orthodontic tooth movement in a cell culture model”

is my own work. I have only used the sources indicated and have not made unauthorised use of services of a third party. Where the work of others has been quoted or reproduced, the source is always given.

I further declare that the dissertation presented here has not been submitted in the same or similar form to any other institution for the purpose of obtaining an academic degree.

München, 26.03.2025

place, date

Hosseini, Samira

Signature doctoral candidate

Confirmation of congruency

Confirmation of congruency between printed and electronic version of the doctoral thesis

Hosseini, Samira

Surname, first name

Street

Zip code, town, country

I hereby declare, that the submitted thesis entitled:

“Effect of hydrogen peroxide-induced oxidative stress on simulated orthodontic tooth movement in a cell culture model”

is congruent with the printed version both in content and format.

München, 26.03.2025

place, date

Hosseini, Samira

Signature doctoral candidate

To both my Persian and German families,

for their endless love, support and belief in me.

And to all who inspired me to learn.

Table of content

List of abbreviations

BECN1	Beclin 1
BGLAP	Bone gamma-carboxyglutamate protein
CASP3	Caspase 3
CASP8	Caspase 8
CXCL8/IL8	C-X-C Motif Chemokine Ligand 8 (aka IL8, interleukin-8)
ELISA	Enzyme-linked immunosorbent assay
FC	Fold change
H_2O_2	Hydrogen peroxide
hOBs	Human osteoblasts
hPDLCs	Human periodontal ligament cells
IL6	Interleukin 6
MAP1LC3A/LC3	Microtubule-Associated Protein 1 Light Chain 3 Alpha (aka LC3)
MIQE	Minimum Information for Publication of Quantitative Real-Time PCR Experiments
OS	Oxidative stress
OTM	Orthodontic tooth movement
P2RX7	Purinergic Receptor P2X7
$P_{adj.}$	Adjusted *p*-value
PGE2	Prostaglandin E2
PTGS2/COX2	Prostaglandin Endoperoxide Synthase 2 (aka COX2, cyclooxygenase 2)
ROS	Reactive oxygen species
RT-qPCR	Reverse transcription quantitative polymerase chain reaction
RUNX2	RUNX Family Transcription Factor 2
TNFRSF11B/OPG	TNF Receptor Superfamily Member 11b (aka OPG, osteoprotegerin)

List of publications

Hosseini S, Diegelmann J, Folwaczny M, Frasheri I, Wichelhaus A, Sabbagh H, Seidel C, Baumert U, Janjic Rankovic M. Investigation of Impact of Oxidative Stress on Human Periodontal Ligament Cells Exposed to Static Compression. Int J Mol Sci. 2024 Dec 17;25(24):13513.

DOI: https://doi.org/10.3390/ijms252413513
PMID: https://www.ncbi.nlm.nih.gov/pubmed/39769281
PMCID: https://www.ncbi.nlm.nih.gov/pmc/articles/PMC11678643

Hosseini S, Diegelmann J, Folwaczny M, Sabbagh H, Otto S, Kakoschke TK, Wichelhaus A, Baumert U, Janjic Rankovic M. Investigation of Oxidative-Stress Impact on Human Osteoblasts During Orthodontic Tooth Movement Using an In Vitro Tension Model. Int J Mol Sci. 2024 Dec 17;25(24):13525.

DOI: https://doi.org/10.3390/ijms252413525
PMID: https://www.ncbi.nlm.nih.gov/pubmed/39769290
PMCID: https://www.ncbi.nlm.nih.gov/pmc/articles/PMC11677893

Your contribution to the publications

1.1 Contribution to paper I

Conceptualization, methodology, validation, formal analysis, investigation, data curation, writing-original draft preparation, writing-review and editing.

- Together with my supervisors, I established the hydrogen peroxide (H_2O_2) stimulation model for human periodontal ligament cells (hPDLCs), using information extracted from the relevant literature. Conducted a H_2O_2 concentration gradient study on hPDLCs, assessing effects after 24 h of H_2O_2 stimulation. Performed cell viability and cytotoxicity evaluation to identify the optimal H_2O_2 concentration range for the second part of this study.
- Developed a dual-stimulation experimental setup with supervisors, combining H_2O_2 exposure and *in vitro* compressive force model (WAB).
- Cultivation of human primary periodontal ligament cells (hPDLCs). Cell stimulation with the selected concentrations of H_2O_2 followed by compressive force application or recovery period. Conducted laboratory experiments including cell viability and cytotoxicity assessments, sample preparation, reverse transcription quantitative polymerase chain reaction (RT-qPCR) and enzyme-linked immunosorbent assays (ELISA).
- For RT-qPCR, I employed *in silico* methods to evaluate PCR primer pairs for genes of interest and reference genes. I identified suitable reference genes using experimental samples according to MIQE (Minimum Information for Publication of Quantitative Real-Time PCR Experiments) guidelines. Took part in analysing and interpreting RT-qPCR and ELISA datasets of results.
- Prepared initial manuscript drafts and participated in revision of manuscript including addressing the feedback of all co-authors as well as reviewers during manuscript submission.

1.2 Contribution to paper II

Conceptualization, methodology, validation, formal analysis, investigation, data curation, writing-original draft preparation, writing-review and editing.

- Collaborated with supervisors to establish a suitable H_2O_2 stimulation model for human osteoblasts (hOBs), based on relevant methodologies in the literature. Initially tested the H_2O_2 concentration gradient on hOBs, evaluating effects at 8 h and 24 h intervals to determine the optimal H_2O_2

concentration for the second part of this study using cell viability and cytotoxicity assessment, both quantitative and qualitative.

- Designed an innovative experimental setup with supervisors, containing a combination of the H_2O_2 model and the previously established *in vitro* tensile force application apparatus.
- Conducted the primary cell culture of hOBs. Stimulated the cells with H_2O_2 for 24 h followed by further tensile force stimulation or recovery. Performed laboratory techniques including cell viability, cell cytotoxicity, sample preparation, RT-qPCR and ELISA. Utilized *in silico* assessment methods for primer assessment of target and reference genes. Examined the reference genes using samples collected during the experiment. Involved in the data analysis of the RT-qPCR and ELISA results. Prepared the original manuscript drafts. Revised the manuscript draft incorporating feedback from the co-authors and addressing comments from the reviewers.

2. Introductory summary

The PhD project entitled “Effect of hydrogen peroxide-induced oxidative stress on simulated orthodontic tooth movement in a cell culture model” was conducted at the Department of Orthodontics and Dentofacial Orthopaedics, University Hospital, Ludwig-Maximilians-Universität München, under the supervision of PD Dr. rer. nat. Uwe Baumert, Prof. Dr. med. dent. Andrea Wichelhaus and Prof. Dr. Dr. Matthias Folwaczny.

2.1 Orthodontic tooth movement

In orthodontics, therapeutic forces are applied to correct abnormally positioned teeth and orthodontic tooth movement (OTM) is the result of this force application (Wichelhaus 2018). Following the application of continuous mechanical forces to teeth, complex aseptic inflammatory cellular and molecular responses are triggered in the surrounding tissues (Davidovitch 1991; Vansant et al. 2018). This effect is particularly evident in the periodontal ligament (PDL) and alveolar bone where human periodontal ligament cells (hPDLCs) and human osteoblasts (hOBs) are recognized as key cells in the mechanosensing process (Janjic et al. 2018). The outcome of mechanical stimulation is bone removal in the direction of the force and bone apposition in the opposite direction (Davidovitch 1991) (Figure 1), with static compression and tension forces playing dominant roles in these processes.

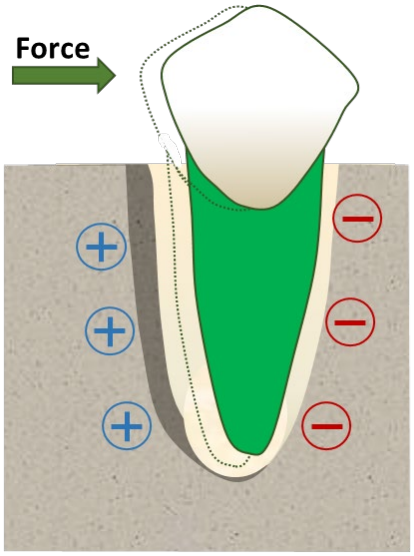

Figure 1. Bone remodelling during OTM. Bone apposition on the tension side and resorption on the compression side as the result of the long-term force application. [Figure adapted from Janjic et al. (2018), Figure 1 (b); licensed under CC BY 4.0/Cropped from the original figure and colours have been modified]

2.2 Reactive oxygen species and oxidative stress

2.2.1 Oxidative stress

Oxidative stress (OS) refers to a metabolic condition in cells and tissues which occurs due to an imbalance between the production and accumulation of reactive oxygen species (ROS) on one hand, and the body's capability to either eliminate and neutralize these compounds or repair the resulting cellular damage on the other hand (Hosseini et al. 2024b; Pizzino et al. 2017). ROS, including hydrogen peroxide (H_2O_2), hydroxyl radicals (•OH), superoxide radicals ($O_2^{\bullet-}$), and singlet oxygen ($^1O_2$), are generated as metabolic byproducts in biological systems (Pizzino et al. 2017). These compounds are involved in essential cellular processes such as inflammatory signalling, apoptosis and differentiation (Pizzino et al. 2017). For these mechanisms to operate effectively, the concentrations of ROS must be appropriately regulated (Pizzino et al. 2017).

ROS is known to present a dual nature in cellular biology. At moderate physiological concentrations, ROS function as important signalling molecules in various cellular functions, including cell differentiation, proliferation, apoptosis and autophagy pathways (Pizzino et al. 2017). However, high concentrations can be detrimental. When ROS levels become excessive, they can lead to significant harm to cellular components such as lipids, proteins, and nucleic acids, which can compromise cell viability and lead to cell death (Pizzino et al. 2017; Zhu et al. 2021).

2.2.2 Influence of oxidative stress on the periodontium

Periodontitis is a widespread chronic inflammatory condition characterized by ongoing alveolar bone resorption. During periodontitis, persistent inflammation in periodontal tissues results in PDL and alveolar bone loss. This is followed by tooth loss and mastication problems, significantly impacting overall well-being and life quality (Durham et al. 2013; Schröder et al. 2021; Tonetti et al. 2017). There have been several studies reporting that oxidative stress (OS) plays an important role in the pathogenesis of different chronic inflammations including periodontitis, particularly in its initiation and progression (Chen et al. 2022; Mittal et al. 2014; Wei et al. 2021). Studies have also demonstrated higher levels of OS were observed in gingival crevicular fluid, in saliva, and in serum of patients with periodontal disease (Almerich-Silla et al. 2015; Chen et al. 2019b; Wang et al. 2017). This pathological condition leads into a direction in which neutrophils become excessively activated. This hyperactivation of neutrophils triggers an increased production of ROS as part of the body's defensive mechanism (Wei et

al. 2021). Increased levels of OS can cause cytotoxic effects on periodontal tissue. It is reported that ROS affects the osteogenic differentiation of hPDLCs by stimulating the production of inflammatory mediators, both *in vitro* and *in vivo* (Chen et al. 2022).

2.2.3 Influence of oxidative stress on OTM

During the recent years, the number of adult patients seeking orthodontic treatment increased remarkably. This leads to a higher prevalence of individuals with periodontal disease in orthodontic practices seeking orthodontic care (Christensen and Luther 2015). Both orthodontic tooth movement and periodontal disease are associated with inflammation and alveolar bone remodelling (Schröder et al. 2021).

2.3 Establishment of an oxidative stress *in vitro* loading model

Various biological processes including inflammation, bone remodelling, autophagy, and apoptosis are known to be influenced by either mechanical force or OS (Zhu et al. 2022). However, the specific interplay between OS and OTM remains unexplored and poorly understood. Despite the recognized importance of OS in such physiological mechanisms, its precise role in the context of OTM is still a subject of considerable uncertainty and requires investigation (Hosseini et al. 2024b). Accordingly, in the presented Ph.D. thesis, two projects were conducted in which the two cell types playing a dominant role in OTM, hPDLCs and hOBs, were subjected to mechanical stimulation with either static compression or static tension after OS stimulation using H_2O_2.

2.3.1 ROS stimulation model establishment

Force stimulations were applied using the “weight approach”-based (WAB) model (Janjic et al. 2018) and the static tension *in vitro* loading model (Sun et al. 2021), mimicking orthodontic forces, with or without preinduction with oxidative stress.

For this purpose, we combined an *in vitro* oxidative stress stimulation method with the two *in vitro* mechanical stimulation models (Hosseini et al. 2024a; Hosseini et al. 2024b). This method would allow us to study cellular and molecular mechanisms of OTM in an increased OS environment. According to the literature, OS has been induced by adding H_2O_2 to the cell culture medium (Chen et al. 2019a; Tan et al. 2021; Wei et al. 2021). To determine the optimal concentration of H_2O_2 not affecting cell proliferation and viability, dose-response experiments

was carried out for each cell type. The cells were stimulated with H_2O_2 concentrations ranging from 50 µM to 500 µM for 24 h. Afterwards, cell viability and proliferation of the cells were assessed to identify "optimal" H_2O_2 concentrations not affecting cell viability and proliferation (Hosseini et al. 2024a; Hosseini et al. 2024b). These were then used in the next step of the experiment where OS exposure was combined with mechanical stimulation.

Herein, the cells were first stimulated 24 h with medium containing the predetermined H_2O_2 "optimal" concentrations and afterwards subjected to mechanical stimulation of either compression or tension for additional 24 h. Experimental force levels applied in this study were as following: 2.0 g/cm^2 for static compressive force and 10 % and 15 % stretching for static tension force, both for the duration of 24 h. These force magnitudes are described in the literature as the "optimal" forces for application in experiments (Janjic et al. 2018; Sun et al. 2021). An "optimal" force is known as the force level not effecting cell viability and proliferation but leading to a modified expression of genes and metabolites. Cell viability and proliferation were assessed. OS/force-related genes and metabolites expression regulation was analysed in genes/metabolites related to inflammation, bone remodelling, autophagy and apoptosis. Gene expression at the transcriptional level was assessed using RT-qPCR and included the following genetic loci: (a) inflammation: *CXCL8*/*IL8*, *IL6*, *PTRGS2*/*COX2*; (b) bone remodelling: *RUNX2*, *P2RX7*, *BGLAP*, *TNFRSF11B*/*OPG*; (c) autophagy: *MAP1LC3A*/*LC3*, *BECN1*; (d) apoptosis: *CASP3*, *CASP8*. Additionally, IL6 and PGE2 secretion were determined by ELISA (Hosseini et al. 2024a; Hosseini et al. 2024b).

Taken together, the main goal of this project was to examine the effect of increased oxidative stress environment on molecular events during OTM. Herein and to our knowledge, we established for the first time a dual model to study the effects of OS on mechanically stimulated hPDLCs and hOBs. The fundamental operating techniques of these two experimental setups can be simply defined by two approaches: tensile forces are applied through the deformation of the substrate (Sun et al. 2021), while compressive forces are applied through the application of weight (Janjic et al. 2018).

A brief overview of the two mentioned force application models is given in the following sub-chapters.

2.3.2 Compressive force stimulation using WAB model

To mimic the orthodontic compressive force, the weight approach-based (WAB) in vitro loading model was utilized (Figure 2) (Janjic et al. 2018). The WAB model has been used since its introduction (Kanai 1992) to investigate the effects of

static, compressive, unidirectional force on cellular responses during OTM (Janjic et al. 2018). This model makes it possible to study the cellular and molecular pathways, especially bone resorption and osteoclastogenesis induction, on the compression side during orthodontic tooth movement. In this model, cells are precultured in culture dishes and subjected to mechanical loading by placing a glass slide over the cell monolayer, with a glass cylinder filled with lead granules positioned on top to apply controlled weight. The proper force distribution is ensured by the glass slide, and the amount of the compressive force can be modulated by adjusting the number of lead granules in the cylinder (Janjic et al. 2018; Kanai 1992; Kanzaki et al. 2002).

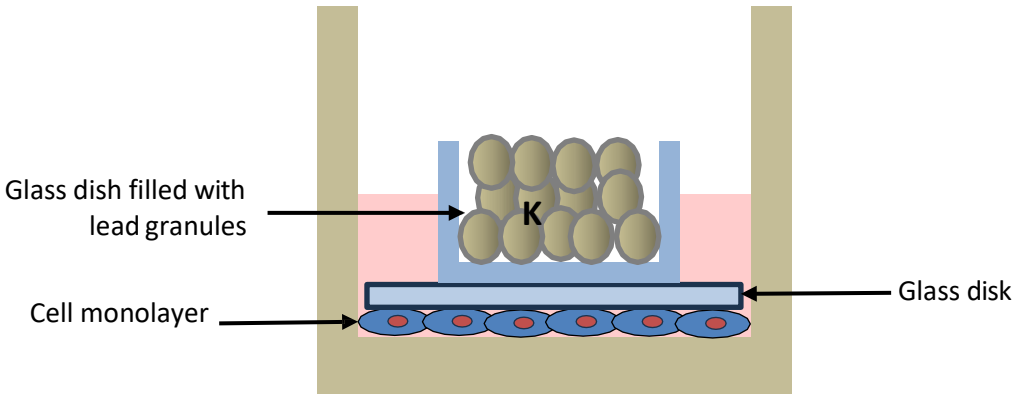

Figure 2. Schematic drawing of the WAB in vitro loading model. [Figure redrawn from Janjic et al. (2018), Figure 2 (a); licensed under CC BY 4.0]

In the first study (Hosseini et al. 2024a), static mechanical compression was applied to hPDLCs. Periodontal ligament cells, in general, play a crucial role in mechanosensing by responding to mechanical loads applied to teeth, particularly in response to orthodontic forces (Sokos et al. 2015; Yang et al. 2015). When subjected to static compression, these cells trigger a cascade of biochemical reactions that drive bone resorption and tooth movement (Yang et al. 2015). Accordingly, our first study was designed to better understand how hPDLCs respond to compressive stimulation combined with OS pre-stimulation.

2.3.3 Tension force stimulation using a custom-made tension apparatus

Different *in* vitro models have been developed to study cellular responses to tensile mechanical force (Sun et al. 2021). These models focused on two key parameters: temporal variation (continuous "static" or intermittent "dynamic" force) and direction of the force application (uniaxial tension along a single principal axis

or equibiaxial tension across all directions) (Sun et al. 2021). In the current project, a custom-made tension apparatus was used to apply static equibiaxial tensile force (Figure 3) (Sun et al. 2022).

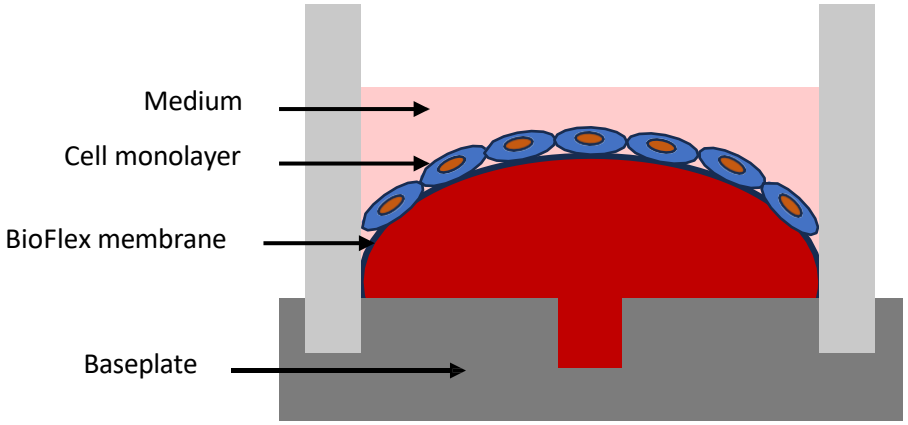

Figure 3. Schematic drawing of experimental setup used to apply tensile strain. [Figure redrawn from Sun et al. (2022), Figure 1; licensed under CC BY 4.0]

In the second study (Hosseini et al. 2024b), static tensile force was applied to hOBs to investigate the role of tensile forces in promoting bone formation by triggering osteogenic regulation (Sun et al. 2021). As known, bone formation consists of matrix formation and mineralization and osteoblasts are key players in this process (Šromová et al. 2023). These cells contribute to matrix protein synthesis and mineralization in response to mechanical loading (Šromová et al. 2023; Xiao et al. 2023). Moreover, they play a significant role in tension-induced osteogenesis, further highlighting their involvement in bone remodelling (Xiao et al. 2023). In this regard, our second study was designed to better understand how hOBs respond to tension stimulation in combination with OS pre-stimulation.

2.4 Clinical relevance of the project

Better understanding of the cellular and biological responses could enhance both the effectiveness and duration of orthodontic tooth movement (OTM). This understanding will particularly help to improve treatment strategies for adult patients, who often require more efficient interdisciplinary treatment approaches with lower risks. From a therapeutic point, improved knowledge of biology and mechanobiology of the underlying mechanisms in regulation of OTM, will guide to the development of more targeted orthodontic materials, leading to a “biologization” of orthodontic therapy. Further research is required to bridge the gap between biological concepts and clinical practice. This concept could implement personalized treatment strategies based on each patient's individual biological response and

would also consider age-related variations and/or coexistence of other oral pathologies such as periodontitis. Given that OS is a common factor in numerous oral diseases, the findings from this research could be used as an initial step for future clinical studies.

2.5 Summary of the papers and key findings

Both studies employed an in vitro model using H_2O_2 to induce OS and examined its impact on hPDLCs and hOBs under mechanical forces relevant to OTM. In both cell types, pre-exposure to H_2O_2 altered mechanosensing under mechanical force, and affected cell viability and proliferation.

In hPDLCs, changes in gene expression related to inflammation (*IL6*, *CXCL8*/*IL8*, *PTGS2*/*COX2*), bone remodelling (*RUNX2*, *TNFRSF11B*/*OPG*, *BGLAP*), apoptosis (*CASP3*, *CASP8*), and autophagy (*MAP1LC3A*/*LC3*, *BECN1*) were examined (Hosseini et al. 2024a). Static compression upregulated *PTGS2/COX2* expression, particularly in H_2O_2-prestimulated groups, which was accompanied by increased PGE2 levels. Similarly, static compression enhanced *CXCL8/IL8* expression, especially when pretreatment with H_2O_2 was done. *IL6* expression was downregulated. H_2O_2 pre-exposure reduced osteogenesis-related gene expression after compression. While autophagy-related genes showed a slight upregulation, apoptosis-related genes were generally downregulated (Hosseini et al. 2024a).

In hOBs, changes in gene expression related to inflammation (*IL6*, *CXCL8*/*IL8*, *PTGS2*/*COX2*), bone remodelling (*RUNX2*, *TNFRSF11B*/*OPG*, *P2RX7*), apoptosis (*CASP3*, *CASP8*), and autophagy (*MAP1LC3A*/*LC3*, *BECN1*) were examined (Hosseini et al. 2024b). OS influenced tension-induced mechanotransduction. In general, 15 % of tension force upregulated the expression of examined genes. While tension alone upregulated genes related to osteogenic differentiation, OS pre-stimulation did not significantly enhance this effect. Key inflammatory markers (*CXCL8*/*IL8*, *IL6*, *PTGS2*/*COX2*) and apoptosis/autophagy-related genes (*CASP3*, *CASP8*, *MAP1LC3A*/*LC3*, *BECN1*) showed varied responses. Additionally, increased *PTGS2*/*COX2* expression with higher concentrations of H_2O_2 correlated with elevated PGE2 levels (Hosseini et al. 2024b).

The findings of these two *in vitro* projects confirm the altering-effects of OS on both cell types. The results also showed the potential prolonged influence of OS on important cellular processes related to inflammation, bone remodelling, autophagy and apoptosis during OTM. These findings and modulations of gene expressions show the complexity of OS in relation to mechanical stimulation and

underscore the need for more studies in more physiologically relevant environments, *in vivo*. Such studies will lead to the betterment of clinical orthodontic treatments by having more personalized treatment plans specially in adult patients with presented periodontal diseases. Such studies will improve clinical orthodontic treatment by enabling more personalized treatment planning, particularly for adult patients with coexisting chronic inflammatory oral conditions, such as periodontal disease.

3. Paper I

Investigation of Impact of Oxidative Stress on Human Periodontal Ligament Cells Exposed to Static Compression

Hosseini S, Diegelmann J, Folwaczny M, Frasheri I, Wichelhaus A, Sabbagh H, Seidel C, Baumert U, Janjic Rankovic M.

Int J Mol Sci. 2024 Dec 17;25(24):13513.

DOI: 10.3390/ijms252413513
PMID: 39769281
PMCID: PMC11678643

(37 pages including supplements)

International Journal of Molecular Sciences

MDPI

Article

Investigation of Impact of Oxidative Stress on Human Periodontal Ligament Cells Exposed to Static Compression

Samira Hosseini [1], Julia Diegelmann [2], Matthias Folwaczny [2], Iris Frasheri [2], Andrea Wichelhaus [1], Hisham Sabbagh [1,*], Corrina Seidel [1], Uwe Baumert [1] and Mila Janjic Rankovic [1,*]

[1] Department of Orthodontics and Dentofacial Orthopedics, LMU University Hospital, LMU Munich, 80336 Munich, Germany; samirahosseini1251@gmail.com (S.H.); kfo.sekretariat@med.uni-muenchen.de (A.W.); corinna.seidel@med.uni-muenchen.de (C.S.); uwe.baumert@med.uni-muenchen.de (U.B.)

[2] Department of Conservative Dentistry and Periodontology, LMU University Hospital, LMU Munich, 80336 Munich, Germany; julia.diegelmann@med.uni-muenchen.de (J.D.); matthias.folwaczny@med.uni-muenchen.de (M.F.); iris.frasheri@med.uni-muenchen.de (I.F.)

* Correspondence: hisham.sabbagh@med.uni-muenchen.de (H.S.); mila.janjic@med.uni-muenchen.de (M.J.R.)

Abstract: Oxidative stress (OS) is a common feature of many inflammatory diseases, oral pathologies, and aging processes. The impact of OS on periodontal ligament cells (PDLCs) in relation to oral pathologies, including periodontal diseases, has been investigated in different studies. However, its impact on orthodontic tooth movement (OTM) remains poorly understood. This study used an in vitro model with human PDLCs previously exposed to H_2O_2 to investigate the effects of OS under a static compressive force which simulated the conditions of OTM. Human PDLCs were treated with varying concentrations of H_2O_2 to identify sub-lethal doses that affected viability minimally. To mimic compromised conditions resembling OTM under OS, the cells were pretreated with the selected H_2O_2 concentrations for 24 h. Using an in vitro loading model, a static compressive force (2 g/cm^2) was applied for an additional 24 h. The cell viability, proliferation, and cytotoxicity were evaluated using live/dead and resazurin assays. Apoptosis induction was assessed based on caspase-3/7 activity. The gene expression related to bone remodeling (*RUNX2*, *TNFRSF11B*/*OPG*, *BGLAP*), inflammation (*IL6*, *CXCL8*/*IL8*, *PTGS2*/*COX2*), apoptosis (*CASP3*, *CASP8*), and autophagy (*MAP1LC3A*/*LC3*, *BECN1*) was analyzed using RT-qPCR. This study suggests an altering effect of previous OS exposure on static-compression-related mechanosensing. Further research is needed to fully elucidate these mechanisms.

Keywords: oxidative stress; human periodontal ligament cells; static compressive force; bone remodeling; orthodontic tooth movement

Citation: Hosseini, S.; Diegelmann, J.; Folwaczny, M.; Frasheri, I.; Wichelhaus, A.; Sabbagh, H.; Seidel, C.; Baumert, U.; Janjic Rankovic, M. Investigation of Impact of Oxidative Stress on Human Periodontal Ligament Cells Exposed to Static Compression. *Int. J. Mol. Sci.* **2024**, *25*, 13513. https://doi.org/10.3390/ijms252413513

Academic Editor: Luigi Canullo

Received: 13 November 2024
Revised: 12 December 2024
Accepted: 13 December 2024
Published: 17 December 2024

1. Introduction

Oxidative stress (OS) arises from an imbalance between the production of reactive oxygen species (ROS) and the host's ability to detoxify them or repair the resulting damage [1,2]. In recent years, research has emphasized the role of OS in various oral pathologies, particularly chronic inflammatory conditions like periodontal disease, as well as in physiological processes such as aging [3–7].

The inflammatory response to the presence of periodontal pathogens increases the production of ROS [7–9]. Various studies have confirmed a positive correlation between elevated ROS levels and the degree of periodontal tissue inflammation [10]. Excessive ROS accumulation causes OS, leading to the damage of cells and tooth-supporting tissues. This damage triggers the release of more inflammatory mediators, creating a continually reinforcing feedback loop of inflammation and OS [7,9]. This cycle negatively impacts periodontal ligament cells (PDLCs), a dominant cell type in the periodontal ligament (PDL), leading to their dysfunction, apoptosis, and reduced regenerative capacity [11,12]. This

ongoing damage and inflammation can result in the destruction of periodontal tissues and impair bone turnover, thus disrupting the balance between bone formation and resorption [13,14]. Additionally, this process negatively affects cellular functions such as autophagy and apoptosis [11,15]. These findings suggest that ROS accumulation might contribute to imbalances in bone metabolism and could adversely affect orthodontic tooth movement (OTM) and post-treatment stability [14].

PDLCs are also known for their crucial role during OTM, where mechanical forces are applied to the teeth to correct their alignment. These forces lead to biological responses in the surrounding tissues, resulting in tooth movement. Elevated pro-inflammatory responses of PDLCs may occur as a consequence of this mechanical stimulation [16]. Particularly, the compression side during OTM is characterized by the presence of sterile inflammation and the increased expression of inflammatory mediators by the PDLCs [16,17]. However, with the exception of few studies that have confirmed increased ROS generation on the compression side during OTM [18,19], the impact of OS and ROS accumulation on OTM at the molecular level is still largely unknown. While lower concentrations of ROS can stimulate tissue-related processes and support regeneration, excessive ROS accumulation—e.g., in chronic inflammatory disorders or with aging-related decline in antioxidant defense—is linked to tissue-destructive processes [3,20–22].

Given the growing elderly population and the increasing number of adult orthodontic patients with underlying degenerative inflammatory conditions, the goal of our study was to investigate whether pre-exposure to OS alters the cellular response and how this may influence static-compression-related mechanosensing in hPDLCs. For these purposes, we used a combination of two well-established setups: one for OS simulation and the other for OTM simulation. Hydrogen peroxide (H_2O_2), a key mediator of OS, has been widely used in experimental settings to simulate OS conditions in cell cultures [11,20,23–28]. By introducing controlled levels of H_2O_2, the cellular environment observed in aging or disease states can be simulated. On the other hand, in vitro models for the application of mechanical stimulation have been well established in the field of orthodontics for investigating molecular events related to mechanosensing [29]. They allow for an in-depth analysis of the complex situation in vivo and investigation of the molecular biology of OTM. One of these models is the weight-approach-based (WAB) in vitro model for the application of static compression [17,30] that we used in this study. These two models for OS and OTM allowed us to simplify the in-depth analysis of the complex situation in vivo and investigate the molecular biology of OTM, focusing on just one cell type and one type of force.

In this study, suitable experimental parameters were established based on cell viability and proliferation. OS/WAB-related gene expression regulation was analyzed in genes related to bone remodeling (*RUNX2*, *BGLAP*, *TNFRSF11B*/*OPG*), inflammation (*IL6*, *CXCL8*/*IL8*, *PTGS2*), autophagy *(MAP1LC3A*/*LC3*, *BECN1*), and apoptosis (*CASP3*, *CASP8*).

2. Results

Initially, based on the recommendations from the literature, an appropriate H_2O_2 concentration range for use in hPDLC culture was tested. Based on cell viability and cytotoxicity assessments, as well as apoptosis marker expression, three concentrations (50 µM, 100 µM, and 200 µM) were selected for use in the experiments.

Afterwards, the effect of ROS stimulation in the hPDLC culture was examined using three selected doses of H_2O_2. Two timepoints for gene expression investigation were selected, one directly after H_2O_2 incubation (the "direct" phase) and the other after 24 h of recovery in H_2O_2-free medium (the "recovery" phase). In this way, it was possible not only to see how different ROS concentrations affected the gene expression related to inflammation, bone remodeling, and tissue homeostasis but also to confirm and examine the consequent long-term changes in cellular behavior.

Finally, we examined the effects of the application of a compression force to the cells after 24 h of recovery from H_2O_2 stimulation. The justification for the application of OS stimulation prior to mechanical stimulation is based on the clinical recommendations to start orthodontic treatment during the remission stage of existing chronical inflammatory disorders.

2.1. Hydrogen Peroxide (H_2O_2) Concentration Testing

Firstly, as part of establishing an OS model, a range of H_2O_2 concentrations for use in the hPDLC culture was evaluated based on the recommendations from the literature [11,20,24]. To determine the optimal concentrations of H_2O_2 that induce cytotoxic effects without compromising the cell viability, the hPDLCs were exposed to rising concentrations of H_2O_2 from 0 µM to 500 µM. Following an assessment of apoptosis and cell viability, concentrations of 50 µM, 100 µM, and 200 µM were identified as suitable for further experimental steps (Figure 1).

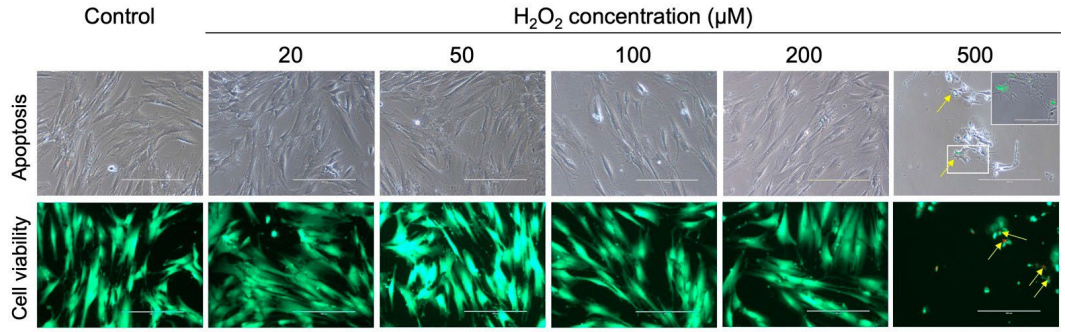

Figure 1. Effect of different hydrogen peroxide concentrations on apoptosis induction (upper row) and cell viability (lower row) in hPDLCs. Upper row: Apoptosis detection using CellEvent™ Caspase-3/7 Detection Reagent (green fluorescence; yellow arrows) in hPDLCs exposed to different H_2O_2 concentrations (0 µM to 500 µM). Insert: Area with higher magnification shows green fluorescence. Lower row: Live/dead cell staining of hPDLCs treated with the different H_2O_2 concentrations. Green cells indicate viability, whereas dead cells are either detached or stained red (yellow arrows). Fluorescence microscopy was carried out using an EVOS®*fl* microscope (Invitrogen, Carlsbad, CA, USA) (Scale bar: 200 µm).

The results from the resazurin test, used to quantitatively assess cytotoxicity and cell viability, supported the selection of 50 µM, 100 µM, and 200 µM of H_2O_2 as minimally cytotoxic while retaining cellular viability (Figure 2). These findings were in line with the qualitative results from the microscopic imaging.

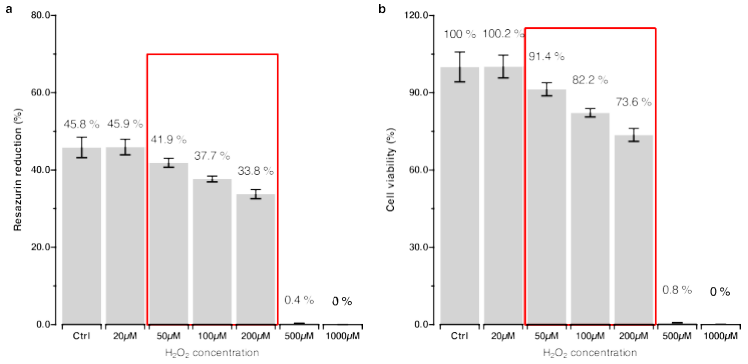

Figure 2. Percentage reduction in resazurin. (**a**) Cytotoxic effect of H_2O_2; (**b**) cell viability calculated as normalized resazurin reduction relative to that in the control group. 50 µM, 100 µM, and 200 µM were identified as the lowest concentrations of H_2O_2 that showed a cytotoxic effect, however, without a pronounced effect on cell viability.

2.2. Investigation of H_2O_2's Effect on Gene Expression Directly After Incubation and 24 h Post-Incubation

To assess the effect of OS on the hPDLCs' gene expression profile, we focused on the impact of H_2O_2 (50 µM, 100 µM, and 200 µM) on the cells directly after its application ("direct") and 24 h post-incubation ("recovery"). The expression of genes related to bone remodeling, inflammation, autophagy and apoptosis was assessed using RT-qPCR (Figure 3).

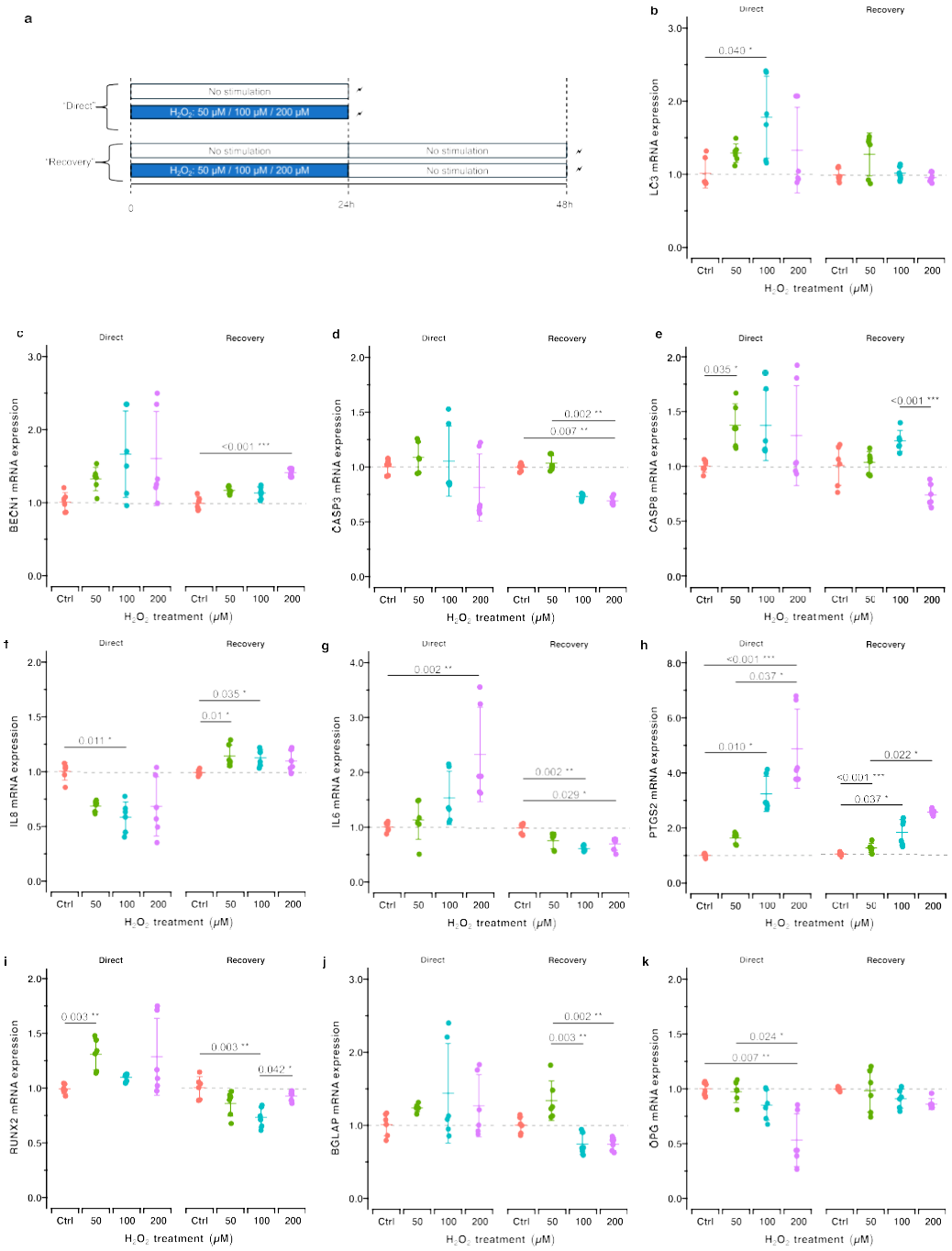

Figure 3. Effect of OS induction alone on gene expression immediately after H_2O_2 incubation ("direct") and 24 h post-incubation ("recovery"). (**a**) Experimental design. (**b–k**) RT-qPCR results for

genes related to autophagy ((**b**,**c**) *MAP1LC3A/LC3*, *BECN1*), apoptosis ((**d**,**e**), *CASP3*, *CASP8*), inflammation ((**f**,**h**), *CXCL2/IL8*, *IL6*, *PTGS2/COX2*), and bone remodeling ((**i**,**k**), *RUNX2*, *P2RX7*, *TNFRSF11B/OPG*). For each genetic locus, the gene expression directly after H_2O_2 exposure (left panel, "direct") and after an additional 24 h of cultivation in H_2O_2-free cell culture medium (right panel, "recovery") is depicted. Adjusted *p*-values ($p_{adj.}$) based on multiple comparisons within each group are reported: *, $p_{adj.} < 0.05$; **, $p_{adj.} < 0.01$; ***, $p_{adj.} < 0.001$.

The autophagy-related genes *MAP1LC3A/LC3* and *BECN1* showed an overall upregulation which was statistically significant, directly after stimulation with 100 µM of H_2O_2 for *MAP1LC3A/LC3* and after recovery from 200 µM of H_2O_2 for *BECN1* (Figure 3b,c). The apoptosis-related genes caspase-3 (*CASP3*) and caspase-8 (*CASP8*) showed no significant changes in expression across the H_2O_2-stimulated groups, except for a decrease in *CASP3* expression after recovery from the treatment with 200 µM H_2O_2 and an increase in *CASP8* expression immediately following stimulation with 50 µM H_2O_2 (Figure 3d,e).

Our results showed a complex time- and H_2O_2-dose-dependent regulation pattern of the key inflammatory mediators *PTGS2/COX2*, *CXCL8/IL8*, and *IL6* in response to H_2O_2 stimulation (Figure 3f–h). *CXCL8/IL8* showed a biphasic response: initial downregulation immediately after H_2O_2 exposure, followed by upregulation after the 24 h recovery period (Figure 3f). Interestingly, IL6 had the opposite pattern: immediate upregulation after H_2O_2 exposure, followed by downregulation after recovery (Figure 3g). *PTGS2/COX2* displayed consistent upregulation with increasing H_2O_2 concentrations both in the "direct" and "recovery" groups in a dose-dependent manner (Figure 3h).

Overall, the bone-remodeling-related genes exhibited a stable expression pattern, characterized by minimal up- or downregulation in different conditions (Figure 3i–k). *RUNX2* showed a significant increase directly after stimulation with 50 µM H_2O_2 and furthermore a decrease after recovery from 100 µM H_2O_2 (Figure 3i). *BGLAP* demonstrated a significant decrease in expression after recovery from 100 and 200 µM H_2O_2 stimulation compared to that with 50 µM H_2O_2 (Figure 3j). *TNFRSF11B/OPG* was downregulated in the direct phase, with statistical significance observed only at the highest concentration tested (200 µM H_2O_2) (Figure 3k).

2.3. Expression of Genes and Metabolites Related to Inflammation, Bone Remodeling, Apoptosis, and Autophagy in Compressed Cells With and Without H_2O_2 Preincubation

Next, we examined the effect of the application of H_2O_2 in the recovery phase followed by the application of static compression using the "WAB model" [17,30]. The expression patterns of genes and proteins related to inflammation, bone remodeling, apoptosis, and autophagy were analyzed (Figure 4).

2.3.1. Inflammation

Upregulation in the expression of the *PTGS2/COX2* gene was observed after the application of static compression in all groups. Especially in the H_2O_2-prestimulated groups, a dose-dependent pattern, with the maximal upregulation in the group "200 µM H_2O_2 and WAB" ($p_{adj.} < 0.001$) (Figure 4b), was found. An almost identical pattern for PGE2 concentration was measured in the corresponding cell culture supernatants (Figure 4c). The compression force also increased *CXCL8/IL8* expression (Figure 4f). Like *PTGS2/COX2*, the *CXCL8/IL8* upregulation was more pronounced in the groups pretreated with H_2O_2 in a dose-dependent manner. On the contrary, *IL6* gene expression was generally downregulated after static compression, with or without H_2O_2 prestimulation (Figure 4d). The IL6 protein concentration in the cell culture supernatant showed the same pattern except in the group pretreated with 200 µM H_2O_2, where upregulation, though not statistically significant, was observed (Figure 4e).

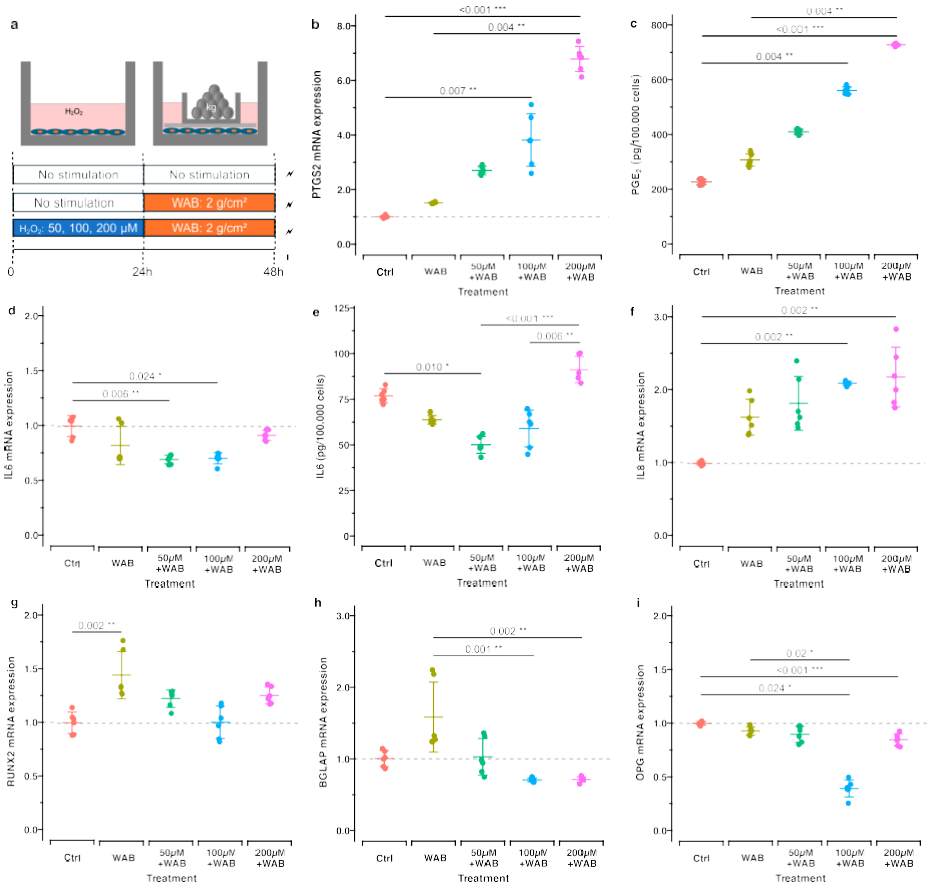

Figure 4. Expression of genes and metabolites related to inflammation, bone remodeling, apoptosis, and autophagy in mechanically stimulated cells with and without previous H_2O_2 stimulation. (**a**) Experimental setup: The control group (Ctrl) received neither H_2O_2 nor compression stimulation. The compression group (WAB) was stimulated with static compression (2 g/cm^2) after 24 h of no stimulation. The H2O2/WAB group was stimulated for 24 h with 50 µM, 100 µM, or 200 µM H_2O_2 followed by 24 h of static compression at 2 g/cm^2. (**b–f**) Expression of inflammation-related genes and metabolites and (**g–i**) genes related to bone remodeling is reported. Adjusted *p*-values ($p_{adj.}$) based on multiple comparisons within each group are reported: *, $p_{adj.} < 0.05$; **, $p_{adj.} < 0.01$; ***, $p_{adj.} < 0.001$.

2.3.2. Bone Remodeling

Although not always statistically significantly, all groups of compressed cells previously exposed to H_2O_2 showed lower gene expression levels related to osteogenesis in comparison to those in the WAB group where only compression was applied (Figure 4g–i). A significant increase in *RUNX2* gene expression was noted as an effect of static compression in the groups of cells without pretreatment in the OS condition (Figure 4g). In contrast, *TNFRSF11B*/*OPG* showed no significant changes in expression, except after the application of a compression force following recovery from 100 µM H_2O_2 stimulation (Figure 4i). The osteogenic gene *BGLAP* showed a significant decrease in expression after applying a compression force to cells preincubated with 100 µM and 200 µM H_2O_2 compared to that in the cells that just received static compression (Figure 4h).

2.3.3. Apoptosis and Autophagy

The apoptosis-related genes *CASP3* and *CASP8* exhibited either no regulation or a minimal tendency to be downregulated, which was more pronounced in the groups with previous H_2O_2 stimulation (Figure 5a,b). *CASP3* was significantly downregulated in response to compression following prestimulation with 100 µM or 200 µM H_2O_2 (Figure 5b). In contrast, the genes related to autophagy showed a slight, although a mostly statisti-

cally non-significant, upregulation tendency (Figure 5c,d). The *BECN1* expression was significantly increased after the application of the WAB method in the group previously stimulated with 200 µM H_2O_2. *MAP1LC3A/LC3* had a pronounced increase in expression following the application of the WAB method after pretreatment with 50 µM H_2O_2 (Figure 5c).

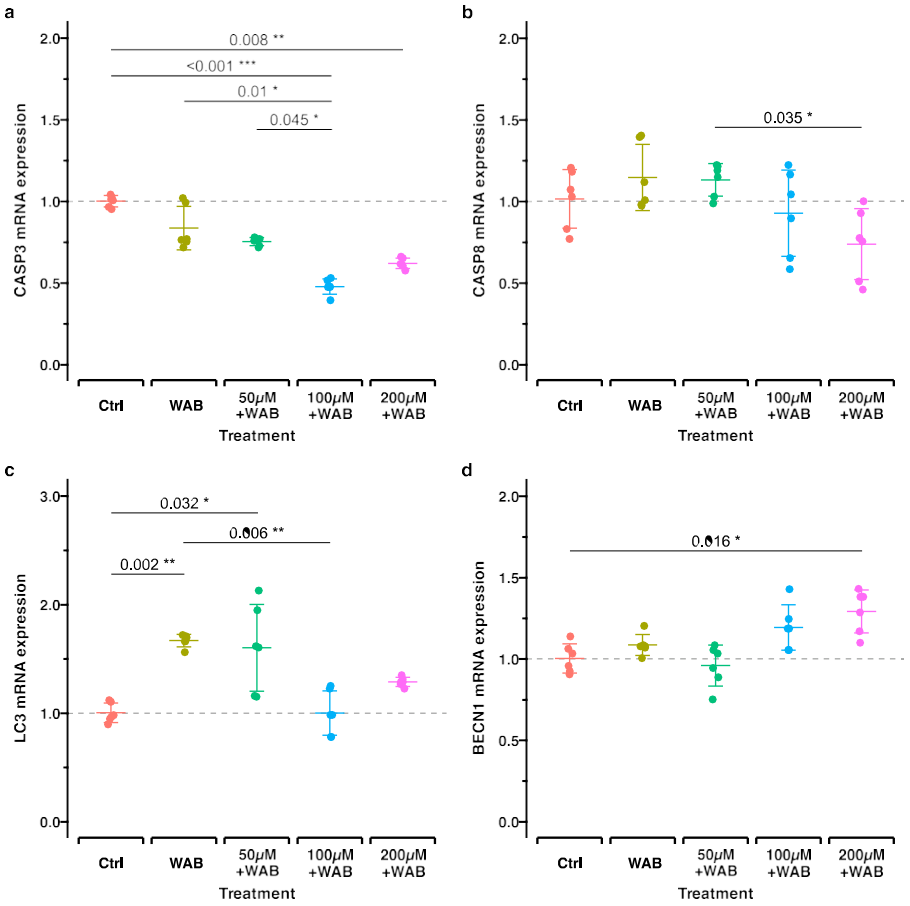

Figure 5. RT-qPCR results for autophagy (**a**,**b**)- and apoptosis (**c**,**d**)-related genes. Adjusted *p*-values based on multiple comparisons between each experimental treatment are shown. The groups are the same as in Figure 4. Adjusted *p*-values ($p_{adj.}$) based on multiple comparisons between each experimental treatment are shown as follows: *, $p_{adj.} < 0.05$; **, $p_{adj.} < 0.01$; ***, $p_{adj.} < 0.001$.

2.4. Assessment of Cell Viability and Proliferation Under Static Compression With and Without Oxidative Stress

Next, we analyzed the cell proliferation in the hPDLCs treated with H_2O_2 and subjected to static compression via calculations of the resazurin reduction (Figure 6). These experiments indicated a reduced proliferation in the groups pre-exposed to H_2O_2, with a more pronounced effect in the groups that received both OTM and H_2O_2 stimulation. Similar results were obtained through live/dead staining of the cells (Figure 7).

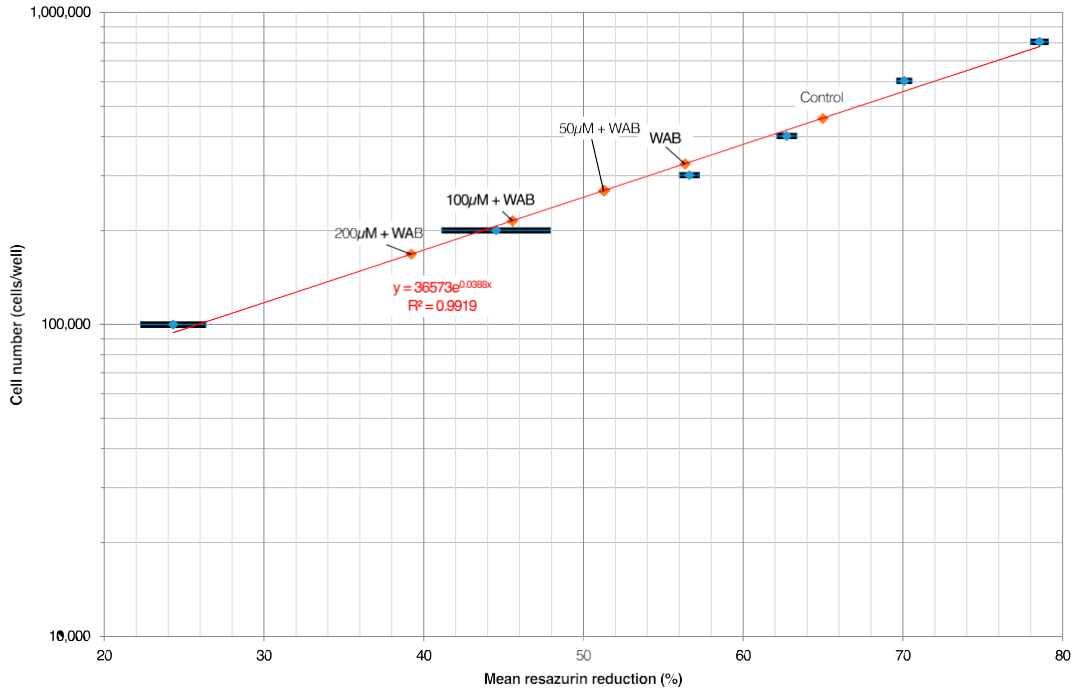

Figure 6. Resazurin-reduction-based growth curve. A standard curve was generated as described in the Section 4 to examine the cell growth during the experiments. Cells from the 5th passage were seeded in triplicate (100,000; 200,000; 300,000; 400,000; 600,000; and 800,000 cells/well). Exponential regression was used to calculate the standard curve (red line) (Microsoft Excel). Cellular growth of the hPDLCs in the different experimental conditions is shown with red diamonds (⌥) on the fitted curve, and data from the standard curve are shown with blue diamonds (⌥).

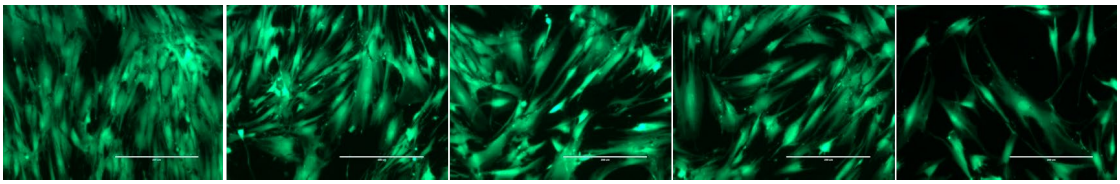

H_2O_2 (μM)	0	0	50	100	200
Compression (g/cm²)	0	2	2	2	2

Figure 7. Results of the live/dead cell staining from the WAB in vitro model, with/without H_2O_2 stimulation for a qualitative assessment of the cell viability of the cells in different experimental groups. Green cells indicate viability, and unattached dead cells are either washed away or stained red (Scale bar: 200 μm).

3. Discussion

The periodontal ligament (PDL) is a specialized connective tissue that plays a crucial role in anchoring the teeth within the alveolar bone, transmitting occlusal forces, providing sensory feedback, and contributing to the repair and regeneration of the periodontal tissues [31]. Its functionality is closely linked to its multi-potential progenitor cells, as well as its diverse cellular composition. Among its different cell types, PDL fibroblasts play a significant functional role, especially in the process of responding to mechanical forces [29,32–34]. These fibroblasts are crucial not only for maintaining the stability and health of the periodontium but also in mechanosensing processes, including those induced by orthodontic forces [29]. Depending on the type of force applied, they either support anabolic or catabolic processes. The compression side during orthodontic tooth movement (OTM) is characterized by a pronounced inflammatory response, increased bone resorption

activity, reduced proliferation, and the activation of cell-destiny-related pathways. Excessive ROS accumulation, such as that seen in periodontal disease, is also associated with catabolic events [35,36]. Herein, we explored the influence of oxidative stress (OS) exposure on hPDLCs immediately after ROS stimulation using H_2O_2, as well as an additional 24 h post-incubation.

Additionally, we investigated how pre-existing OS affects the cellular physiology related to OTM, particularly in response to a compressive force. In this study, we focused on gene/substance expression related to inflammation (*IL6*, *CXCL8*/*IL8*, *PTGS2*/*COX2*, PGE2), bone remodeling (*RUNX2*, *BGLAP*, *TNFRSF11B*/*OPG*), autophagy (*MAP1LC3A*/*LC3*, *BECN1*), and apoptosis (*CASP3*, *CASP8*) and analyzed these at the transcriptional, translational, and activity levels via RT-qPCR and/or ELISA. While our results generally confirm the catabolic influence of OS, they also demonstrate the long-lasting altering effects of ROS exposure on gene expression. Additionally, our findings indicate that ROS exposure affects the mechanosensing processes during OTM, emphasizing the need for caution when treating older patients with pre-existing chronic inflammatory conditions.

3.1. Inflammation

Herein, we investigated the expression of the inflammatory markers *IL6*, *CXCL8*/*IL8*, *PTGS2*/*COX2*, and PGE2 in hPDLCs in response to OS and a static compressive force, both known to trigger inflammatory responses. These markers were selected due to their pivotal roles in the inflammatory cascade and their relevance to both periodontal pathology and OTM [17,37–42]. In this regard, studies have shown an increase in, for example, IL6 in gingival crevicular fluid during orthodontic tooth movement [43,44]. As such, we decided to track the regulation of IL6 at both the gene and protein expression levels.

3.1.1. H_2O_2 Stimulation—Direct vs. 24 h Post-Incubation

It is known that increased OS and exposure to H_2O_2 can lead to the elevated expression of inflammatory markers [45]. In line with this, the herein-investigated markers *IL6* and *PTGS2*/*COX2* showed dose-dependent upregulation directly after H_2O_2 stimulation. On the other hand, contrary to the findings from literature [46], *CXCL8*/*IL8* decreased directly after H_2O_2 stimulation. In this study, we also showed that changes in gene expression were still visible 24 h after H_2O_2 stimulation, although to a lesser extent. The results presented herein indicate that H_2O_2 exposure alters the pro-inflammatory response; however, they also demonstrate its long-lasting effect. Further studies on the relationship of OS and pro-inflammatory markers at the cellular and molecular levels are needed to strengthen this evidence base.

3.1.2. H_2O_2 Stimulation Followed by Static Compression

Although not statistically significant, slight gene expression upregulation in response to a static compressive force could be observed for *PTGS2*/*COX2* and *CXCL8*/*IL8*. This is in line with published studies [47–55]. Nevertheless, preincubation with H_2O_2 induced more pronounced dose-dependent upregulation of *PTGS2*/*COX2* and *CXCL8*/*IL8* gene expression, demonstrating an enhancing pro-inflammatory effect of ROS stimulation. The PGE2 concentration in the corresponding supernatants followed the *PTGS2*/*COX2* expression pattern as determined using RT-qPCR, which is consistent with its known role as a key enzyme involved in PGE2 synthesis [51–54]. Contrary to the findings in the literature [48–50,56], *IL6* gene expression showed slight downregulation, which was generally confirmed using IL6 ELISA, with the exception of prestimulation with 200 µM H_2O_2, which might indicate an altered inflammatory response to a higher exposure to OS. These results confirm an alteration in the inflammatory response, highlighting the complex interplay between OS and mechanical stimuli in regulating key inflammatory mediators.

3.2. Bone Remodeling

hPDLCs play an important role in activating molecular pathways related to both bone formation and resorption [57]. Herein, we analyzed the expression of the osteogenic marker genes *RUNX2*, *BGLAP*, and *TNFRSF11B*/*OPG* in the hPDLCs. *RUNX2* [58,59] is one of the essential transcription factors during bone development, also known to directly regulate the expression of *BGLAP* and *TNFRSF11B*/*OPG*, highlighting their interconnected roles in bone physiology [60]. *BGLAP* is a non-collagenous protein secreted by osteoblasts and is involved in bone mineralization and calcium ion homeostasis [61]. *TNFRSF1B*/*OPG* acts as a decoy receptor for RANKL (receptor activator of nuclear factor kappa B ligand), inhibiting its interaction with RANK (receptor activator of NF-kappaB) and thereby preventing osteoclast differentiation and bone resorption [62].

3.2.1. H_2O_2 Stimulation—Direct vs. 24 h Post-Incubation

Our results showed a moderate upregulation of *RUNX2* directly after stimulation with the lower dose of H_2O_2 (50 µM) or no change with the higher doses (100/200 µM). Recently published studies [20,24] reported the downregulation of *RUNX2* in hPDLCs directly after stimulation with 100 µM H_2O_2 for 24 h. However, in both studies, the cells were precultured in an osteogenic induction medium before H_2O_2 stimulation, which might explain the difference. Nevertheless, according to our results, downregulation of *RUNX2* was measured 24 h post-incubation, showing delayed negative influence on osteogenesis. Similarly, 24 h post-incubation downregulation was observed in *BGLAP* gene expression in groups treated with 100/200 µM H_2O_2. In contrast to these findings, *TNFRSF11B*/*OPG* showed immediate dose dependent downregulation with recovery effect 24 h post-incubation.

3.2.2. H_2O_2 Stimulation Followed by Static Compression

There are limited research data examining the regulation of *RUNX2* after the stimulation of hPDLCs with a static compressive force using the WAB in vitro model [63,64]. All of the studies identified so far reported either the downregulation of *RUNX2* gene expression or no stimulation at all within the first 24 h of the application of a static compressive force. In contrast, herein, *RUNX2* was upregulated by the application of a compressive force, while in cases of previous H_2O_2 exposure, no change in gene expression was observable. Similarly, when comparing the reaction to static compression between the cells with and without previous H_2O_2 exposure, *BGLAP* was also significantly less expressed in the cells treated with 100 µM and 200 µM H_2O_2 compared to the cells that just received the force. Our results showed a significant decrease in *TNFRSF11B*/*OPG* in the cells pretreated with 100 µM and 200 µM of H_2O_2 and then subjected to the compression force. In contrast, no significant change in *TNFRSF11B*/*OPG* was observed in the cells that underwent the mechanical force, which is in accordance with previous results [65]. Nevertheless, different studies have reported different expressions of *TNFRSF11B*/*OPG* in hPDLCs subjected to mechanical compression, examining different magnitudes and durations of compression [54,66–69].

3.3. Autophagy and Apoptosis

OS has been shown to be involved in various biological and cellular pathways, including apoptosis and autophagy [15]. The overproduction of ROS can have destructive effects on the structure of cell organelles and biomolecules [15], triggering cell-destiny-related pathways. Recent studies have found that autophagy protects PDLCs from apoptosis and promotes recovery in an inflammatory microenvironment. In periodontitis, autophagy helps to eliminate the periodontal pathogen infection and modulates the immune inflammatory response [70]. Similarly, these pathways are also activated by mechanosensing [71,72]. To obtain a better insight into these relationships, we focused on *CASP3* and *CASP8*, with both playing an important role in cell apoptosis, and the autophagy-related markers *BECN1* and *MAP1LC3A*/*LC3* [73]. While *BECN1* plays a crucial role in the early stages of au-

tophagy, *MAP1LC3A/LC3* is an essential marker in the final stages, specifically during autophagosome formation [74].

3.3.1. H_2O_2 Stimulation—Direct vs. 24 h Post-Incubation

Previous studies have shown increased rates of apoptosis and autophagy in PDLCs and periodontal ligament stem cells following OS stimulation [11,26,27,75]. Although the upregulation of the autophagy-related genes *MAP1LC3A/LC3* and *BECN1* was not always statistically significant herein, a general tendency toward upregulation was observed after H_2O_2 stimulation, aligning with previous findings [26]. However, these effects diminished in most cases 24 h post-incubation. In contrast, no clear expression pattern was observed for the apoptosis-related genes *CASP3* and *CASP8*. Given the limited research on hPDLCs regarding OS, autophagy, and apoptosis, further studies are essential to clarify the precise impact of OS on these cellular mechanisms [73].

3.3.2. H_2O_2 Stimulation Followed by Static Compression

Studies have reported contradictory effects of a compressive force on autophagy-related markers. One study reported a decrease in LC3II/I and BECN1 protein after 24 h of a 1.5 g/cm^2 compressive force [67], whereas another reported an increase in BECN1 protein and the ratio of LC3II/I after 24 h of stimulation with a 2 g/cm^2 compressive force in hPDLCs [76], along with elevated CASP3 protein levels. Herein, the apoptosis-related genes exhibited either no regulation or a minimal downregulation tendency, which was slightly more pronounced in groups with previous H_2O_2 stimulation. On the contrary, the genes related to autophagy seemed to show a slight, although statistically non-significant in most cases, upregulation tendency.

3.4. This Study's Strengths/Limitations and Future Perspectives

OS has not been thoroughly investigated in relationship to mechanosensing in hPDLCs. In this study, we combined two established models: one using H_2O_2 to simulate OS and the WAB model as the other to mimic orthodontic static compressive forces. To our knowledge, this represents the first attempt to investigate the combined effects of static compression forces and OS on hPDLCs.

Direct exposure of cells to oxidative chemicals like H_2O_2 is a commonly used method for simulating OS [77]. H_2O_2, an ROS frequently generated during inflammation, including periodontal disease [7,78–80], makes this approach particularly relevant to studying OS in PDLCs. This method is supported by well-established protocols, allowing for precise control over the concentration and exposure time [81]. For a more physiological simulation of OS, alternative models involving the knockout or suppression of antioxidant defense genes have been proposed [82]. While such approaches can provide a more realistic representation of chronic OS, they come with certain limitations. Many genes have multiple functions, meaning that knocking out a single gene can trigger unexpected phenotypic changes unrelated to OS. Additionally, cells may activate compensatory pathways to offset the loss of gene function, potentially obscuring the true effects of the knockout. Furthermore, permanent gene knockout complicates the study of time-dependent processes, which was particularly relevant in our study, as we aimed to simulate the "recovery effect" following periodontal therapy.

While in vitro models have limitations in replicating the biological complexity of living organisms [83], this study lays a foundation for more sophisticated analyses by focusing on key mechanistic insights in a controlled setting. We specifically used hPDLCs in a 2D cellular monolayer, providing a direct view of their response to OS and compressive forces. However, in living tissues, interactions with neighboring cells, the extracellular matrix, and signaling molecules [84,85] influence these processes. Therefore, future studies, such as those using coculture or three-dimensional (3D) models, would further enhance our understanding by mimicking the in vivo environment more closely, allowing for intercellular communication and a more physiologically relevant structure [86]. Our study

relied on a qPCR-based analysis of *MAP1LC3A/LC3* and *BECN1* as markers to assess cell autophagy. While these markers are widely known autophagy regulators [87,88], their roles in other cellular pathways and the lack of direct measurement of autophagic flux limit the specificity of our conclusions. Future studies including such direct assays will provide a more comprehensive evaluation of autophagic activity [89]. Incorporating additional functional assays, such as TUNEL assays for apoptosis detection [90], would provide a more comprehensive understanding of how oxidative stress and mechanical force impact hPDLC physiology. Additionally, a broader exploration at the gene and protein levels, incorporating cells from multiple donors of varying ages and sexes, as well as further in vivo studies, could provide valuable insights into the variability in these responses. Such studies would help account for individual differences in biology and physiology, bringing us closer to understanding how these factors contribute to OTM and related bone remodeling processes in vivo. Future research should include animal models to validate our findings in a more physiologically relevant context, enabling a deeper understanding of the interplay between OS, gene regulation, and tissue remodeling during orthodontic treatment.

4. Materials and Methods

4.1. Primary Cell Culture

Human PDLCs were isolated from the middle third of the roots of caries-free molars from a healthy 18-year-old male that were extracted due to orthodontic reasons. Written informed consent from the patient or his legal custodian was obtained. This study was conducted in accordance with the Declaration of Helsinki, and the study protocol was approved by the ethics committee of the Ludwig-Maximilians-Universität München (project number 21-0931).

HPDLCs were obtained from tissue samples utilizing a modified explant technique [91] and were cultured in Dulbecco's Modified Eagle's Medium/Nutrient Mixture F-12 Ham (DMEM/F-12) (D6421; Sigma-Aldrich, St. Louis, MO, USA) supplemented with 10% FBS (F7524; Sigma-Aldrich, St. Louis, MO, USA), 2% MEM vitamins (M6895; Biochrom, Berlin, Germany), and 1% antibiotic/antimycotic (15240-062; Life Technologies, Carlsbad, CA, USA). The cells were maintained in a humidified environment with 5% CO_2 at 37 °C and passaged at regular intervals using 0.05% trypsin–EDTA solution (L2143; Biochrom, Berlin, Germany). Cells from passages 5 and 6 were used in all of the experimental procedures.

4.2. H_2O_2 Concentration Gradient Selection

To identify the appropriate concentration of H_2O_2 for the experiment, cell viability, cytotoxicity, and apoptosis were analyzed after the stimulation of the hPDLCs with different H_2O_2 concentrations (9681.4; Carl Roth GmbH + Co. KG, Karlsruhe, Germany). The cells were seeded at a density of $1.5 \rightarrow 10^5$ cells/well into 6-well plates (657160; Greiner Bio One, Frickenhausen, Germany) in triplicate and incubated overnight in a CO_2 incubator (5% CO_2, 37 °C, humidified atmosphere). On the next day, the cells were stimulated with H_2O_2 concentrations of 20 µM, 50 µM, 100 µM, 200 µM, and 500 µM [11,20,24] and incubated for 24 h. Wells containing the cell culture medium without H_2O_2 were considered as medium controls. The cytotoxicity of H_2O_2 in terms of cell viability was monitored using a resazurin-based assay, as previously published [92]. Cell viability and apoptosis were visually assessed as described below.

Quantitative assessment of cell viability/cytotoxicity: Cell viability and cytotoxicity were assayed using a resazurin assay as previously described [92] with one minor modification: the cells were incubated with resazurin-containing medium for 2 h instead of 3 h. The cell viability was then calculated as the normalized resazurin reduction relative to the control group.

Qualitative assessment of cell viability and apoptosis using fluorescence microscopy: Following the resazurin test, all of the wells were washed twice with phosphate-buffered saline (PBS, RNBL5636; Sigma-Aldrich, St. Louis, MO, USA). From each experimental group, two wells were used for live/dead cell staining, and one well was used for apoptosis

detection. For apoptosis detection, the CellEvent™ Caspase-3/7 Green Reagent kit (R37111; Life Technologies, Carlsbad, CA, USA) was employed according to the manufacturer's instructions. The cell viability of the hPDLCs at all concentrations was evaluated using a live/dead cell staining kit (L3224; Invitrogen/ThermoFisher Scientific, Carlsbad, CA, USA) according to the manufacturer's instructions. After 30 min of incubation at room temperature in the dark, fluorescence microscopy was conducted (EVOS®*fl*, Invitrogen, Carlsbad, CA, USA) for both the live/dead and caspase 3/7 apoptosis tests. Photographs of randomly selected fields were captured using 10→ and 20→ microscope objectives.

4.3. Effect of Oxidative Stress Induction on Gene Expression in "Direct" and "Recovery" Setups

To assess the effect of H_2O_2 on the cells, we defined two setups: one for investigating the effect of H_2O_2 treatment directly after 24 h (the "direct" setup) and another one after an additional 24 h post-incubation (the "recovery" setup) (Figure 3a). For this purpose, the cells were seeded and incubated overnight as described above. The next day, the cell culture medium was replaced with culture medium containing the determined H_2O_2 concentrations (50 µM, 100 µM, or 200 µM) in triplicate ($n = 3$). Wells which received the cell culture medium without H_2O_2 were considered controls. Cell lysates of the "direct" setup were collected after 24 h of incubation from each well using 750 µL RNA lysis buffer (R0160-1-50; Zymo, Irvine, CA, USA) according to the manufacturer's instructions and stored at −80 °C for further RT-qPCR tests (Section 4.5). For the "recovery" setup, fresh normal cell culture medium was added to all of the wells. Twenty-four hours post-incubation, the cell lysates were prepared and stored according to the same method.

4.4. Application of Compressive Force During the H_2O_2 "Recovery" Phase

To investigate the effect of H_2O_2 recovery and/or the compression force, the cells were evenly seeded as described above in two identical setups of experiments, each consisting of five experimental conditions: One setup was then used for cell viability and proliferation testing, and the other one was used for RT-qPCR (Section 4.5) and ELISA (Section 4.6). For each experimental group, three biological replicates were allocated ($n = 3$). All of the plates were incubated overnight as described above. The cells were stimulated with or without 50 µM, 100 µM, and 200 µM H_2O_2 the following day and incubated for 24 h.

4.4.1. Application of Force with the WAB Model

After 24 h of stimulation with or without the abovementioned concentrations of H_2O_2 in a CO_2 incubator, a physiological compressive force of 2.0 g/cm^2 was applied to the cells for a further 24 h (Figure 4a). Immediately prior to the application of force, the old culture medium was removed, and all of the wells were washed twice with PBS. Fresh culture medium was then added (2.5 mL/well). The compressive force was applied using a sterile glass disc and a small container with lead granules, as described in previously [92].

4.4.2. Cell Proliferation and Cell Viability

As previously described by Janjic Rankovic et al. [92], a resazurin standard curve was prepared as follows. Cells from the 5th passage were seeded in triplicate (100,000; 200,000; 300,000; 400,000; 600,000; and 800,000 cells per well). "*Percentage reduction of resazurin*" was calculated according to the manufacturer's instructions, and a standard curve (cell number vs. percentage reduction in resazurin) was established using exponential regression (Microsoft Excel for Windows 365 MSO Version 2404, Microsoft Corporation, Redmond, WA, USA) (Figure 6). After the application of force with the WAB method (Section 4.4.1) the compression setup was carefully disassembled, and the resazurin assessment was conducted as described above. The cell number per well was calculated using the prepared standard curve.

Additionally, cell viability was assessed qualitatively using the abovementioned live/dead cell staining kit according to the manufacturer's instructions. After the release of the force and the removal of the resazurin test supernatants, all of the wells were

washed twice with PBS, and microphotographs were captured as previously outlined (Section 4.2)

4.4.3. Sample Preparation for RT-qPCR and ELISA

After 48 h of cellular stimulation, the cell culture supernatants from the respective setup were collected. Afterwards, the adherent cells were washed twice with sterile PBS. Cell lysates were then prepared as explained above (Section 4.3). In between, the collected cell culture supernatants were centrifuged and stored at −80 °C for the ELISA analysis [93].

4.5. Reverse Transcription Quantitative Polymerase Chain Reaction (RT-qPCR)

An analysis of *PTGS2*/*COX2*, *IL6*, *CXCL8*/*IL8*, *RUNX2*, *TNFRSF11B*/*OPG*, *BGLAP*, *CASP3*, *CASP8*, *MAP1LC3A*/*LC3*, and *BECN1* gene expression following H_2O_2 stimulation and/or the application of compressive force was carried out for all experimental groups according to previously described protocols [92,93]. Below is an overview of the sample preparation and quantitative RT-PCR (RT-qPCR) process. Additionally, a checklist according to the "*Minimum Information for Publication of Quantitative Real-Time PCR Experiment*" (MIQE) guidelines [94] is available in Supplementary Table S2.1.

Total RNA preparation and cDNA synthesis: RNA isolation and cDNA synthesis were conducted utilizing the QuickRNA™ MicroPrep Kit (R1051; Zymo, Irvine, CA, USA) and the SuperScript™ IV First-Strand Synthesis System (18091050, Thermo Fisher Scientific, Waltham, MA, USA), respectively, and based on previously published data [92,93].

PCR primer selection: As previously published [92], the primer sequences for all of the genes were sourced from public databases and were tested in silico according to the MIQE guidelines [95] (Supplementary Table S2.1). Unmodified primers were acquired from a commercial source (TIB Molbiol Syntheselabor GmbH, Berlin, Germany). Gradient PCR using the qPCR cycling program as specified in the MIQE checklist was performed to determine the optimal annealing temperatures. The primer specificity was confirmed through agarose gel electrophoresis. To assess the efficiencies of each primer, serial dilutions of cDNA were used to create specific standard curves. These data were then quantified using the LightCycler® 480 with the primer pairs as described in Supplementary File S2.

Reference gene selection: A panel of reference genes (*EEF1A1*, *GAPDH*, *PPIB*, *RNA18SN5*, *RPL0*, *RPL22*, and *YWHAZ*) was selected from public sources [96,97]. cDNA from the experimental groups "Control", "100 µM H_2O_2", "100 µM H_2O_2 + WAB", "50 µM H_2O_2", "50 µM H_2O_2 + WAB", "WAB", "50 µM H_2O_2" (directly after 24 h of stimulation), and "100 µM H_2O_2" (directly after 24 h of stimulation) was used to evaluate the reference genes. Gene-specific primers were then used to conduct RT-qPCR (Supplementary File S2). RefFinder [98,99] was used to analyze the raw Cq values (Supplementary Table S2.2). This web-based tool integrates four different algorithms (BestKeeper [100], NormFinder [101], geNorm [102], and the comparative ΔCt method [103]) to compare and rank candidate reference genes. Based on the rankings, the most stable genes (*RPL22* and *EEF1A1*) were used as the reference genes in RT-qPCR (Figure 8).

Quantitative PCR: The LightCycler® 480 SYBR Green I Master Kit (04887352001; Roche Diagnostics GmbH, Mannheim, Germany) was used to conduct RT-qPCR according to the manufacturer's protocol (5 µL of cDNA (1:10 prediluted) in each PCR reaction). The details are mentioned in the MIQE checklist (Supplementary File S1). The PCR primer specifications are summarized in Table 1.

Gene expression calculation: After averaging (geometric mean) the reference genes (*RPL22* and *EEF1A1*) for a given WAB/H_2O_2 concentration combination, the $2^{-\Delta\Delta Cq}$ method was applied for quantification of the gene expression [102,104]. For each experimental group, six qPCR reactions were analyzed: two technical replicates from each of the three biological replicates (N = 3, n = 6).

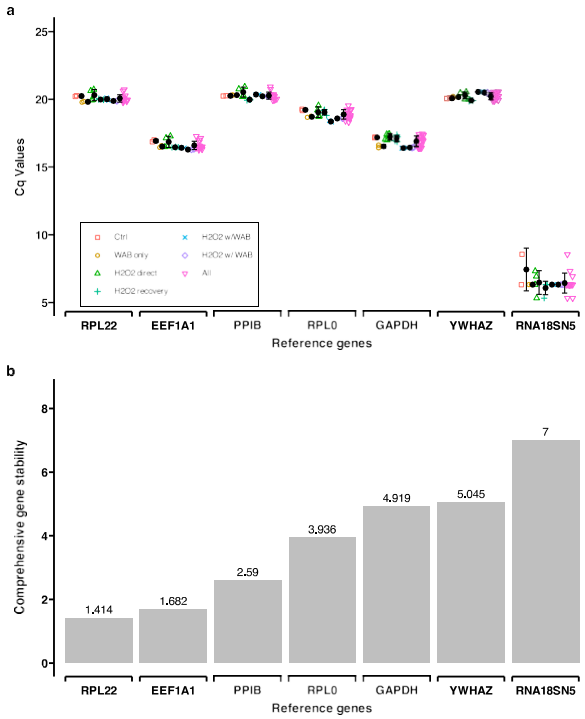

Figure 8. Reference gene selection was undertaken using RefFinder. (**a**) Cq values for the panel of reference genes. Six quantitative polymerase chain reaction (qPCR) runs were analyzed, representing three biological replicates and two technical replicates each (Supplementary Table S2.3). (**b**) Analysis of comprehensive gene stability for the panel of reference genes. Lower values indicate higher gene stability (Supplementary File S2).

Table 1. Specification of the PCR primers used for gene quantification.

Gene	GenBank Accession Number	Primer Sequence (f: 5′-Forward Primer-3′; r: 5′-Reverse Primer-3′)	Annealing Temp. (°C)	Amplicon Size (bp)	Reference
PTGS2/COX2	NM_000963.4	f: AAGCCTTCTCTAACCTCTCC r: GCCCTCGCTTATGATCTGTC	58	234	[92,105]
IL6	NM_000600.5	f: TGGCAGAAAACAACCTGAACC r: TGGCTTGTTCCTCACTACTCTC	58	168	[92,105]
CXCL8/IL8	NM_000584.4	f: CAGAGACAGCAGAGCACACAA r: TTAGCACTCCTTGGCAAAAC	55	170	[106]
RUNX2	NM_001015051.4	f: GCGCATTCCTCATCCCAGTA r: GGCTCAGGTAGGAGGGGTAA	58	176	[92,107]
BGLAP	NM_199173.6	f: AGCGAGGTAGTGAAGAGAC r: GAAAGCCGATGTGGTCAG	64	142	[108]
BECN1	NM_003766.5	f: AGGTTGAGAAAGGCGAGACA r: AATTGTGAGGACACCCAAGC	58	196	[109]
MAP1LC3A/LC3	NM_032514.4	f: CGTCCTGGACAAGACCAAGT r: TCCTCGTCTTTCTCCTGCTC	58	183	[109]
CASP3	NM_004346.4	f: TGGAGGCCGACTTCTTGTAT r: ACTGTTTCAGCATGGCACAA	58	111	[110]
CASP8	NM_001228.5	f: GGAGGAGTTGTGTGGGGTAA r: CCTGCATCCAAGTGTGTTCC	58	207	[111]
TNFRSF11B	NM_002546.4	f: TCAAGCAGGAGTGCAATCG r: AGAATGCCTCCTCACACAGG	64	342	[112]
EEF1A1	NM_001402.6	f: CCTGCCTCTCCAGGATGTCTAC r: GGAGCAAAGGTGACCACCATAC	61	105	[93,97]
PPIB	NM_000942.5	f: TTCCATCGTGTAATCAAGGACTTC r: GCTCACCGTAGATGCTCTTTC	55	88	[93,97]

4.6. Enzyme-Linked Immunosorbent Assay (ELISA)

Cell culture supernatants from all of the wells were collected for ELISA as described. The IL6 and PGE2 concentrations in the cell culture supernatants were determined through ELISA (IL6: DuoSet human IL6 ELISA kit, DY206-05, R&D Systems, Minneapolis, MN, USA; PGE2: PGE2 High-Sensitivity ELISA kit, ADI-931-001, Enzo Life Sciences AG, Lausen, Switzerland) on a Varioscan microplate reader (Thermo Electron Corporation, Vantaa, Finland). Each marker molecule and experimental condition combination was tested in three biological replicates, with each measured twice. The results were reported as "pg per 100,000 cells", using the well-specific cell numbers determined previously.

4.7. Statistics

Descriptive statistics on the gene expression and ELISA results are reported as the mean and standard deviation (SD), median, and minimum/maximum. All of the calculations were based on three biological replicates, with two technical replicates for each gene/experimental condition combination. For each gene locus and marker molecule, differences between the different magnitudes of tensile strain and durations were evaluated using the Kruskal–Wallis test followed by multiple comparisons with Bonferroni correction applied ($p_{adj.}$). All of the statistical procedures were carried out using IBM SPSS Statistics 29 (IBM Corp., Armonk, NY, USA) and were two-tailed, considering $p_{adj.}$ values < 0.05 as significant.

5. Conclusions

The results of this in vitro study not only confirm the catabolic effects of OS but also highlight the prolonged influence of ROS exposure (24 h post-incubation) on the expression of genes that regulate inflammation, bone metabolism, and cell fate in hPDLCs. Furthermore, our findings suggest that ROS alters mechanosensing in hPDLCs during the application of static compression force, directly impacting the expression of these key genes.

This alteration could potentially shift the balance between bone resorption and formation, leading to complications in orthodontic treatment. Understanding these mechanisms is essential for developing personalized treatment options that align with the unique biological characteristics of each patient. Additionally, our study highlights the need to create strategies aiming to reduce OS, thereby enhancing the effectiveness and safety of orthodontic treatments. By addressing these factors, we can improve and ensure more tailored successful orthodontic care, particularly in elderly patients or patients with chronic inflammatory diseases, where ROS levels are known to be elevated.

Supplementary Materials: The following supporting information can be downloaded at https://www.mdpi.com/article/10.3390/ijms252413513/s1.

Author Contributions: Conceptualization, S.H., A.W., U.B. and M.J.R.; methodology, S.H., J.D., M.F., U.B. and M.J.R.; software, U.B.; validation, S.H., M.F., H.S., C.S., A.W., I.F., U.B. and M.J.R.; formal analysis, S.H., U.B. and M.J.R.; investigation, S.H., U.B. and M.J.R.; resources, A.W., U.B., M.F. and M.J.R.; data curation, S.H., U.B. and M.J.R.; writing—original draft preparation, S.H., U.B. and M.J.R.; writing—review and editing, S.H., J.D., M.F., H.S., C.S., A.W., I.F., U.B. and M.J.R.; supervision, M.F., A.W., U.B. and M.J.R.; project administration, U.B. and M.J.R.; funding acquisition, M.J.R. All authors have read and agreed to the published version of the manuscript.

Funding: This study was supported by a grant from the Funding Program for Research and Teaching (FöFoLe; LMU Medical Faculty) to M.J.R. (project number 1155).

Institutional Review Board Statement: This study was conducted according to the guidelines of the Declaration of Helsinki. Approval for the collection and use of hPDLCs was obtained from the ethics committee of the Ludwig-Maximilians-Universität München (project number 045-09; first date of approval: 24 March 2009; latest amendment approved on 23 July 2019).

Informed Consent Statement: Informed consent was obtained from all of the subjects donating bony tissue for the cell isolation used in this study.

Data Availability Statement: All of the authors confirm that all related data supporting the findings of this study are given in the article and its Supplementary Materials.

Acknowledgments: The authors would like to give great thanks to Christine Schreindorfer and Laure Djaleu (both from the Department of Orthodontics, University Hospital, LMU Munich) and Brigitte Hackl (Department of Conservative Dentistry and Periodontology, University Hospital, LMU Munich) for their assistance regarding the lab work.

Conflicts of Interest: The authors declare no conflicts of interest.

Abbreviations

BECN1	Beclin 1
BGLAP	Bone gamma-carboxyglutamate protein
CASP3	Caspase 3
CASP8	Caspase 8
CXCL8/IL8	C-X-C Motif Chemokine Ligand 8 (aka IL8 (interleukin-8))
ELISA	Enzyme-linked immunosorbent assay
FC	Fold change
H_2O_2	Hydrogen peroxide
hPDLCs	Human periodontal ligament cells
IL6	Interleukin 6
MAP1LC3A/LC3	Microtubule-Associated Protein 1 Light Chain 3 Alpha (aka LC3)
MIQE	Minimum Information for Publication of Quantitative Real-Time PCR Experiment
OS	Oxidative stress
OTM	Orthodontic tooth movement
$P_{adj.}$	Adjusted *p*-value
PGE2	Prostaglandin E2
PTGS2/COX2	Prostaglandin Endoperoxide Synthase 2 (aka COX2 (cyclooxygenase 2))
ROS	Reactive oxygen species
RT-qPCR	Reverse transcription quantitative polymerase chain reaction
RUNX2	RUNX Family Transcription Factor 2
TNFRSF11B/OPG	TNF Receptor Superfamily Member 11b (aka OPG (osteoprotegerin))

References

1. Pizzino, G.; Irrera, N.; Cucinotta, M.; Pallio, G.; Mannino, F.; Arcoraci, V.; Squadrito, F.; Altavilla, D.; Bitto, A. Oxidative Stress: Harms and Benefits for Human Health. *Oxid. Med. Cell. Longev.* **2017**, *2017*, 8416763. [CrossRef]
2. Noubiap, J.J.; Sanders, P.; Nattel, S.; Lau, D.H. Biomarkers in Atrial Fibrillation: Pathogenesis and Clinical Implications. *Card. Electrophysiol. Clin.* **2021**, *13*, 221–233. [CrossRef] [PubMed]
3. Checa, J.; Aran, J.M. Reactive Oxygen Species: Drivers of Physiological and Pathological Processes. *J. Inflamm. Res.* **2020**, *13*, 1057–1073. [CrossRef] [PubMed]
4. Iakovou, E.; Kourti, M. A Comprehensive Overview of the Complex Role of Oxidative Stress in Aging, the Contributing Environmental Stressors and Emerging Antioxidant Therapeutic Interventions. *Front. Aging Neurosci.* **2022**, *14*, 827900. [CrossRef]
5. Maldonado, E.; Morales-Pison, S.; Urbina, F.; Solari, A. Aging Hallmarks and the Role of Oxidative Stress. *Antioxidants* **2023**, *12*, 651. [CrossRef] [PubMed]
6. Abdelazim, A.M.; Abomughaid, M.M. Oxidative stress: An overview of past research and future insights. *All Life* **2024**, *17*, 2316092. [CrossRef]
7. Shang, J.; Liu, H.; Zheng, Y.; Zhang, Z. Role of oxidative stress in the relationship between periodontitis and systemic diseases. *Front. Physiol.* **2023**, *14*, 1210449. [CrossRef]
8. Maquera-Huacho, P.M.; Spolidorio, D.P.; Manthey, J.A.; Grenier, D. Eriodictyol Suppresses *Porphyromonas gingivalis*-Induced Reactive Oxygen Species Production by Gingival Keratinocytes and the Inflammatory Response of Macrophages. *Front. Oral Health* **2022**, *3*, 847914. [CrossRef] [PubMed]
9. Tomofuji, T.; Irie, K.; Sanbe, T.; Azuma, T.; Ekuni, D.; Tamaki, N.; Yamamoto, T.; Morita, M. Periodontitis and increase in circulating oxidative stress. *Jpn. Dent. Sci. Rev.* **2009**, *45*, 46–51. [CrossRef]
10. Tothova, L.; Celec, P. Oxidative Stress and Antioxidants in the Diagnosis and Therapy of Periodontitis. *Front. Physiol.* **2017**, *8*, 1055. [CrossRef]

11. Wei, Y.; Fu, J.; Wu, W.; Ma, P.; Ren, L.; Yi, Z.; Wu, J. Quercetin Prevents Oxidative Stress-Induced Injury of Periodontal Ligament Cells and Alveolar Bone Loss in Periodontitis. *Drug Des. Devel. Ther.* **2021**, *15*, 3509–3522. [CrossRef]
12. Chen, Y.; Ji, Y.; Jin, X.; Sun, X.; Zhang, X.; Chen, Y.; Shi, L.; Cheng, H.; Mao, Y.; Li, X.; et al. Mitochondrial abnormalities are involved in periodontal ligament fibroblast apoptosis induced by oxidative stress. *Biochem. Biophys. Res. Commun.* **2019**, *509*, 483–490. [CrossRef]
13. Tao, H.; Ge, G.; Liang, X.; Zhang, W.; Sun, H.; Li, M.; Geng, D. ROS signaling cascades: Dual regulations for osteoclast and osteoblast. *Acta Biochim. Biophys. Sin.* **2020**, *52*, 1055–1062. [CrossRef]
14. Inchingolo, F.; Inchingolo, A.M.; Latini, G.; Ferrante, L.; Trilli, I.; Del Vecchio, G.; Palmieri, G.; Malcangi, G.; Inchingolo, A.D.; Dipalma, G. Oxidative Stress and Natural Products in Orthodontic Treatment: A Systematic Review. *Nutrients* **2023**, *16*, 113. [CrossRef]
15. He, L.; He, T.; Farrar, S.; Ji, L.; Liu, T.; Ma, X. Antioxidants Maintain Cellular Redox Homeostasis by Elimination of Reactive Oxygen Species. *Cell. Physiol. Biochem.* **2017**, *44*, 532–553. [CrossRef] [PubMed]
16. Davidovitch, Z. Tooth movement. *Crit. Rev. Oral Biol. Med.* **1991**, *2*, 411–450. [CrossRef]
17. Janjic, M.; Docheva, D.; Trickovic Janjic, O.; Wichelhaus, A.; Baumert, U. In Vitro Weight-Loaded Cell Models for Understanding Mechanodependent Molecular Pathways Involved in Orthodontic Tooth Movement: A Systematic Review. *Stem Cells Int.* **2018**, *2018*, 3208285. [CrossRef] [PubMed]
18. Funakoshi, M.; Yamaguchi, M.; Asano, M.; Fujita, S.; Kasai, K. Effect of Compression Force on Apoptosis in Human Periodontal Ligament Cells. *J. Hard Tissue Biol.* **2013**, *22*, 41–50. [CrossRef]
19. Yang, Y.; Liu, Q.; Lu, X.; Ma, J.; Mei, D.; Chen, Q.; Zhao, T.; Chen, J. Sanhuang decoction inhibits autophagy of periodontal ligament fibroblasts during orthodontic tooth movement by activating PI3K-Akt-mTOR pathway. *Biomed. Pharmacother.* **2023**, *166*, 115391. [CrossRef]
20. Tan, L.; Cao, Z.; Chen, H.; Xie, Y.; Yu, L.; Fu, C.; Zhao, W.; Wang, Y. Curcumin reduces apoptosis and promotes osteogenesis of human periodontal ligament stem cells under oxidative stress in vitro and in vivo. *Life Sci.* **2021**, *270*, 119125. [CrossRef]
21. Redza-Dutordoir, M.; Averill-Bates, D.A. Activation of apoptosis signalling pathways by reactive oxygen species. *Biochim. Biophys. Acta* **2016**, *1863*, 2977–2992. [CrossRef]
22. de Almeida, A.; de Oliveira, J.; da Silva Pontes, L.V.; de Souza Junior, J.F.; Goncalves, T.A.F.; Dantas, S.H.; de Almeida Feitosa, M.S.; Silva, A.O.; de Medeiros, I.A. ROS: Basic Concepts, Sources, Cellular Signaling, and its Implications in Aging Pathways. *Oxid. Med. Cell. Longev.* **2022**, *2022*, 1225578. [CrossRef] [PubMed]
23. Cavalla, F.; Osorio, C.; Paredes, R.; Valenzuela, M.A.; Garcia-Sesnich, J.; Sorsa, T.; Tervahartiala, T.; Hernandez, M. Matrix metalloproteinases regulate extracellular levels of SDF-1/CXCL12, IL-6 and VEGF in hydrogen peroxide-stimulated human periodontal ligament fibroblasts. *Cytokine* **2015**, *73*, 114–121. [CrossRef] [PubMed]
24. Chen, H.; Huang, X.; Fu, C.; Wu, X.; Peng, Y.; Lin, X.; Wang, Y. Recombinant Klotho Protects Human Periodontal Ligament Stem Cells by Regulating Mitochondrial Function and the Antioxidant System during H_2O_2-Induced Oxidative Stress. *Oxid. Med. Cell. Longev.* **2019**, *2019*, 9261565. [CrossRef]
25. Costa, F.P.D.; Puty, B.; Nogueira, L.S.; Mitre, G.P.; Santos, S.M.D.; Teixeira, B.J.B.; Kataoka, M.; Martins, M.D.; Barboza, C.A.G.; Monteiro, M.C.; et al. Piceatannol Increases Antioxidant Defense and Reduces Cell Death in Human Periodontal Ligament Fibroblast under Oxidative Stress. *Antioxidants* **2019**, *9*, 16. [CrossRef]
26. Kuang, Y.; Hu, B.; Feng, G.; Xiang, M.; Deng, Y.; Tan, M.; Li, J.; Song, J. Metformin prevents against oxidative stress-induced senescence in human periodontal ligament cells. *Biogerontology* **2020**, *21*, 13–27. [CrossRef] [PubMed]
27. Liu, Y.; Yang, H.; Wen, Y.; Li, B.; Zhao, Y.; Xing, J.; Zhang, M.; Chen, Y. Nrf2 Inhibits Periodontal Ligament Stem Cell Apoptosis under Excessive Oxidative Stress. *Int. J. Mol. Sci.* **2017**, *18*, 1076. [CrossRef]
28. Ueno, T.; Yamada, M.; Igarashi, Y.; Ogawa, T. *N*-acetyl cysteine protects osteoblastic function from oxidative stress. *J. Biomed. Mater. Res. A* **2011**, *99*, 523–531. [CrossRef] [PubMed]
29. Yang, L.; Yang, Y.; Wang, S.; Li, Y.; Zhao, Z. In vitro mechanical loading models for periodontal ligament cells: From two-dimensional to three-dimensional models. *Arch. Oral Biol.* **2015**, *60*, 416–424. [CrossRef]
30. Kanai, K. Initial effects of continuously applied compressive stress to human periodontal ligament fibroblasts. *J. Jpn. Orthod. Soc.* **1992**, *51*, 153–163.
31. Marchesan, J.T.; Scanlon, C.S.; Soehren, S.; Matsuo, M.; Kapila, Y.L. Implications of cultured periodontal ligament cells for the clinical and experimental setting: A review. *Arch. Oral Biol.* **2011**, *56*, 933–943. [CrossRef] [PubMed]
32. Lekic, P.; McCulloch, C.A. Periodontal ligament cell population: The central role of fibroblasts in creating a unique tissue. *Anat. Rec.* **1996**, *245*, 327–341. [CrossRef]
33. Chen, Y.J.; Shie, M.Y.; Hung, C.J.; Wu, B.C.; Liu, S.L.; Huang, T.H.; Kao, C.T. Activation of focal adhesion kinase induces extracellular signal-regulated kinase-mediated osteogenesis in tensile force-subjected periodontal ligament fibroblasts but not in osteoblasts. *J. Bone Miner. Metab.* **2014**, *32*, 671–682. [CrossRef]
34. Roguljic, H.; Matthews, B.G.; Yang, W.; Cvija, H.; Mina, M.; Kalajzic, I. In vivo identification of periodontal progenitor cells. *J. Dent. Res.* **2013**, *92*, 709–715. [CrossRef]
35. Vo, T.T.T.; Chu, P.M.; Tuan, V.P.; Te, J.S.; Lee, I.T. The Promising Role of Antioxidant Phytochemicals in the Prevention and Treatment of Periodontal Disease via the Inhibition of Oxidative Stress Pathways: Updated Insights. *Antioxidants* **2020**, *9*, 1211. [CrossRef] [PubMed]

36. Sui, L.; Wang, J.; Xiao, Z.; Yang, Y.; Yang, Z.; Ai, K. ROS-Scavenging Nanomaterials to Treat Periodontitis. *Front. Chem.* **2020**, *8*, 595530. [CrossRef]
37. Yucel-Lindberg, T.; Båge, T. Inflammatory mediators in the pathogenesis of periodontitis. *Expert Rev. Mol. Med.* **2013**, *15*, e7. [CrossRef]
38. Nokhbehsaim, M.; Nogueira, A.V.B.; Nietzsche, S.; Eick, S.; Deschner, J. Regulation of Cyclooxygenase 2 by *Filifactor alocis* in Fibroblastic and Monocytic Cells. *Mediators Inflamm.* **2020**, *2020*, 4185273. [CrossRef]
39. Morton, R.S.; Dongari-Bagtzoglou, A.I. Cyclooxygenase-2 is upregulated in inflamed gingival tissues. *J. Periodontol.* **2001**, *72*, 461–469. [CrossRef]
40. Irwin, C.R.; Myrillas, T.T. The role of IL-6 in the pathogenesis of periodontal disease. *Oral Dis.* **1998**, *4*, 43–47. [CrossRef]
41. Mazurek-Mochol, M.; Bonsmann, T.; Mochol, M.; Poniewierska-Baran, A.; Pawlik, A. The Role of Interleukin 6 in Periodontitis and Its Complications. *Int. J. Mol. Sci.* **2024**, *25*, 2146. [CrossRef]
42. Finoti, L.S.; Nepomuceno, R.; Pigossi, S.C.; Corbi, S.C.; Secolin, R.; Scarel-Caminaga, R.M. Association between interleukin-8 levels and chronic periodontal disease: A PRISMA-compliant systematic review and meta-analysis. *Medicine* **2017**, *96*, e6932. [CrossRef]
43. Uematsu, S.; Mogi, M.; Deguchi, T. Interleukin (IL)-1ß, IL-6, tumor necrosis factor-↵, epidermal growth factor, and ß2-microglobulin levels are elevated in gingival crevicular fluid during human orthodontic tooth movement. *J. Dent. Res.* **1996**, *75*, 562–567. [CrossRef]
44. Kunii, R.; Yamaguchi, M.; Tanimoto, Y.; Asano, M.; Yamada, K.; Goseki, T.; Kasai, K. Role of interleukin-6 in orthodontically induced inflammatory root resorption in humans. *Korean J. Orthod.* **2013**, *43*, 294–301. [CrossRef]
45. Lennicke, C.; Rahn, J.; Lichtenfels, R.; Wessjohann, L.A.; Seliger, B. Hydrogen peroxide—Production, fate and role in redox signaling of tumor cells. *Cell Commun. Signal.* **2015**, *13*, 39. [CrossRef]
46. Lee, Y.S.; Bak, E.J.; Kim, M.; Park, W.; Seo, J.T.; Yoo, Y.J. Induction of IL-8 in periodontal ligament cells by H_2O_2. *J. Microbiol.* **2008**, *46*, 579–584. [CrossRef]
47. Marciniak, J.; Lossdörfer, S.; Kirschneck, C.; Deschner, J.; Jäger, A.; Wolf, M. Heat shock protein 70 dampens the inflammatory response of human PDL cells to mechanical loading in vitro. *J. Periodontal Res.* **2019**, *54*, 481–488. [CrossRef] [PubMed]
48. Brockhaus, J.; Craveiro, R.B.; Azraq, I.; Niederau, C.; Schröder, S.K.; Weiskirchen, R.; Jankowski, J.; Wolf, M. In Vitro Compression Model for Orthodontic Tooth Movement Modulates Human Periodontal Ligament Fibroblast Proliferation, Apoptosis and Cell Cycle. *Biomolecules* **2021**, *11*, 932. [CrossRef]
49. Marciniak, J.; Lossdörfer, S.; Knaup, I.; Bastian, A.; Craveiro, R.B.; Jäger, A.; Wolf, M. Orthodontic cell stress modifies proinflammatory cytokine expression in human PDL cells and induces immunomodulatory effects via TLR-4 signaling in vitro. *Clin. Oral Investig.* **2020**, *24*, 1411–1419. [CrossRef] [PubMed]
50. Roth, C.E.; Craveiro, R.B.; Niederau, C.; Malyaran, H.; Neuss, S.; Jankowski, J.; Wolf, M. Mechanical Compression by Simulating Orthodontic Tooth Movement in an In Vitro Model Modulates Phosphorylation of AKT and MAPKs via TLR4 in Human Periodontal Ligament Cells. *Int. J. Mol. Sci.* **2022**, *23*, 8062. [CrossRef] [PubMed]
51. Proff, P.; Reicheneder, C.; Faltermeier, A.; Kubein-Meesenburg, D.; Römer, P. Effects of mechanical and bacterial stressors on cytokine and growth-factor expression in periodontal ligament cells. *J. Orofac. Orthop.* **2014**, *75*, 191–202. [CrossRef] [PubMed]
52. Kang, Y.G.; Nam, J.H.; Kim, K.H.; Lee, K.S. FAK pathway regulates PGE_2 production in compressed periodontal ligament cells. *J. Dent. Res.* **2010**, *89*, 1444–1449. [CrossRef]
53. Kanzaki, H.; Chiba, M.; Shimizu, Y.; Mitani, H. Periodontal ligament cells under mechanical stress induce osteoclastogenesis by receptor activator of nuclear factor ⍰B ligand up-regulation via prostaglandin E_2 synthesis. *J. Bone Miner. Res.* **2002**, *17*, 210–220. [CrossRef] [PubMed]
54. Kirschneck, C.; Proff, P.; Maurer, M.; Reicheneder, C.; Römer, P. Orthodontic forces add to nicotine-induced loss of periodontal bone: An in vivo and in vitro study. *J. Orofac. Orthop.* **2015**, *76*, 195–212. [CrossRef] [PubMed]
55. Mayahara, K.; Yamaguchi, A.; Sakaguchi, M.; Igarashi, Y.; Shimizu, N. Effect of Ga-Al-As laser irradiation on *COX-2* and *cPLA$_2$-α* expression in compressed human periodontal ligament cells. *Lasers Surg. Med.* **2010**, *42*, 489–493. [CrossRef]
56. Wang, C.; Yang, Q.; Han, Y.; Liu, H.; Wang, Y.; Huang, Y.; Zheng, Y.; Li, W. A reduced level of the long non-coding RNA SNHG8 activates the NF-kappaB pathway by releasing functional HIF-1alpha in a hypoxic inflammatory microenvironment. *Stem Cell Res. Ther.* **2022**, *13*, 229. [CrossRef]
57. Spitz, A.; Christovam, I.O.; Marañón-Vásquez, G.A.; Masterson, D.F.; Adesse, D.; Maia, L.C.; Bolognese, A.M. Global gene expression profile of periodontal ligament cells submitted to mechanical loading: A systematic review. *Arch. Oral Biol.* **2020**, *118*, 104884. [CrossRef] [PubMed]
58. Ducy, P.; Zhang, R.; Geoffroy, V.; Ridall, A.L.; Karsenty, G. Osf2/Cbfa1: A transcriptional activator of osteoblast differentiation. *Cell* **1997**, *89*, 747–754. [CrossRef] [PubMed]
59. Karsenty, G. Role of Cbfa1 in osteoblast differentiation and function. *Semin. Cell Dev. Biol.* **2000**, *11*, 343–346. [CrossRef] [PubMed]
60. Komori, T. Whole Aspect of Runx2 Functions in Skeletal Development. *Int. J. Mol. Sci.* **2022**, *23*, 5776. [CrossRef] [PubMed]
61. Patti, A.; Gennari, L.; Merlotti, D.; Dotta, F.; Nuti, R. Endocrine actions of osteocalcin. *Int. J. Endocrinol.* **2013**, *2013*, 846480. [CrossRef] [PubMed]

62. Domazetovic, V.; Marcucci, G.; Iantomasi, T.; Brandi, M.L.; Vincenzini, M.T. Oxidative stress in bone remodeling: Role of antioxidants. *Clin. Cases Miner. Bone Metab.* **2017**, *14*, 209–216. [CrossRef]
63. Lee, S.Y.; Yoo, H.I.; Kim, S.H. CCR5-CCL Axis in PDL during Orthodontic Biophysical Force Application. *J. Dent. Res.* **2015**, *94*, 1715–1723. [CrossRef]
64. Huang, Y.; Zhang, Y.; Li, X.; Liu, H.; Yang, Q.; Jia, L.; Zheng, Y.; Li, W. The long non-coding RNA landscape of periodontal ligament stem cells subjected to compressive force. *Eur. J. Orthod.* **2019**, *41*, 333–342. [CrossRef]
65. Kanzaki, H.; Wada, S.; Narimiya, T.; Yamaguchi, Y.; Katsumata, Y.; Itohiya, K.; Fukaya, S.; Miyamoto, Y.; Nakamura, Y. Pathways that Regulate ROS Scavenging Enzymes, and Their Role in Defense Against Tissue Destruction in Periodontitis. *Front. Physiol.* **2017**, *8*, 351. [CrossRef]
66. Schröder, A.; Stumpf, J.; Paddenberg, E.; Neubert, P.; Schatz, V.; Köstler, J.; Jantsch, J.; Deschner, J.; Proff, P.; Kirschneck, C. Effects of mechanical strain on periodontal ligament fibroblasts in presence of *Aggregatibacter actinomycetemcomitans* lysate. *BMC Oral Health* **2021**, *21*, 405. [CrossRef]
67. Chen, L.; Mo, S.; Hua, Y. Compressive force-induced autophagy in periodontal ligament cells downregulates osteoclastogenesis during tooth movement. *J. Periodontol.* **2019**, *90*, 1170–1181. [CrossRef]
68. Odagaki, N.; Ishihara, Y.; Wang, Z.; Ei Hsu Hlaing, E.; Nakamura, M.; Hoshijima, M.; Hayano, S.; Kawanabe, N.; Kamioka, H. Role of Osteocyte-PDL Crosstalk in Tooth Movement via SOST/Sclerostin. *J. Dent. Res.* **2018**, *97*, 1374–1382. [CrossRef] [PubMed]
69. Küchler, E.C.; Schröder, A.; Teodoro, V.B.; Nazet, U.; Scariot, R.; Spanier, G.; Proff, P.; Kirschneck, C. The role of 25-hydroxyvitamin-D3 and vitamin D receptor gene in human periodontal ligament fibroblasts as response to orthodontic compressive strain: An in vitro study. *BMC Oral Health* **2021**, *21*, 386. [CrossRef] [PubMed]
70. An, Y.; Liu, W.; Xue, P.; Zhang, Y.; Wang, Q.; Jin, Y. Increased autophagy is required to protect periodontal ligament stem cells from apoptosis in inflammatory microenvironment. *J. Clin. Periodontol.* **2016**, *43*, 618–625. [CrossRef]
71. Jiang, N.; He, D.; Ma, Y.; Su, J.; Wu, X.; Cui, S.; Li, Z.; Zhou, Y.; Yu, H.; Liu, Y. Force-Induced Autophagy in Periodontal Ligament Stem Cells Modulates M1 Macrophage Polarization via AKT Signaling. *Front. Cell Dev. Biol.* **2021**, *9*, 666631. [CrossRef]
72. Hatai, T.; Yokozeki, M.; Funato, N.; Baba, Y.; Moriyama, K.; Ichijo, H.; Kuroda, T. Apoptosis of periodontal ligament cells induced by mechanical stress during tooth movement. *Oral Dis.* **2001**, *7*, 287–290. [CrossRef]
73. Zhu, L.; Xie, H.; Liu, Q.; Ma, F.; Wu, H. Klotho inhibits H_2O_2-induced oxidative stress and apoptosis in periodontal ligament stem cells by regulating UCP2 expression. *Clin. Exp. Pharmacol. Physiol.* **2021**, *48*, 1412–1420. [CrossRef] [PubMed]
74. Chifenti, B.; Locci, M.T.; Lazzeri, G.; Guagnozzi, M.; Dinucci, D.; Chiellini, F.; Filice, M.E.; Salerno, M.G.; Battini, L. Autophagy-related protein LC3 and Beclin-1 in the first trimester of pregnancy. *Clin. Exp. Reprod. Med.* **2013**, *40*, 33–37. [CrossRef] [PubMed]
75. Zhao, Y.; Liu, H.; Xi, X.; Chen, S.; Liu, D. TRIM16 protects human periodontal ligament stem cells from oxidative stress-induced damage via activation of PICOT. *Exp. Cell Res.* **2020**, *397*, 112336. [CrossRef]
76. Li, B.; Shi, Y.; Fu, Y. Apocynin inhibits compressive force-induced apoptosis and autophagy of periodontal ligament stem cells. *Oral Dis.* **2023**, *29*, 2837–2844. [CrossRef]
77. Ransy, C.; Vaz, C.; Lombès, A.; Bouillaud, F. Use of H_2O_2 to Cause Oxidative Stress, the Catalase Issue. *Int. J. Mol. Sci.* **2020**, *21*, 9149. [CrossRef] [PubMed]
78. Dahiya, P.; Kamal, R.; Gupta, R.; Bhardwaj, R.; Chaudhary, K.; Kaur, S. Reactive oxygen species in periodontitis. *J. Indian Soc. Periodontol.* **2013**, *17*, 411–416. [CrossRef]
79. Yu, J.Y.; Lee, S.Y.; Son, Y.O.; Shi, X.; Park, S.S.; Lee, J.C. Continuous presence of H_2O_2 induces mitochondrial-mediated, MAPK- and caspase-independent growth inhibition and cytotoxicity in human gingival fibroblasts. *Toxicol. Vitr.* **2012**, *26*, 561–570. [CrossRef]
80. Castro, M.F.d.; Chami, Y.M.T.; Oliveira, J.d.; Perozini, C.; Sendyk, W.R.; Koga-Ito, C.Y.; Pallos, D.; Tanaka, M.H. Comparative Evaluation of Hydrogen Peroxide Levels in Patients with Periodontal Disease and Healthy Individuals–Pilot Study. *J. Adv. Med. Med. Res.* **2024**, *36*, 135–142. [CrossRef]
81. Blazquez-Castro, A.; Stockert, J.C. In vitro human cell responses to a low-dose photodynamic treatment vs. mild H_2O_2 exposure. *J. Photochem. Photobiol. B* **2015**, *143*, 12–19. [CrossRef] [PubMed]
82. Goffart, S.; Tikkanen, P.; Michell, C.; Wilson, T.; Pohjoismäki, J. The Type and Source of Reactive Oxygen Species Influences the Outcome of Oxidative Stress in Cultured Cells. *Cells* **2021**, *10*, 1075. [CrossRef] [PubMed]
83. Kapałczyńska, M.; Kolenda, T.; Przybyła, W.; Zaja̧czkowska, M.; Teresiak, A.; Filas, V.; Ibbs, M.; Bliz´niak, R.; Łuczewski, Ł.; Lamperska, K. 2D and 3D cell cultures – A comparison of different types of cancer cell cultures. *Arch. Med. Sci.* **2018**, *14*, 910–919. [CrossRef] [PubMed]
84. Yue, B. Biology of the extracellular matrix: An overview. *J. Glaucoma* **2014**, *23*, S20–S23. [CrossRef] [PubMed]
85. Frantz, C.; Stewart, K.M.; Weaver, V.M. The extracellular matrix at a glance. *J. Cell Sci.* **2010**, *123*, 4195–4200. [CrossRef]
86. Zhao, C. Cell culture: In vitro model system and a promising path to in vivo applications. *J. Histotechnol.* **2023**, *46*, 1–4. [CrossRef] [PubMed]
87. Kang, R.; Zeh, H.J.; Lotze, M.T.; Tang, D. The Beclin 1 network regulates autophagy and apoptosis. *Cell Death Differ.* **2011**, *18*, 571–580. [CrossRef] [PubMed]

88. Mizushima, N.; Yoshimori, T. How to interpret LC3 immunoblotting. *Autophagy* **2007**, *3*, 542–545. [CrossRef]
89. Klionsky, D.J.; Abdel-Aziz, A.K.; Abdelfatah, S.; Abdellatif, M.; Abdoli, A.; Abel, S.; Abeliovich, H.; Abildgaard, M.H.; Abudu, Y.P.; Acevedo-Arozena, A.; et al. Guidelines for the use and interpretation of assays for monitoring autophagy (4th edition). *Autophagy* **2021**, *17*, 1–382.
90. Kyrylkova, K.; Kyryachenko, S.; Leid, M.; Kioussi, C. Detection of apoptosis by TUNEL assay. *Methods Mol. Biol.* **2012**, *887*, 41–47. [PubMed]
91. Somerman, M.J.; Archer, S.Y.; Imm, G.R.; Foster, R.A. A comparative study of human periodontal ligament cells and gingival fibroblasts in vitro. *J. Dent. Res.* **1988**, *67*, 66–70. [CrossRef]
92. Janjic Rankovic, M.; Docheva, D.; Wichelhaus, A.; Baumert, U. Effect of static compressive force on in vitro cultured PDL fibroblasts: Monitoring of viability and gene expression over 6 days. *Clin. Oral Investig.* **2020**, *24*, 2497–2511. [CrossRef] [PubMed]
93. Sun, C.; Janjic Rankovic, M.; Folwaczny, M.; Stocker, T.; Otto, S.; Wichelhaus, A.; Baumert, U. Effect of Different Parameters of In Vitro Static Tensile Strain on Human Periodontal Ligament Cells Simulating the Tension Side of Orthodontic Tooth Movement. *Int. J. Mol. Sci.* **2022**, *23*, 1525. [CrossRef] [PubMed]
94. Bustin, S.A.; Beaulieu, J.F.; Huggett, J.; Jaggi, R.; Kibenge, F.S.; Olsvik, P.A.; Penning, L.C.; Toegel, S. MIQE précis: Practical implementation of minimum standard guidelines for fluorescence-based quantitative real-time PCR experiments. *BMC Mol. Biol.* **2010**, *11*, 74. [CrossRef]
95. Bustin, S.A.; Benes, V.; Garson, J.A.; Hellemans, J.; Huggett, J.; Kubista, M.; Mueller, R.; Nolan, T.; Pfaffl, M.W.; Shipley, G.L.; et al. The MIQE Guidelines: *M*inimum *I*nformation for Publication of *Q*uantitative Real-Time PCR *E*xperiments. *Clin. Chem.* **2009**, *55*, 611–622. [CrossRef]
96. Chirieleison, S.M.; Marsh, R.A.; Kumar, P.; Rathkey, J.K.; Dubyak, G.R.; Abbott, D.W. Nucleotide-binding oligomerization domain (NOD) signaling defects and cell death susceptibility cannot be uncoupled in X-linked inhibitor of apoptosis (XIAP)-driven inflammatory disease. *J. Biol. Chem.* **2017**, *292*, 9666–9679. [CrossRef]
97. Nazet, U.; Schröder, A.; Spanier, G.; Wolf, M.; Proff, P.; Kirschneck, C. Simplified method for applying static isotropic tensile strain in cell culture experiments with identification of valid RT-qPCR reference genes for PDL fibroblasts. *Eur. J. Orthod.* **2020**, *42*, 359–370. [CrossRef] [PubMed]
98. Xie, F.; Xiao, P.; Chen, D.; Xu, L.; Zhang, B. miRDeepFinder: A miRNA analysis tool for deep sequencing of plant small RNAs. *Plant Mol. Biol.* **2012**, *80*, 75–84. [CrossRef]
99. RefFinder. Available online: https://www.ciidirsinaloa.com.mx/RefFinder-master/ (accessed on 7 November 2024).
100. Pfaffl, M.W.; Tichopad, A.; Prgomet, C.; Neuvians, T.P. Determination of stable housekeeping genes, differentially regulated target genes and sample integrity: BestKeeper—Excel-based tool using pair-wise correlations. *Biotechnol. Lett.* **2004**, *26*, 509–515. [CrossRef]
101. Andersen, C.L.; Jensen, J.L.; Ørntoft, T.F. Normalization of real-time quantitative reverse transcription-PCR data: A model-based variance estimation approach to identify genes suited for normalization, applied to bladder and colon cancer data sets. *Cancer Res.* **2004**, *64*, 5245–5250. [CrossRef] [PubMed]
102. Vandesompele, J.; De Preter, K.; Pattyn, F.; Poppe, B.; Van Roy, N.; De Paepe, A.; Speleman, F. Accurate normalization of real-time quantitative RT-PCR data by geometric averaging of multiple internal control genes. *Genome Biol.* **2002**, *3*, 00341–003411. [CrossRef] [PubMed]
103. Silver, N.; Best, S.; Jiang, J.; Thein, S.L. Selection of housekeeping genes for gene expression studies in human reticulocytes using real-time PCR. *BMC Mol. Biol.* **2006**, *7*, 33. [CrossRef]
104. Livak, K.J.; Schmittgen, T.D. Analysis of relative gene expression data using real-time quantitative PCR and the 2^{-DDC}T Method. *Methods* **2001**, *25*, 402–408. [CrossRef] [PubMed]
105. Shi, J.; Baumert, U.; Folwaczny, M.; Wichelhaus, A. Influence of static forces on the expression of selected parameters of inflammation in periodontal ligament cells and alveolar bone cells in a co-culture in vitro model. *Clin. Oral Investig.* **2019**, *23*, 2617–2628. [CrossRef] [PubMed]
106. Jones, R.L.; Hannan, N.J.; Kaitu'u, T.J.; Zhang, J.; Salamonsen, L.A. Identification of chemokines important for leukocyte recruitment to the human endometrium at the times of embryo implantation and menstruation. *J. Clin. Endocrinol. Metab.* **2004**, *89*, 6155–6167. [CrossRef] [PubMed]
107. Shi, J.; Folwaczny, M.; Wichelhaus, A.; Baumert, U. Differences in *RUNX2* and *P2RX7* gene expression between mono- and coculture of human periodontal ligament cells and human osteoblasts under compressive force application. *Orthod. Craniofac. Res.* **2019**, *22*, 168–176. [CrossRef]
108. Gartland, A.; Buckley, K.A.; Dillon, J.P.; Curran, J.M.; Hunt, J.A.; Gallagher, J.A. Isolation and culture of human osteoblasts. *Methods Mol. Med.* **2005**, *107*, 29–54.
109. Zhuang, H.; Hu, D.; Singer, D.; Walker, J.V.; Nisr, R.B.; Tieu, K.; Ali, K.; Tredwin, C.; Luo, S.; Ardu, S.; et al. Local anesthetics induce autophagy in young permanent tooth pulp cells. *Cell Death Discov.* **2015**, *1*, 15024. [CrossRef]
110. Wang, Y.; Du, C.; Wan, W.; He, C.; Wu, S.; Wang, T.; Wang, F.; Zou, R. shRNA knockdown of integrin-linked kinase on hPDLCs migration, proliferation, and apoptosis under cyclic tensile stress. *Oral Dis.* **2020**, *26*, 1747–1754. [CrossRef] [PubMed]

111. Cao, Z.; Zhang, H.; Cai, X.; Fang, W.; Chai, D.; Wen, Y.; Chen, H.; Chu, F.; Zhang, Y. Luteolin Promotes Cell Apoptosis by Inducing Autophagy in Hepatocellular Carcinoma. *Cell. Physiol. Biochem.* **2017**, *43*, 1803–1812. [CrossRef]
112. Yang, Y.; Yang, Y.; Li, X.; Cui, L.; Fu, M.; Rabie, A.B.; Zhang, D. Functional analysis of core binding factor a1 and its relationship with related genes expressed by human periodontal ligament cells exposed to mechanical stress. *Eur. J. Orthod.* **2010**, *32*, 698–705. [CrossRef]

Supplement 1 to manuscript

"Investigation of Oxidative Stress Impact on Human Periodontal Ligament Cells Exposed to Static Compression"

Contents

Supplementary Table S2.1: MIQE checklist for the RT-qPCR workflow

Reference: Bustin et al. (2010). BMC Mol Biol; 11:74.

	Details	Checklist
Sample/Template		
Source	If cancer, was biopsy screened for adjacent normal tissue?	Human alveolar-bone derived osteoblasts (hOBs) were obtained anonymously from a male donor undergoing a surgical procedure based orthodontic treatment and isolated according to established procedures (Somerman et al. 1988).
Method of preservation	Liquid N2/RNAlater/formalin	Cell lysates were snap frozen in liquid N2 and stored at -80°C until all samples were collected.
Storage time (if appropriate)	If using samples >6 months old	Not applicable.
Handling	Fresh/frozen/formalin	Cell lysates were prepared using RNA lysis buffer from Quick-RNA™ MicroPrep kit (R1051; Zymo). They were snap-frozen in liquid nitrogen, and then stored at -80°C until further use for RNA extraction.
Extraction method	TriZol/columns	Defrosted cells lysates were passed through QIAshredder™ columns (Qiagen) to shear genomic DNA. The Quick-RNA™ Miniprep Kit (Zymo) was used for further RNA purification. After primary column purification, DNase I digestion was applied to reduce genomic DNA contamination as described by the manufacturer (Zymo). Finally, DNase/RNase-free water was used to elute the RNA from the columns. Before storage in the -80°C, RNase inhibitor RNasin® (Promega) was added to each preparation.
RNA: DNA-free	Intron-spanning primers/no RT control	Most primers were intron-spanning (Supplementary Table 2.2). Treatment with QIAshredder™ columns (Qiagen) and DNase I digestion were applied to reduce genomic DNA contamination according to the manufacturer's instructions (Zymo).
Concentration	Nanodrop/ribogreen/microfluidics	Purity and concentration of extracted RNA were detected photometrically (Nanodrop ND-1000; PeqLab). Ratio of $A_{260/280}$>1.8 was found, indicating free of protein contamination during RNA preparations.
RNA: integrity	Microfluidics/3':5' assay	No.
Inhibition-free	Method of testing	Serial dilution of cDNA as shown in “Primer efficiency” in Supplementary Table S2.3 below.
Assay optimisation/validation		
Accession number	RefSeq XX_1234567	Table 1 in the manuscript and Supplementary Table S2.2.

	Details	Checklist
Amplicon details	Exon location, amplicon size	Supplementary Table S2.2
Primer sequence	Even if previously published	Table 3 in the manuscript; Supplementary Tables S2.2 and S2.3.
*Probe sequence**	Identify LNA or other substitutions	No probes were used.
In silico	BLAST/Primer-BLAST/m-fold	Primer-BLAST, UCSC In-Silico PCR, and ENSEMBL were used for *in silico* testing.
empirical	Primer concentration/annealing temperature	The optimal annealing temperatures were first identified by gradient PCR (TProfessional Gradient; Biometra, Goettingen, Germany) and then were finalized by qPCR on Roche LightCycler® 480 (LC480). Optimal annealing temperatures are recorded in Supplementary Table S2.3 below.
Priming conditions	Oligo-dT/random/combination/target-specific	The SuperScript® IV First Strand Synthesis System (Invitrogen) was used for cDNA synthesis with random hexamers provided. For each cDNA synthesis reaction, 600 ng total RNA was used. Target-specific primers for qPCR were used after assessment (Table 1 of the manuscript; Supplementary Table S2.3).
PCR efficiency	Dilution curve	Information on serial dilutions and primer efficiency was summarized in Supplementary Table S2.3. For each gene, two technical replicates were used for each dilution for qPCR. For analysis of qPCR including the standard curves, LC480 software version 1.5.0.39 was used.
Linear dynamic range	Spanning unknown targets	The analyzing software for qPCR appointed the linear dynamic range automatically.
Limits of detection	LOD detection/accurate quantification	The analyzing software for qPCR appointed the LOD automatically.
Intra-assay variation	Copy numbers not Cq	Each gene was detected on one individual plate.
RT/PCR		
Protocols	Detailed description, concentrations, volumes	For real-time PCR, LightCycler® 480 SYBR Green I Master kit (04887352001; Roche Diagnostics GmbH, Mannheim, Germany) was used to detect gene expression of PTGS2/COX2, IL6, CXCL8/IL8, RUNX2, CASP3, CASP8, MAP1LC3A/LC3, BECN1, TNFRSF11B/OPG and BGLAP using the LightCycler® 480 with LC480 software version 1.5.0.39 (both from Roche Molecular Diagnostics, Basel, Switzerland). According to the manufacturer' protocol, 5 µl diluted cDNA (1:10 with double distilled, sterile water), 1 µl gene-specific forward primer, 1 µl gene-specific reverse primers, 3 µl PCR water and 10 µl qPCR mastermix were added for reaction. PCR reactions proceeded as follows: 10 min of initial denaturation at 95 °C and 45 cycles of amplifications. Each amplification consisted of three steps: 15 s of denaturation at 95 °C, 15 s of specific annealing temperature for each primer pair and 15 s of elongation at 72 °C.

	Details	Checklist
Reagents	Supplier, Lot number	Primers for genes were synthesized using sequences from related literatures. The primers were verified by *in silico* tests using related bioinformatic tools given in **Supplementary Table S2.2**. All primers were synthesized by TIB Molbiol Syntheselabor GmbH (Berlin, Germany). Information on the kits used (Quick-RNA™ MicroPrep kit; SuperScript® IV First Strand Synthesis kit, Invitrogen; LightCycler® 480 SYBR Green I Master kit, Roche) were all given in the manuscript.
Duplicate RT	ΔCq	No, but two technical replicates were repeated for each biological replicate at minimum.
NTC	Cq & melt curves	Yes
NAC	ΔCq beginning:end of qPCR	No, as no probes were used.
Positive control	Inter-run calibrators	No, each gene was tested on one plate with all samples included.
Data analysis		
Specialist software	e.g., QBAsePlus	IBM SPSS Statistics 29 (IBM Corp., Armonk, NY, USA)
Statistical justification	e.g., biological replicates	For each force magnitude for every force duration, three biological replicates were used. Each biological replicate was repeated with two technical replicates, giving a total of 6 amplifications of qPCR.
Transparent, validated normalization	e.g., GeNorm summary	After testing with RT-qPCR using cDNA from some samples and assessment with RefFinder, *RPL22* and *EEF1A1* were proved to be most stable in this experiment among the panel of reference genes. Therefore, *RPL22* and *EEF1A1* were used as reference genes for following analysis.

Supplementary Table S2.2: *In-silico* analysis of the RT-qPCR primer

Official gene symbol	**Reference sequence** (NCBI GenBank)	**5'-forward primer-3'** (length / T_m / %GC / Self-comp./Self-3'-comp.)	**5'-reverse primer-3'** (length / T_m / %GC / Self-comp./Self-3'-comp.)	**Amplicon length (bp)**	**Amplicon location** (bp of Start/Stop)	**Intron spanning** (length, bp)	**In silico qPCR specificity**	**Variants targeted** (Transcript/ Splice)	**Reference**
Genes of interest									
PTGS2	NM_000963.4	AAGCCTTCTCTAACCTCTCC (20 / 55.9°C / 50% / 5/0)	GCCCTCGCTTATGATCTGTC (20 / 58.2°C / 55% / 4/1)	234	510 / 743	Yes (430)	Yes (BLAST, UCSC)	Yes	Janjic Rankovic et al. (2020); Shi et al. (2019a)
IL6	NM_000600.5	TGGCAGAAAACAACCTGAACC (21 / 56.5°C / 48% / 3/0)	TGGCTTGTTCCTCACTACTCTC (22 / 56.9°C / 50% / 2/0)	168	317 / 484	Yes (707)	Yes (BLAST, UCSC)	Yes	Janjic Rankovic et al. (2020); Shi et al. (2019a)
CXCL8 / IL8	NM_000584.4	CAGAGACAGCAGAGCACACAA (21 / 60.5°C / 52% / 2/0)	TTAGCACTCCTTGGCAAAAC (20 / 56.5°C / 45% / 5/0)	170	10 / 179	Yes (819)	Yes (BLAST)	Yes	(Jones et al. 2004)
RUNX2	NM_001015051.4	GCGCATTCCTCATCCCAGTA (20 / 56.9°C / 55% / 4/2)	GGCTCAGGTAGGAGGGGTAA (20 / 56.9°C / 60% / 3/1)	176	947 / 1122	Yes (20131)	Yes (BLAST, UCSC)	Yes	Shi et al. (2019b); Janjic Rankovic et al. (2020)
BGLAP	NM_199173.6	AGCGAGGTAGTGAAGAGAC (19 / 52.6°C / 53% / 2/1)	GAAAGCCGATGTGGTCAG (18 / 52.3°C / 56% / 2/1)	142	175 / 316	Yes (201)	Yes (BLAST, UCSC)	Yes	Gartland et al. (2005)
BECN1	NM_003766.5	AGGTTGAGAAAGGCGAGACA (20 / 58.9°C / 50% / 2/0)	AATTGTGAGGACACCCAAGC (20 / 58.3°C / 50% / 4/2)	196	1297 / 1492	Yes (726)	Yes (BLAST)	Yes	Zhuang et al. (2015)
MAP1LC3A/LC3	NM_032514.4	CGTCCTGGACAAGACCAAGT (20 / 59.6°C / 55% / 7/2)	TCCTCGTCTTTCTCCTGCTC (20 / 58.8°C / 55% / 2/0)	183	286 / 468	Yes (179)	Yes (BLAST)	Yes	Zhuang et al. (2015)
CASP3	NM_004346.4	TGGAGGCCGACTTCTTGTAT (20 / 58.4°C / 50% / 4/2)	ACTGTTTCAGCATGGCACAA (20 / 58.6°C / 45% / 4/2)	111	801 / 911	Yes (1535)	Yes (BLAST)	Yes	Wang et al. (2020)
CASP8	NM_001228.5	GGAGGAGTTGTGTGGGGTAA (20 / 58.9°C / 55% / 2/1)	CCTGCATCCAAGTGTGTTCC (20 / 59.1°C / 55% / 4/0)	207	931 / 1137	Yes (1873)	Yes (BLAST)	Yes	Cao et al. (2017)
TNFRSF11B	NM_002546.4	TCAAGCAGGAGTGCAATCG (19 / 54.9°C / 53% / 6/4)	AGAATGCCTCCTCACACAGG (20 / 56.3°C / 55% / 4/1)	342	342 / 683	Yes (6020)	Yes (BLAST, UCSC)	Yes	Yang et al. (2010)
Reference genes									
RPL0	NM_001002.4	GAAACTCTGCATTCTCGCTTCC (22 / 57.4°C / 50% / 4/0)	GACTCGTTTGTACCCGTTGATG (22 / 57.1°C / 50% / 4/0)	120	702 / 821	Yes (1091)	Yes (BLAST/UCSC)	Yes	Sun et al. (2022), Nazet et al. (2020)
RPL22	NM_000983.4	TGATTGCACCCACCCTGTAG (20 / 56.6°C / 55% / 4/2)	GGTTCCCAGCTTTTCCGTTC (20 / 56.4°C / 55% / 4/0)	98	91 / 188	Yes (4597)	Yes (BLAST/UCSC)	Yes	Sun et al. (2022), Nazet et al. (2020)
GAPDH	NM_002046.7	CTCCTGTTCGACAGTCAGCC (20 / 57.4°C / 60% / 6/1)	CGACCAAATCCGTTGACTCC (20 / 55.9°C/ 55%/ 3/1)	103	12 / 114	Yes, rev. primer on exon junction	Yes (BLAST/UCSC)	Yes	Sun et al. (2022), Chirieleison et al. (2017)
EEF1A1	NM_001402.6	CCTGCCTCTCCAGGATGTCTAC (22 / 59.0°C / 59% / 5/2)	GGAGCAAAGGTGACCACCATAC (22 / 58.7°C / 55% / 6/2)	105	804 / 908	Yes (87)	Yes (BLAST/UCSC)	Yes	Sun et al. (2022), Nazet et al. (2020)
PPIB	NM_000942.5	TTCCATCGTGTAATCAAGGACTTC (24 / 56.7°C / 42% / 4/2)	GCTCACCGTAGATGCTCTTTC (21 / 56.1°C / 52% / 4/0)	88	313 / 400	Yes (3194)	Yes (BLAST/UCSC)	Yes	Sun et al. (2022), Nazet et al. (2020)
YWHAZ	NM_003406.4	AGGAGATTACTACCGTTACTTGGC (24 / 57.8°C / 46% / 4/2)	AGCTTCTTGGTATGCTTGTTGTG (23 / 57.4°C / 43% / 4/0)	91	491 / 581	Yes (617)	Yes (BLAST/UCSC)	Yes	Sun et al. (2022), Nazet et al. (2020)

Official gene symbol	**Reference sequence** (NCBI GenBank)	**5'-forward primer-3'** (length / T_m / %GC / Self-comp./Self-3'-comp.)	**5'-reverse primer-3'** (length / T_m / %GC / Self-comp./Self-3'-comp.)	**Amplicon length (bp)**	**Amplicon location** (bp of Start/Stop)	**Intron spanning** (length, bp)	**In silico qPCR specificity**	**Variants targeted** (Transcript/ Splice)	**Reference**
RNA18SN5	NR_003286.4	AACTGCGAATGGCTCATTAAATC (23 / 55.8°C / 39% / 6/3)	GCCCGTCGGCATGTATTAG (19 / 55.2°C / 58% / 5/1)	103	84 / 186	No (rRNA)	No (RNA45S5 also targeted)	-	Sun et al. (2022), Nazet et al. (2020)
POLR2A	NM_000937.5	TCGCTTACTGTCTTCCTGTTGG (22 / 57.8°C / 50% / 3/0)	TGTGTTGGCAGTCACCTTCC (20 / 57.4°C / 55% / 3/3)	108	3811 / 3918	Yes (468)	Yes (BLAST/UCSC)	Yes	Sun et al. (2022), Nazet et al. (2020)

T_m, melting temperature of primer or qPCR product (amplicon); %GC, percent of guanin/cytosine content; bp, base pairs; Self-comp., self-complementary; Self-3'-comp., self 3' complementary.

To perform silico analysis of RT-qPCR primers, their targets and corresponding amplification products, the following programs and online resources were used. All URLs were valid on 02-12-2020.

a. Primer-BLAST (URL: https://www.ncbi.nlm.nih.gov/tools/primer-blast/) was used to check the melting temperature (T_m) and the "length" of each primer, their "in silico qPCR specificity", possible co-amplification of genomic DNA, "Self-comp." and "Self-3'-comp".
    i. Settings for "Refseq mRNA": max primer annealing: 65; intron length range: 100 – 100000, max. target amplicon size: 40000
    ii. Settings for "Refseq representative genomes": max primer annealing: 65; intron length range: 100 – 100000, max. target amplicon size: 40000
b. UCSC In-Silico PCR (URL: https://genome.ucsc.edu/cgi-bin/hgPcr) was used to check "In silico qPCR specificity" and RT-qPCR in genomic context.
c. "Amplicon (length)", "Amplicon location (bp of Start/Stop)", "Intron-spanning (length)" was identified or calculated by either Primer-BLAST or UCSC In-Silico PCR
d. ENSEMBL (URL: https://www.ensembl.org) was used to check "Variants targeted (Transcript/Splice)".

Supplementary Table S2.3: Primer validation by RT-qPCR

Gene symbol	Primer sequence (f: 5'-forward primer-3'; r: 5'-reverse primer-3')	Reference	Specificity by melting curve / T_m (°C)	Specificity by agarose gel / amplicon size (bp)	Annealing temp. (°C)	Dilution series used for efficiency testing – starting from 1:10 prediluted cDNA	Primer efficiency			
							Efficiency	Error	Slope	Y intercept
Genes of interest										
PTGS2	f: AAGCCTTCTCTAACCTCTCC r: GCCCTCGCTTATGATCTGTC	Janjic Rankovic et al. (2020); Shi et al. (2019a)	Yes / 81.7	234	58	1:1, 1:10, 1:100, 1:1000	2.028	0.0768	-3.257	35.67
IL6	f: TGGCAGAAAACAACCTGAACC r: TGGCTTGTTCCTCACTACTCTC	Janjic Rankovic et al. (2020); Shi et al. (2019a)	Yes / 80.3	168	58	1:1, 1:10, 1:100, 1:1000	1.999	0.0277	-3.325	39.05
CXCL8	f: CAGAGACAGCAGAGCACACAA r: TTAGCACTCCTTGGCAAAAC	(Jones et al. 2004)	Yes/ 84.5	170	55	1:1, 1:4, 1:16, 1:64, 1:256	2.082	0.025	-3.141	34.17
RUNX2	f: GCGCATTCCTCATCCCAGTA r: GGCTCAGGTAGGAGGGGTAA	Shi et al. (2019b); Janjic Rankovic et al. (2020)	Yes / 85.3	176	58	1:1, 1:10, 1:100, 1:1000	1.94	0.00746	-3.475	39.04
BGLAP	f: AGCGAGGTAGTGAAGAGAC r: GAAAGCCGATGTGGTCAG	Gartland et al. (2005)	Yes / 86.7	142	64	1:1, 1:4, 1:16, 1:64, 1:256	1.916	0.0196	-3.541	36.33
BCN1	f: AGGTTGAGAAAGGCGAGACA r: AATTGTGAGGACACCCAAGC	Zhuang et al. (2015)	Yes/ 82.7	196	58	1:1, 1:10, 1:100, 1:1000	2.037	0.0676	-3.237	33.41
MAP1LC3A	f: CGTCCTGGACAAGACCAAGT r: TCCTCGTCTTTCTCCTGCTC	Zhuang et al. (2015)	Yes/ 87.8	183	58	1:1, 1:10, 1:100, 1:1000	1.951	0.0674	-3.445	34.7
CASP3	f: TGGAGGCCGACTTCTTGTAT r: ACTGTTTCAGCATGGCACAA	Wang et al. (2020)	Yes/ 81.7	111	58	1:1, 1:10, 1:100, 1:1000	1.984	0.01	-3.362	37.23
CASP8	f: GGAGGAGTTGTGTGGGGTAA r: CCTGCATCCAAGTGTGTTCC	Cao et al. (2017)	Yes/ 81.0	207	58	1:1, 1:10, 1:100, 1:1000	2.033	0.0614	-3.245	35.23
TNFRSF11B	f: TCAAGCAGGAGTGCAATCG r: AGAATGCCTCCTCACACAGG	Yang et al. (2010)	Yes / 84.8	342	64	1:1, 1:10, 1:100, 1:1000, 1:10000	1.915	0.0164	-3.545	37.27
Reference genes										
RPL0	f: GAAACTCTGCATTCTCGCTTCC r: GACTCGTTTGTACCCGTTGATG	Sun et al. (2022), Nazet et al. (2020)	Yes / 83.8	120	64	1:1, 1:10, 1:100, 1:1000, 1:10000	1.947	0.027	-3.455	32.54
RPL22	f: TGATTGCACCCACCCTGTAG r: GGTTCCCAGCTTTTCCGTTC	Sun et al. (2022), Nazet et al. (2020)	Yes / 80.1	98	61	1:1, 1:10, 1:100, 1:1000, 1:10000	2.004	0.007	-3.313	33.4
GAPDH	f: CAACTACATGGTTTACATGTTC r: GCCAGTGGACTCCACGAC	Sun et al. (2022), Chirieleison et al. (2017)	Yes / 84.4	103	52	1:1, 1:10, 1:100, 1:1000, 1:10000	1.968	0.002	-3.4	30.4
EEF1A1	f: CCTGCCTCTCCAGGATGTCTAC r: GGAGCAAAGGTGACCACCATAC	Sun et al. (2022), Nazet et al. (2020)	Yes / 82.4	105	61	1:1, 1:10, 1:100, 1:1000, 1:10000	2.038	0.002	-3.235	29.41
PPIB	f: TTCCATCGTGTAATCAAGGACTTC r: GCTCACCGTAGATGCTCTTTC	Sun et al. (2022), Nazet et al. (2020)	Yes / 82.4	88	55	1:1, 1:10, 1:100, 1:1000, 1:10000	1.992	0.007	-3.341	33.77
YWHAZ	f: AGGAGATTACTACCGTTACTTGGC r: AGCTTCTTGGTATGCTTGTTGTG	Sun et al. (2022), Nazet et al. (2020)	Yes / 81.3	91	55	1:1, 1:10, 1:100, 1:1000, 1:10000	2.019	0.012	-3.276	33.48
RNA18SN5	f: AACTGCGAATGGCTCATTAAATC r: GCCCGTCGGCATGTATTAG	Sun et al. (2022), Nazet et al. (2020)	Yes / 80.4	103	55	1:1, 1:10, 1:100, 1:1000, 1:10000	2.022	0.021	-3.271	19.26
POLR2A	f: TCGCTTACTGTCTTCCTGTTGG r: TGTGTTGGCAGTCACCTTCC	Sun et al. (2022), Nazet et al. (2020)	Yes / 83.7	108	58	1:1, 1:10, 1:100, 1:1000, 1:10000	2.046	0.016	-3.216	34.72

References

Cao Z, Zhang H, Cai X, Fang W, Chai D, Wen Y, Chen H, Chu F, Zhang Y (2017). Luteolin Promotes Cell Apoptosis by Inducing Autophagy in Hepatocellular Carcinoma. Cell Physiol Biochem; 43(5):1803-1812.

Chirieleison SM, Marsh RA, Kumar P, Rathkey JK, Dubyak GR, Abbott DW (2017). Nucleotide-binding oligomerization domain (NOD) signaling defects and cell death susceptibility cannot be uncoupled in X-linked inhibitor of apoptosis (XIAP)-driven inflammatory disease. J Biol Chem; 292(23):9666-9679.

Gartland A, Buckley KA, Dillon JP, Curran JM, Hunt JA, Gallagher JA (2005). Isolation and culture of human osteoblasts. Methods Mol Med; 107:29-54.

Janjic Rankovic M, Docheva D, Wichelhaus A, Baumert U (2020). Effect of static compressive force on in vitro cultured PDL fibroblasts: monitoring of viability and gene expression over 6 days. Clin Oral Investig; 24(7):2497-2511.

Jones RL, Hannan NJ, Kaitu'u TJ, Zhang J, Salamonsen LA (2004). Identification of chemokines important for leukocyte recruitment to the human endometrium at the times of embryo implantation and menstruation. J Clin Endocrinol Metab; 89(12):6155-67.

Nazet U, Schroder A, Spanier G, Wolf M, Proff P, Kirschneck C (2020). Simplified method for applying static isotropic tensile strain in cell culture experiments with identification of valid RT-qPCR reference genes for PDL fibroblasts. Eur J Orthod; 42(4):359-370.

Shi J, Baumert U, Folwaczny M, Wichelhaus A (2019a). Influence of static forces on the expression of selected parameters of inflammation in periodontal ligament cells and alveolar bone cells in a co-culture in vitro model. Clin Oral Investig; 23(6):2617-2628.

Shi J, Folwaczny M, Wichelhaus A, Baumert U (2019b). Differences in RUNX2 and P2RX7 gene expression between mono- and coculture of human periodontal ligament cells and human osteoblasts under compressive force application. Orthod Craniofac Res; 22(3):168-176.

Somerman MJ, Archer SY, Imm GR, Foster RA (1988). A comparative study of human periodontal ligament cells and gingival fibroblasts in vitro. J Dent Res; 67(1):66-70.

Sun C, Janjic Rankovic M, Folwaczny M, Stocker T, Otto S, Wichelhaus A, Baumert U (2022). Effect of Different Parameters of In Vitro Static Tensile Strain on Human Periodontal Ligament Cells Simulating the Tension Side of Orthodontic Tooth Movement. Int J Mol Sci; 23(3).

Wang Y, Du C, Wan W, He C, Wu S, Wang T, Wang F, Zou R (2020). shRNA knockdown of integrin-linked kinase on hPDLCs migration, proliferation, and apoptosis under cyclic tensile stress. Oral Dis; 26(8):1747-1754.

Yang Y, Yang Y, Li X, Cui L, Fu M, Rabie AB, Zhang D (2010). Functional analysis of core binding factor a1 and its relationship with related genes expressed by human periodontal ligament cells exposed to mechanical stress. Eur J Orthod; 32(6):698-705.

Zhuang H, Hu D, Singer D, Walker JV, Nisr RB, Tieu K, Ali K, Tredwin C, Luo S, Ardu S, Hu B (2015). Local anesthetics induce autophagy in young permanent tooth pulp cells. Cell Death Discov; 1:15024.

Supplement 2 to manuscript

"Investigation of Oxidative Stress Impact on Human Periodontal Ligament Cells Exposed to Static Compression"

URL: https://www.ciidirsinaloa.com.mx/RefFinder-master/ (2024-04-26)

RefFinder is a user-friendly web-based comprehensive tool developed for evaluating and screening reference genes from extensive experimental datasets. It integrates the currently available major computational programs (**geNorm**, **Normfinder**, **BestKeeper**, and **the comparative ΔCt method**) to compare and rank the tested candidate reference genes. Based on the rankings from each program, it assigns an appropriate weight to an individual gene and calculated the geometric mean of their weights for the overall final ranking.

Citation: **F Xie, P Xiao, D Chen, L Xu, B Zhang. 2012. miRDeepFinder: a miRNA analysis tool for deep sequencing of plant small RNAs. Plant molecular biology 80 (1), 75-84.**

References

1. BestKeeper: Pfaffl MW, Tichopad A, Prgomet C, Neuvians TP. 2004. Determination of stable housekeeping genes, differentially regulated target genes and sample integrity: BestKeeper--Excel-based tool using pair-wise correlations. Biotechnology letters 26:509-515.
2. NormFinder: Andersen CL, Jensen JL, Orntoft TF. 2004. Normalization of real-time quantitative reverse transcription-PCR data: a model-based variance estimation approach to identify genes suited for normalization, applied to bladder and colon cancer data sets. Cancer research 64:5245-5250.
3. Genorm: Vandesompele J, De Preter K, Pattyn F, Poppe B, Van Roy N, De Paepe A, Speleman F. 2002. Accurate normalization of real-time quantitative RT-PCR data by geometric averaging of multiple internal control genes. Genome biology 3:RESEARCH0034.
4. The comparative delta-Ct method: Silver N, Best S, Jiang J, Thein SL. 2006. Selection of housekeeping genes for gene expression studies in human reticulocytes using real-time PCR. BMC molecular biology 7:33.

Contents

Raw data (Cq values)

Treatment	PPIB	GAPDH	RPL22	YWHAZ	EEF1A1	RPL0	RNA18SN5
Control	20.16	16.81	20.21	20.05	16.44	19.17	8.24
Control	20.19	16.85	20.14	20.09	16.59	19.07	6.00
H_2O_2 100µM	19.95	16.53	19.88	19.94	16.02	19.13	5.00
H_2O_2 100µM	19.84	17.00	19.90	19.97	16.06	19.08	6.00
H_2O_2 100µM + WAB	20.13	16.13	19.80	20.43	15.86	18.50	6.00
H_2O_2 100µM + WAB	20.15	16.08	19.83	20.48	15.89	18.47	6.00
H_2O_2 50µM	19.90	16.59	19.99	19.90	16.08	18.71	6.00
H_2O_2 50µM	19.88	16.86	19.92	19.88	16.01	18.87	6.00
H_2O_2 50µM +WAB	20.28	16.08	19.85	20.53	16.00	18.21	6.00
H_2O_2 50µM +WAB	20.27	16.07	20.05	20.51	15.99	18.31	6.00
WAB	20.24	16.28	19.78	20.10	16.16	18.57	6.00
WAB	20.22	16.10	19.72	20.20	16.03	18.65	6.00
H_2O_2 100µM (direct)	20.10	16.68	19.88	20.16	16.10	18.62	5.00
H_2O_2 100µM (direct)	20.18	16.65	19.89	20.01	16.06	18.64	6.00
H_2O_2 50µM (direct)	20.67	17.08	20.56	20.44	16.72	19.44	6.61
H_2O_2 50µM (direct)	20.84	17.05	20.66	20.51	16.86	19.09	7.00

	Ctrl (N= 2)	WAB only (N= 2)	H_2O_2 direct (N= 4)	H_2O_2 recovery (N= 4)	H_2O_2 w/WAB (N= 2)	H_2O_2 w/WAB (N= 2)	All (N= 16)
PPIB							
Mean (SD)	20 (0.021)	20 (0.014)	20 (0.36)	20 (0.046)	20 (0.0071)	20 (0.014)	20 (0.26)
Median [Min, Max]	20 [20, 20]	20 [20, 20]	20 [20, 21]	20 [20, 20]	20 [20, 20]	20 [20, 20]	20 [20, 21]
GAPDH							
Mean (SD)	17 (0.028)	16 (0.13)	17 (0.23)	17 (0.22)	16 (0.0071)	16 (0.035)	17 (0.38)
Median [Min, Max]	17 [17, 17]	16 [16, 16]	17 [17, 17]	17 [17, 17]	16 [16, 16]	16 [16, 16]	17 [16, 17]
RPL22							
Mean (SD)	20 (0.049)	20 (0.042)	20 (0.42)	20 (0.048)	20 (0.14)	20 (0.021)	20 (0.27)
Median [Min, Max]	20 [20, 20]	20 [20, 20]	20 [20, 21]	20 [20, 20]	20 [20, 20]	20 [20, 20]	20 [20, 21]
YWHAZ							
Mean (SD)	20 (0.028)	20 (0.071)	20 (0.24)	20 (0.040)	21 (0.014)	20 (0.035)	20 (0.24)
Median [Min, Max]	20 [20, 20]	20 [20, 20]	20 [20, 21]	20 [20, 20]	21 [21, 21]	20 [20, 20]	20 [20, 21]
EEF1A1							
Mean (SD)	17 (0.11)	16 (0.092)	16 (0.41)	16 (0.033)	16 (0.0071)	16 (0.021)	16 (0.30)
Median [Min, Max]	17 [16, 17]	16 [16, 16]	16 [16, 17]	16 [16, 16]	16 [16, 16]	16 [16, 16]	16 [16, 17]
RPL0							
Mean (SD)	19 (0.071)	19 (0.057)	19 (0.39)	19 (0.19)	18 (0.071)	18 (0.021)	19 (0.35)
Median [Min, Max]	19 [19, 19]	19 [19, 19]	19 [19, 19]	19 [19, 19]	18 [18, 18]	18 [18, 19]	19 [18, 19]
RNA18SN5							
Mean (SD)	7.1 (1.6)	6.0 (0)	6.2 (0.87)	5.8 (0.50)	6.0 (0)	6.0 (0)	6.1 (0.74)
Median [Min, Max]	7.1 [6.0, 8.2]	6.0 [6.0, 6.0]	6.3 [5.0, 7.0]	6.0 [5.0, 6.0]	6.0 [6.0, 6.0]	6.0 [6.0, 6.0]	6.0 [5.0, 8.2]

RefFinder – Summary

Ranking Order (Better--Good--Average)

Method	1	2	3	4	5	6	7
Delta CT	RPL22	EEF1A1	PPIB	RPL0	GAPDH	YWHAZ	RNA18SN5
BestKeeper	PPIB	RPL22	YWHAZ	EEF1A1	RPL0	GAPDH	RNA18SN5
Normfinder	EEF1A1	RPL22	PPIB	RPL0	GAPDH	YWHAZ	RNA18SN5
Genorm	RPL22 | EEF1A1		RPL0	GAPDH	PPIB	YWHAZ	RNA18SN5
Recommended comprehensive ranking	**RPL22**	**EEF1A1**	**PPIB**	**RPL0**	**GAPDH**	**YWHAZ**	**RNA18SN5**

Comprehensive Ranking:

Genes	Geomean of ranking values
RPL22	1.41
EEF1A1	1.68
PPIB	2.59
RPL0	3.94
GAPDH	4.95
YWHAZ	5.05
RNA18SN5	7.00

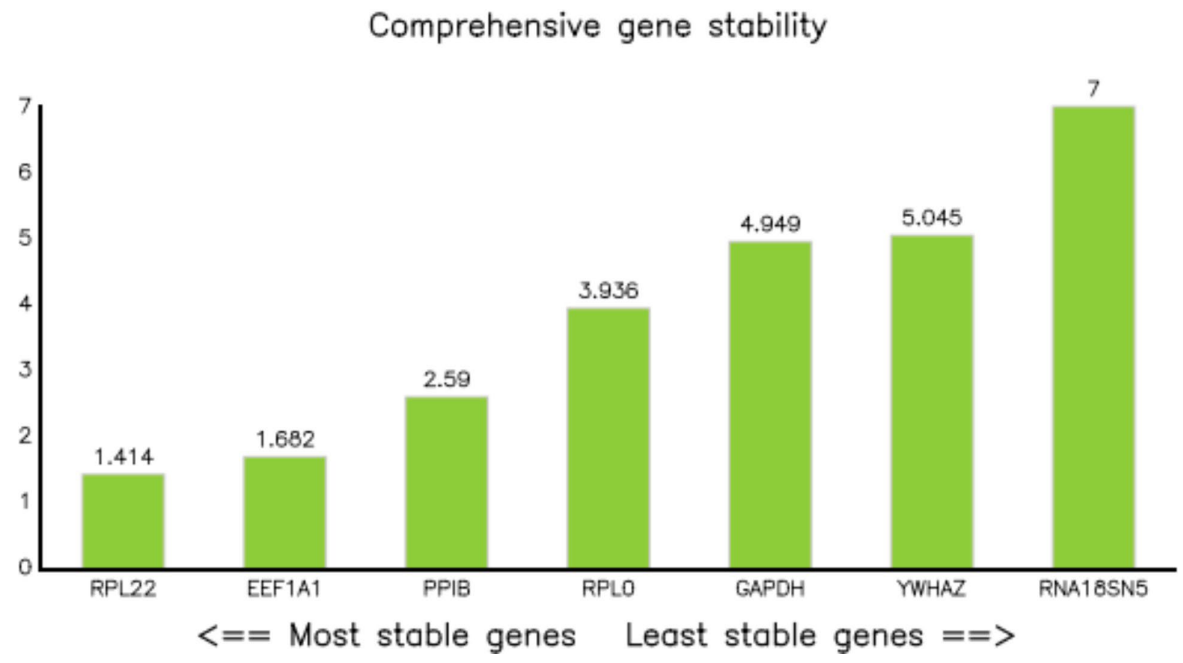

Supplement 2: RefFinder results

Delta CT

Genes	Average of STDEV
RPL22	0.30
EEF1A1	0.31
PPIB	0.35
RPL0	0.38
GAPDH	0.40
YWHAZ	0.43
RNA18SN5	0.68

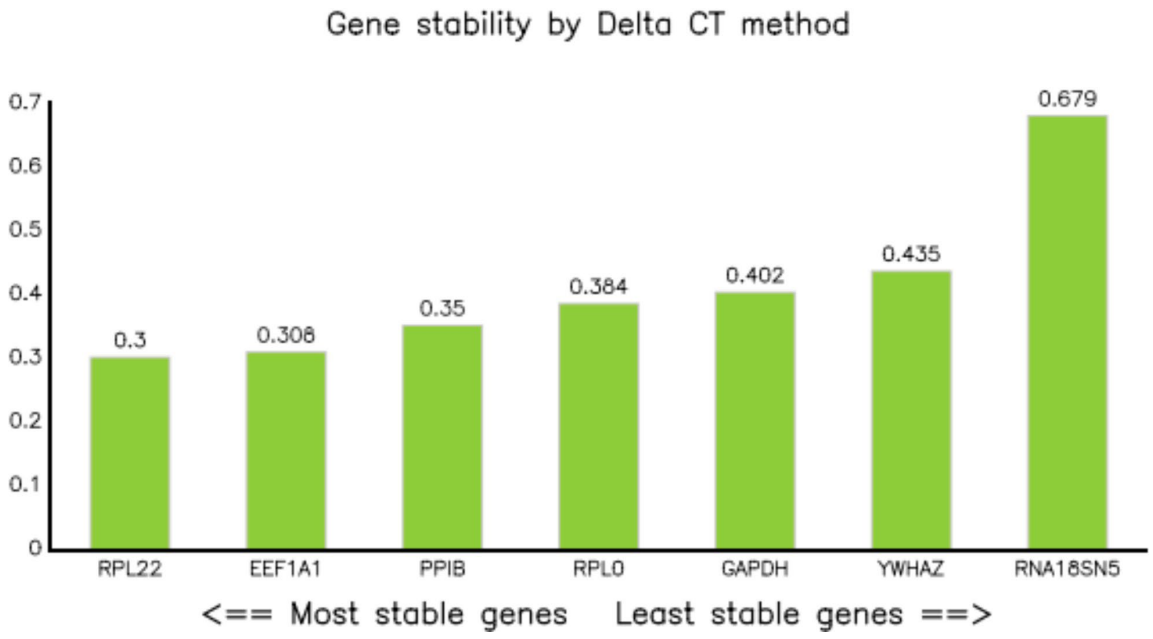

BestKeeper

CP data of housekeeping Genes by BEST KEEPER

	PPIB	GAPDH	RPL22	YWHAZ	EEF1A1	RPL0	RNA18SN5
n	16	16	16	16	16	16	16
geo Mean [CP]	20.19	16.55	20.00	20.20	16.18	18.78	6.08
AR Mean [CP]	20.19	16.55	20.00	20.20	16.18	18.78	6.12
min [CP]	19.84	16.07	19.72	19.88	15.86	18.21	5.00
max [CP]	20.84	17.08	20.66	20.53	16.86	19.44	8.24
std dev [+/- CP]	0.17	0.32	0.20	0.21	0.24	0.30	0.44
CV [% CP]	0.87	1.96	1.00	1.05	1.46	1.58	7.16
min [x-fold]	-1.27	-1.39	-1.22	-1.25	-1.25	-1.48	-2.11
max [x-fold]	1.57	1.45	1.58	1.26	1.61	1.58	4.48
std dev [+/- x-fold]	1.13	1.25	1.15	1.16	1.18	1.23	1.35

Pearson correlation coefficient (r) by BEST KEEPER

	PPIB	GAPDH	RPL22	YWHAZ	EEF1A1	RPL0	RNA18SN5
GAPDH	0.157	-	-	-	-	-	-
p-value	0.561	-	-	-	-	-	-
RPL22	0.735	0.671	-	-	-	-	-
p-value	0.001	0.004	-	-	-	-	-
YWHAZ	0.707	-0.384	0.300	-	-	-	-
p-value	0.002	0.142	0.259	-	-	-	-
EEF1A1	0.718	0.705	0.908	0.150	-	-	-
p-value	0.002	0.002	0.001	0.580	-	-	-
RPL0	0.183	0.853	0.643	-0.343	0.705	-	-
p-value	0.499	0.001	0.007	0.194	0.002	-	-
RNA18SN5	0.414	0.309	0.571	0.156	0.548	0.360	-
p-value	0.111	0.245	0.021	0.563	0.028	0.170	-

Pearson correlation coefficient (r)

BestKeeper vs.	PPIB	GAPDH	RPL22	YWHAZ	EEF1A1	RPL0	RNA18SN5
coeff. of corr. [r]	0.612	0.555	0.822	0.204	0.806	0.583	0.923
p-value	0.012	0.026	0.001	0.448	0.001	0.018	0.001

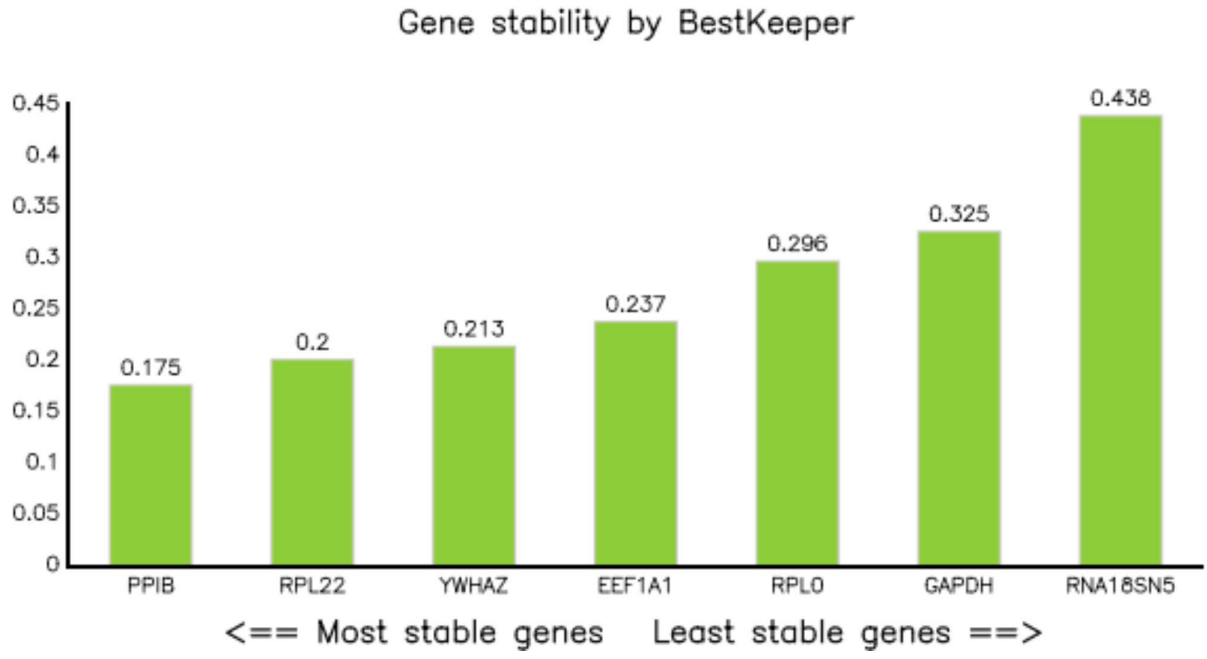

normFinder

Gene name	Stability value
EEF1A1	0.007
RPL22	0.063
PPIB	0.197
RPL0	0.259
GAPDH	0.297
YWHAZ	0.346
RNA18SN5	0.642

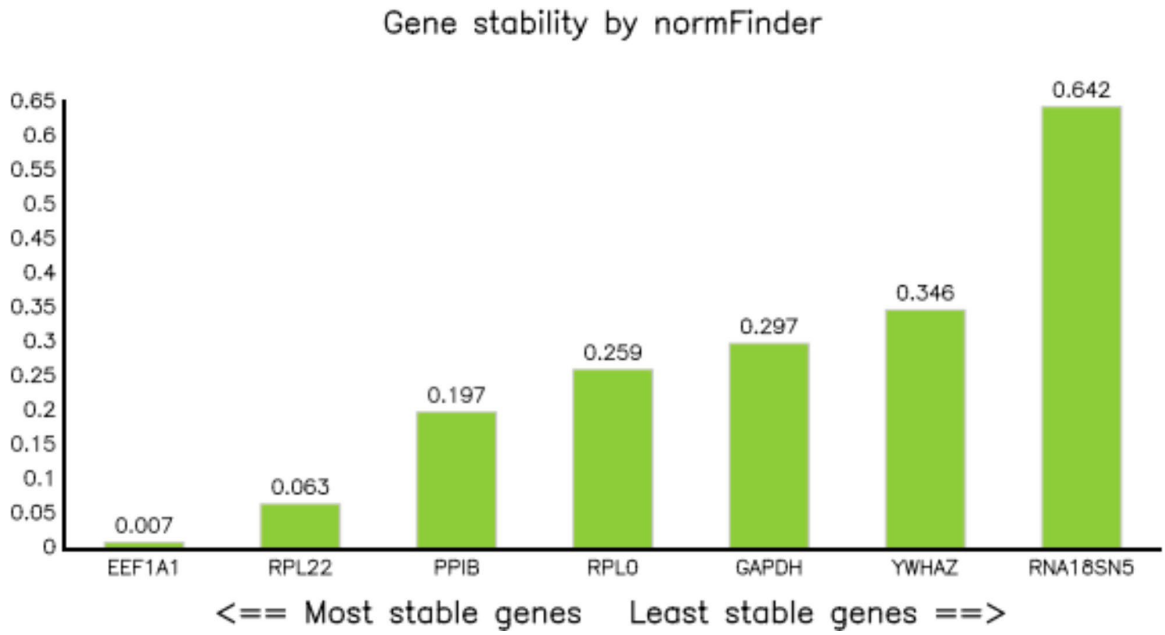

Genorm

Gene name	Stability value
RPL22 | EEF1A1	0.126
RPL0	0.217
GAPDH	0.233
PPIB	0.263
YWHAZ	0.300
RNA18SN5	0.408

4. Paper II

Investigation of Oxidative-Stress Impact on Human Osteoblasts During Orthodontic Tooth Movement Using an In Vitro Tension Model

Hosseini S, Diegelmann J, Folwaczny M, Sabbagh H, Otto S, Kakoschke TK, Wichelhaus A, Baumert U, Janjic Rankovic M

Int J Mol Sci. 2024 Dec 17;25(24):13525.

DOI: 10.3390/ijms252413525
PMID: 39769290
PMCID: PMC11677893.

(44 pages including supplements)

International Journal of
Molecular Sciences

Article

Investigation of Oxidative-Stress Impact on Human Osteoblasts During Orthodontic Tooth Movement Using an In Vitro Tension Model

Samira Hosseini [1], Julia Diegelmann [2], Matthias Folwaczny [2], Hisham Sabbagh [1], Sven Otto [3], Tamara Katharina Kakoschke [3], Andrea Wichelhaus [1], Uwe Baumert [1] and Mila Janjic Rankovic [1,*]

1 Department of Orthodontics and Dentofacial Orthopedics, LMU University Hospital, LMU Munich, 80336 Munich, Germany; samirahosseini1251@gmail.com (S.H.); hisham.sabbagh@med.uni-muenchen.de (H.S.); kfo.sekretariat@med.uni-muenchen.de (A.W.); uwe.baumert@med.uni-muenchen.de (U.B.)
2 Department of Conservative Dentistry and Periodontology, LMU University Hospital, LMU Munich, 80336 Munich, Germany; julia.diegelmann@med.uni-muenchen.de (J.D.); matthias.folwaczny@med.uni-muenchen.de (M.F.)
3 Department of Oral and Maxillofacial Surgery and Facial Plastic Surgery, LMU University Hospital, LMU Munich, 80337 Munich, Germany; sven.otto@med.uni-muenchen.de (S.O.); tamara.kakoschke@med.uni-muenchen.de (T.K.K.)
* Correspondence: mila.janjic@med.uni-muenchen.de

Abstract: In recent years, there has been a growing number of adult orthodontic patients with periodontal disease. The progression of periodontal disease is well-linked to oxidative stress (OS). Nevertheless, the impact of OS on orthodontic tooth movement (OTM) is not fully clarified. Therefore, we applied an OS in vitro-model utilizing H_2O_2 to study its effect on tension-induced mechanotransduction in human osteoblasts (hOBs). Experimental parameters were established based on cell viability and proliferation. Apoptosis detection was based on caspase-3/7 activity. Gene expression related to bone-remodeling (*RUNX2*, *P2RX7*, *TNFRSF11B*/*OPG*), inflammation (*CXCL8*/*IL8*, *IL6*, *PTRGS2*/*COX2*), autophagy (*MAP1LC3A*/*LC3*, *BECN1*), and apoptosis (*CASP3*, *CASP8*) was analyzed by RT-qPCR. IL6 and PGE2 secretion were determined by ELISA. Tension increased the expression of *PTRGS2*/*COX2* in all groups, especially after stimulation with higher H_2O_2 concentration. This corresponds also to the measured PGE2 concentrations. *CXCL8*/*IL8* was upregulated in all groups. Cells subjected to tension alone showed a general upregulation of osteogenic differentiation-related genes; however, pre-stimulation with OS did not induce significant changes especially towards downregulation. *MAP1LC3A*/*LC3*, *BECN1* and *CASP8* were generally upregulated in cells without OS pre-stimulation. Our results suggest that OS might have considerable impacts on cellular behavior during OTM.

Keywords: human osteoblasts; tensile strain; oxidative stress; bone remodeling; orthodontic tooth movement

Citation: Hosseini, S.; Diegelmann, J.; Folwaczny, M.; Sabbagh, H.; Otto, S.; Kakoschke, T.K.; Wichelhaus, A.; Baumert, U.; Janjic Rankovic, M. Investigation of Oxidative-Stress Impact on Human Osteoblasts During Orthodontic Tooth Movement Using an In Vitro Tension Model. *Int. J. Mol. Sci.* **2024**, *25*, 13525. https://doi.org/10.3390/ijms252413525

Academic Editor: Luigi Canullo

Received: 6 November 2024
Revised: 1 December 2024
Accepted: 2 December 2024
Published: 17 December 2024

1. Introduction

Orthodontic tooth movement (OTM) serves as a therapeutic approach to correct misaligned and/or dispositioned teeth. OTM involves mechanical stimulation, eliciting intricate aseptic inflammatory cellular and molecular responses that lead to tissue remodeling. This results in bone resorption on the compression side and bone apposition on the tension side [1]. In recent years, there has been a notable increase in the number of adult orthodontic patients with preexisting periodontal disease [2]. It is well-established that both orthodontic force and periodontal disease exert a significant influence on cellular and tissue homeostasis [3,4]. They stimulate bone remodeling, inflammatory responses, and

pivotal biological processes such as autophagy and apoptosis [5]. Like various inflammatory diseases, periodontal disease is associated with oxidative stress (OS)—a condition arising from an imbalance between the production and accumulation of reactive oxygen species (ROS) in cells and tissues [6–8]. ROS, including hydrogen peroxide (H_2O_2), are highly reactive oxygen metabolites produced in living organisms as a by-product of aerobic processes [9,10]. Under normal conditions, antioxidants neutralize ROS, preventing tissue damage. However, during inflammation, ROS production escalates, overloading the antioxidant defense system and leading to oxidative stress and tissue damage [6,11]. ROS can directly induce tissue damage through lipid peroxidation, DNA damage, protein damage, and enzyme oxidation [6]. Additionally, they serve as important signaling molecules or mediators of inflammation [6], indirectly influencing the production of cytokines, chemokines, and enzymes, interplaying with multiple pathways. For example, oxidative stress can trigger the expression of *IL6*, *CXCL8/IL8*, and *PTGS2/COX2*, which are involved in inflammatory responses and immune modulation [12]. As a signaling factor, ROS are known to influence bone metabolism by affecting osteoblasts. Consequently, a reduced osteoblastogenesis and a disruption in normal cellular signaling pathways might occur, leading to an imbalance between bone formation and resorption [13].

Clinically, orthodontic treatment should be initiated after periodontal therapy during remission [4,14]. This is also linked to improved redox balance and a reduction in inflammatory parameters, mitigating the damaging effects of oxidative stress on cellular function, but not completely restoring it [15,16]. While increased oxidative stress is a hallmark of periodontal disease and is proven to influence many molecular events including bone remodeling, inflammation and cell destiny [7], its effect on OTM is not fully clarified. Therefore, this study aims to address this gap by investigating the interplay between OS and mechanosensitive gene expression in human alveolar osteoblasts (hOBs) under combined conditions of oxidative and mechanical stress.

To establish an OTM-related OS in vitro model, two well-established in vitro setups were combined. The effect of OS was simulated by exposing cells to H_2O_2 [17,18]. Afterwards, the cells were mechanically stimulated using tensile strain [19,20] (Figure 1). Suitable experimental parameters were established based on cell viability and proliferation. Gene expression related to bone remodeling (*RUNX2*, *P2RX7*, *TNFRSF11B/OPG*), inflammation (*IL6*, *CXCL8/IL8*, *PTGS2/COX2*), autophagy (*MAP1LC3A/LC3*, *BECN1*) and apoptosis (*CASP3*, *CASP8*) was examined.

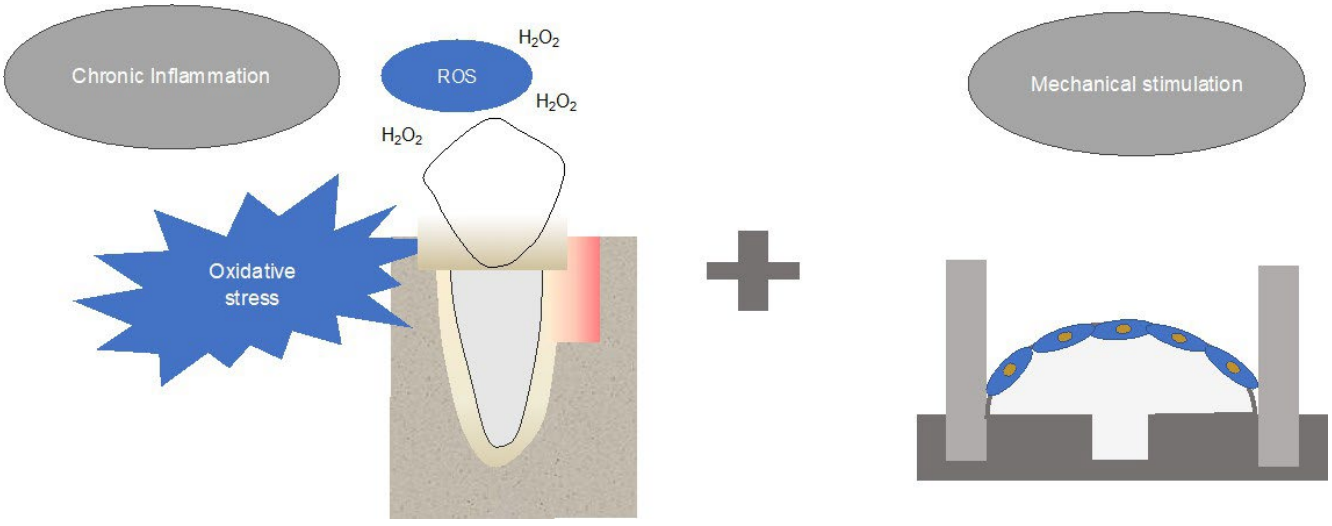

Figure 1. Oxidative stress in vitro-model utilizing H_2O_2 [21] and tensile strain [20] to study its effect on mechanotransduction in primary human alveolar osteoblasts.

2. Results

2.1. Hydrogen Peroxide (H_2O_2) Concentration Testing

To identify the lowest concentrations causing a cytotoxic effect without affecting cell viability, different H_2O_2 concentrations ranging from 20 µM to 500 µM were tested on primary hOBs. Unstimulated (i.e., 0 µM H_2O_2) but otherwise identically treated cells served as controls.

Apoptosis induction and cell viability were assessed qualitatively by caspase-3/7 activity detection using a specific reagent (R37111; Life Technologies, Carlsbad, CA, USA) and a live/dead cell staining kit (L3224; ThermoFisher Scientific, Carlsbad, CA, USA), respectively (Figure 2). The higher the concentration of H_2O_2 applied, the fewer living cells were observed, while caspase-3/7 positive cells became more prominent. These changes were especially visible in groups stimulated with 200 µM and 500 µM of H_2O_2.

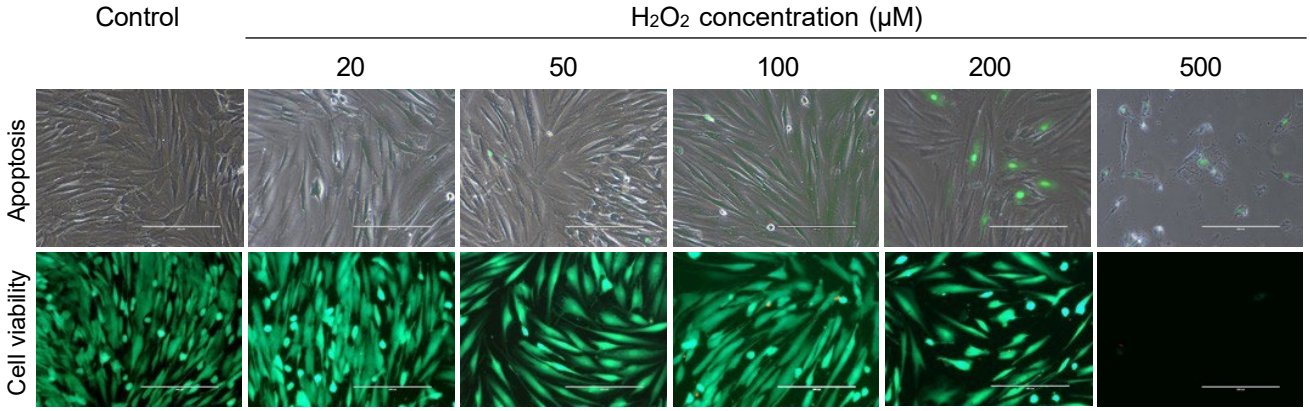

Figure 2. Effects of different hydrogen peroxide concentrations ranging from 0 µM (i.e., control) to 500 µM on apoptosis induction (**upper row**) and cell viability (**lower row**) on primary human osteoblasts. **Upper row:** Apoptosis induction was detected using the CellEvent™ Caspase-3/7 Detection Reagent (R37111; Life Technologies, Carlsbad, CA, USA). Caspase-3/7-positive cells were stained green (overlay of fluorescence and phase contrast). **Lower row:** Cell viability assessment using live/dead cell staining. Green cells represent living cells. Dead cells are either detached and washed away or stained with the red color. (Scale: 200 µm).

The impacts of the different H_2O_2 concentrations on cytotoxicity and cell viability were quantitatively determined using a resazurin-based assay (Figure 3). The findings are in line with the results of the apoptosis and cell viability tests (Figure 2).

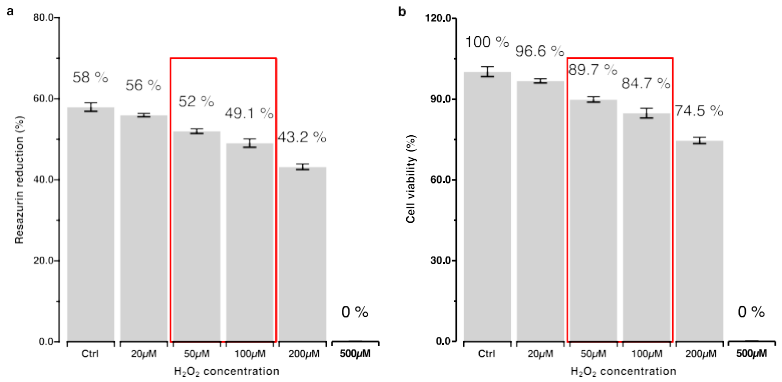

Figure 3. Percentage reduction of resazurin: (**a**) Cytotoxic effect of H_2O_2, (**b**) cell viability calculated as normalized resazurin reduction relative to the control group. 50 µM and 100 µM were identified as the lowest concentrations of H_2O_2 showing a cytotoxic effect; however, these did not have pronounced effects on cell viability.

Based on these results, H_2O_2 concentrations of 50 µM and 100 µM were chosen to further investigate the effects of higher and lower OS exposure levels.

2.2. Effect of Oxidative Stress Induction Alone on Gene Expression Immediately After H_2O_2 Incubation and After Additional 24 h Post-Incubation

Herein, we evaluated the immediate and lasting effects of oxidative stress induction on gene expression. hOBs were stimulated with either 50 µM or 100 µM H_2O_2 for 24 h. The expressions of genes related to bone remodeling, inflammation, autophagy and apoptosis were determined either immediately after the stimulation ("direct") or after an additional 24 h post-incubation period in H_2O_2-free medium ("recovery") (Figure 4, Table 1).

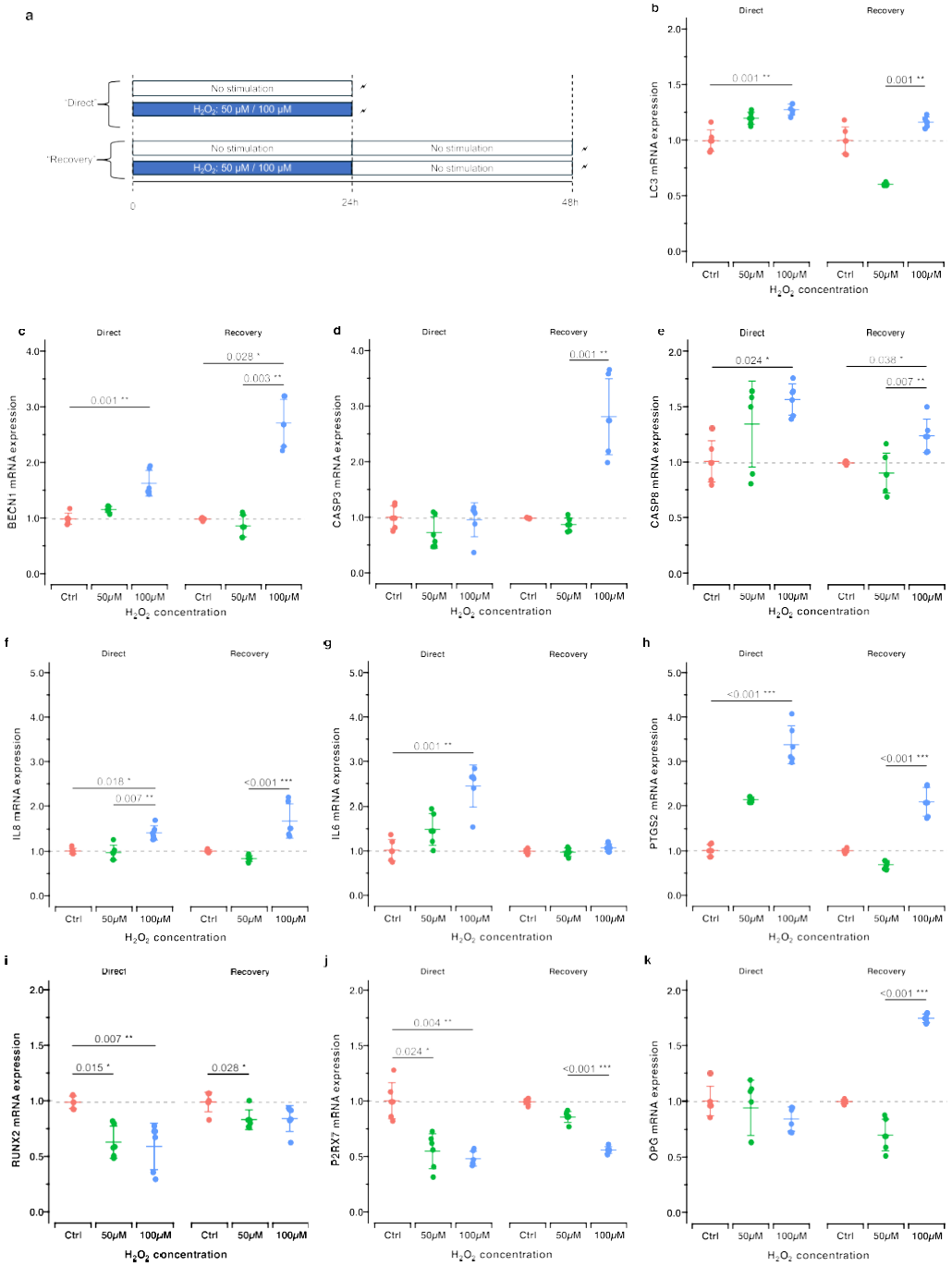

Figure 4. Effect of oxidative stress induction alone on gene expression immediately after H_2O_2 incubation ("direct") and 24 h post-incubation ("recovery"). (**a**) Experimental design. (**b–k**) RT-qPCR

results for genes related to autophagy (**b**,**c**, *MAP1LC3A/LC3*, *BECN1*), apoptosis (**d**,**e**, *CASP3*, *CASP8*), inflammation (**f–h**, *CXCL2/IL8*, *IL6*, *PTGS2/COX2*), and bone remodeling (**i–k**, *RUNX2*, *P2RX7*, *TNFRSF11B/OPG*). For each genetic locus, gene expression directly after H_2O_2 exposure (left panel, "direct") and after an additional 24 h cultivation in H_2O_2-free cell culture medium (right panel, "recovery") is depicted. Adjusted *p*-values based on multiple comparisons within each experimental group are reported: *, $p_{adj.} < 0.05$; **, $p_{adj.} < 0.01$; ***, $p_{adj.} < 0.001$.

Table 1. Summary statistics and comparisons of the effects of 50 µM and 100 µM H_2O_2 on gene expression (*CXCL8/IL8, IL6, PTGS2/COX2, CASP3, CASP8, MAP1LC3A/LC3, BECN1, TNFRSF11B/OPG,* and *P2RX7*) reported as fold change in primary hOBs immediately after H_2O_2 incubation ("direct") and 24 h post-incubation ("recovery"). *p*-values were obtained with the Kruskal–Wallis test (KW) and adjusted by Bonferroni correction for multiple tests (adjusted *p*, $p_{adj.}$).

Analyte	Treatment	Mean	SD	Median	Min	Max	K-W of Treatment		
							***p* Value**	**Post-Hoc Test vs. Ctrl ($p_{adj.}$)**	**Sig. [a]**
Direct									
CXCL8/IL8 (FC)	Ctrl	1.00	0.06	1.00	0.94	1.12	0.004		**
	50 µM	0.97	0.17	0.96	0.81	1.26		1.000	n.s.
	100 µM	1.41	0.16	1.38	1.26	1.69		0.018	*
IL6 (FC)	Ctrl	1.02	0.24	1.00	0.75	1.37	0.001		**
	50 µM	1.49	0.36	1.45	1.01	1.96		0.249	n.s.
	100 µM	2.47	0.47	2.65	1.54	2.86		0.001	**
PTGS2/COX2 (FC)	Ctrl	1.01	0.13	1.00	0.86	1.17	<0.001		***
	50 µM	2.15	0.06	2.15	2.08	2.22		0.153	n.s.
	100 µM	3.39	0.43	3.23	2.99	4.08		<0.001	***
RUNX2 (FC)	Ctrl	1.00	0.06	1.00	0.94	1.07	0.003		**
	50 µM	0.64	0.14	0.60	0.50	0.83		0.015	*
	100 µM	0.61	0.21	0.71	0.31	0.79		0.007	**
CASP3 (FC)	Ctrl	1.02	0.21	1.00	0.76	1.28	0.205		n.s.
	50 µM	0.74	0.29	0.64	0.49	1.11		0.350	n.s.
	100 µM	0.97	0.31	1.11	0.38	1.19		1.000	n.s.
CASP8 (FC)	Ctrl	1.01	0.19	1.00	0.80	1.31	0.026		*
	50 µM	1.35	0.39	1.55	0.81	1.65		0.248	n.s.
	100 µM	1.57	0.14	1.60	1.39	1.77		0.024	*
MAP1LC3A/LC3 (FC)	Ctrl	1.00	0.10	1.00	0.90	1.17	0.002		**
	50 µM	1.20	0.05	1.20	1.13	1.28		0.144	n.s.
	100 µM	1.28	0.05	1.28	1.21	1.34		0.001	**
BECN1 (FC)	Ctrl	1.00	0.10	1.00	0.90	1.19	0.001		**
	50 µM	1.17	0.05	1.17	1.08	1.24		0.388	n.s.
	100 µM	1.64	0.23	1.52	1.44	1.96		0.001	**
TNFRSF11B/OPG (FC)	Ctrl	1.01	0.13	0.98	0.86	1.25	0.128		n.s.
	50 µM	0.94	0.25	1.05	0.63	1.20		1.000	n.s.
	100 µM	0.84	0.11	0.86	0.72	0.95		0.154	n.s.
P2RX7 (FC)	Ctrl	1.01	0.16	1.00	0.83	1.28	0.003		**
	50 µM	0.56	0.16	0.60	0.32	0.73		0.024	*
	100 µM	0.49	0.07	0.46	0.42	0.58		0.004	**
Recovery									
CXCL8/IL8 (FC)	Ctrl	1.00	0.03	1.00	0.96	1.05	<0.001		***
	50 µM	0.83	0.06	0.83	0.73	0.94		0.154	n.s.
	100 µM	1.68	0.39	1.51	1.33	2.21		0.154	n.s.

Table 1. *Cont.*

Analyte	Treatment	Mean	SD	Median	Min	Max	K-W of Treatment		
							p Value	Post-Hoc Test vs. Ctrl ($p_{adj.}$)	Sig. [a]
IL6 (FC)	Ctrl	1.00	0.05	1.00	0.92	1.07	0.142		n.s.
	50 µM	0.98	0.09	0.97	0.84	1.09		1.000	n.s.
	100 µM	1.07	0.09	1.07	0.98	1.21		0.665	n.s.
PTGS2/COX2 (FC)	Ctrl	1.00	0.04	1.00	0.93	1.07	<0.001		***
	50 µM	0.69	0.09	0.70	0.57	0.78		0.154	n.s.
	100 µM	2.10	0.32	2.08	1.73	2.48		0.154	n.s.
RUNX2 (FC)	Ctrl	1.00	0.09	1.01	0.84	1.08	0.024		*
	50 µM	0.84	0.09	0.83	0.78	1.02		0.028	*
	100 µM	0.86	0.12	0.89	0.64	0.95		0.126	n.s.
CASP3 (FC)	Ctrl	1.00	0.01	1.00	0.99	1.01	0.001		**
	50 µM	0.89	0.12	0.88	0.75	1.06		0.575	n.s.
	100 µM	2.83	0.68	2.76	2.00	3.66		0.067	n.s.
CASP8 (FC)	Ctrl	1.00	0.01	1.00	0.98	1.01	0.005		**
	50 µM	0.91	0.18	0.89	0.69	1.17		1.000	n.s.
	100 µM	1.24	0.15	1.24	1.09	1.51		0.038	*
MAP1LC3A/LC3 (FC)	Ctrl	1.01	0.12	1.00	0.88	1.19	0.001		**
	50 µM	0.61	0.01	0.61	0.60	0.63		0.091	n.s.
	100 µM	1.17	0.05	1.17	1.11	1.24		0.388	n.s.
BECN1 (FC)	Ctrl	1.00	0.02	1.00	0.96	1.02	0.003		**
	50 µM	0.87	0.19	0.86	0.66	1.12		1.000	n.s.
	100 µM	2.71	0.42	2.68	2.21	3.19		0.028	*
TNFRSF11B/OPG (FC)	Ctrl	1.00	0.02	1.00	0.97	1.03	<0.001		***
	50 µM	0.70	0.14	0.69	0.52	0.88		0.154	n.s.
	100 µM	1.75	0.04	1.75	1.70	1.80		0.154	n.s.
P2RX7 (FC)	Ctrl	1.00	0.03	1.00	0.96	1.03	<0.001		***
	50 µM	0.86	0.05	0.87	0.78	0.92		0.154	n.s.
	100 µM	0.57	0.03	0.57	0.52	0.62		0.154	n.s.

[a] Sig., significance; *, $p_{adj.} < 0.05$; **, $p_{adj.} < 0.01$; ***, $p_{adj.} < 0.001$; n.s., not significant.

The autophagy or apoptosis-related genes *MAP1LC3A/LC3*, *BECN1* and *CASP8* showed dose-dependent upregulation patterns immediately after H_2O_2 stimulation. Similar gene expression regulation patterns were observed after 24 h post-incubation concerning the apoptosis-related gene *CASP3* ($p_{adj.} = 0.001$) and the autophagy-related gene *BECN1* ($p_{adj.} = 0.028$) stimulated with 100 µM H_2O_2 (Figure 4b–e).

In all three inflammation-related genes, *CXCL8/IL8*, *IL6* and *PTGS2/COX2*, a concentration-dependent upregulated expression was observed directly after H_2O_2 stimulation (Figure 4f–h). After 24 h post-incubation, a recovery effect was observable. While *IL6* gene expression was downregulated to control level, pre-stimulation with 100 µM H_2O_2 led to a persistent upregulation of *CXCL8/IL8* and *PTGS2/COX2* after 24 h post-incubation (*CXCL8/IL8*—$p_{adj.} < 0.001$; *PTGS2/COX2*—$p_{adj.} < 0.001$).

The genes related to bone remodeling were concentration-dependently downregulated directly after H_2O_2 stimulation depending on the concentration (Figure 4i–k). After 24 h post-incubation, a recovery of *RUNX2* and *P2RX7* expression was observed, but still below the corresponding controls. This contrasted with *TNFRSF11B/OPG*, which was downregulated directly after H_2O_2 stimulation, showing partially contradicting results 24 h post-exposure; 50 µM H_2O_2 resulted in a more pronounced downregulation, whereas 100 µM H_2O_2 led to an upregulation compared to the control (mean FC: 1.75).

2.3. Expression of Genes and Metabolites Related to Inflammation, Bone Remodeling, Apoptosis and Autophagy in Mechanically Stimulated Cells with and Without Previous OS Stimulation

Next, we investigated the effects of the static tension on hOBs with and without previous H_2O_2 stimulation focusing on the gene expression related to inflammation, bone remodeling, apoptosis and autophagy (Figure 5a, Table 2). Based on a previously published review [22], our initial intention was to test two different tensile strains—10% as the most frequently used one in studies applying static tension, and 15% to simulate a more tensile strains. However, due to almost identical gene/protein expression patterns, we decided to present only results derived from the 15% tensile strain setup. Nevertheless, results derived from the 10% tension setup are summarized in Supplementary Materials S1.

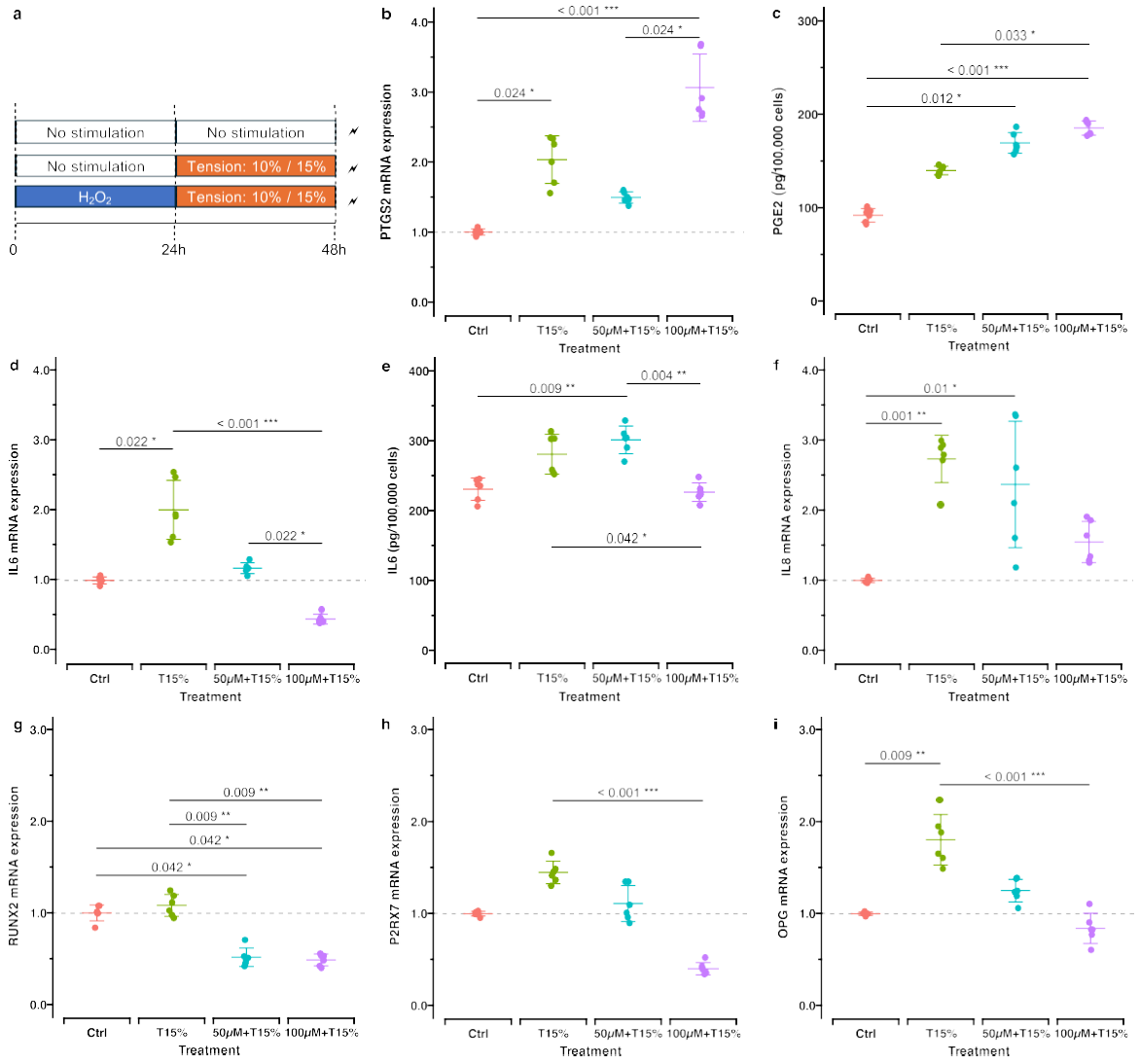

Figure 5. Expressions of genes and metabolites related to inflammation and bone remodeling in mechanically stimulated cells with and without previous H_2O_2 stimulation. (**a**) Experimental setup: the control group (ctrl) received neither H_2O_2 nor tension stimulation. The tension (T10%, T15%) group was stimulated by static tension after 24 h non-stimulation. The H_2O_2/tension group was stimulated for 24 h with 50 µM or 100 µM H_2O_2 followed by 24 h static tension at 10% or 15% stretching. Shown here are the results from 15% tension stimulation. (**b–f**) The expression of inflammation-related genes and metabolites and (**g–i**) genes related to bone remodeling are reported. Shown are the adjusted *p*-values based on multiple comparisons between each experimental treatment (*, $p_{adj.} < 0.05$; **, $p_{adj.} < 0.01$; ***, $p_{adj.} < 0.001$). Results derived from 10% tension are reported in Supplementary Materials S1.

Table 2. Summary statistics and comparison of the expression of genes and metabolites in mechanically stimulated cells with and without previous H_2O_2 stimulation. Data from RT-qPCR experiments are given as fold change, and data from ELISA (PGE2 and IL6) as "pg/100,000 cells". *p*-values were obtained with the Kruskal–Wallis test (K-W) and adjusted by Bonferroni correction for multiple tests (adjusted *p*, $p_{adj.}$).

Analyte	Treatment	Mean	SD	Median	Min	Max	K-W of Treatment		
							p Value	Post-Hoc Test vs. Ctrl ($p_{adj.}$)	Sig.[a]
CXCL8/IL8 (FC)	Ctrl	1.00	0.03	1.00	0.96	1.05	<0.001		***
	T15%	2.74	0.34	2.85	2.08	3.00		0.001	**
	50 µM/T15%	2.37	0.90	2.36	1.19	3.38		0.010	*
	100 µM/T15%	1.55	0.30	1.49	1.25	1.91		0.397	n.s.
IL6 (FC)	Ctrl	1.00	0.05	1.00	0.92	1.07	<0.001		***
	T15%	2.01	0.42	1.93	1.55	2.55		0.022	*
	50 µM/T15%	1.17	0.08	1.17	1.06	1.30		0.989	n.s.
	100 µM/T15%	0.45	0.06	0.42	0.40	0.58		0.784	n.s.
PTGS2/COX2 (FC)	Ctrl	1.00	0.04	1.00	0.93	1.07	<0.001		***
	T15%	2.03	0.34	2.13	1.56	2.35		0.024	*
	50 µM/T15%	1.49	0.08	1.48	1.38	1.59		0.754	n.s.
	100 µM/T15%	3.06	0.48	2.83	2.66	3.69		<0.001	***
RUNX2 (FC)	Ctrl	1.00	0.09	1.01	0.84	1.08	<0.001		***
	T15%	1.09	0.12	1.07	0.95	1.25		1.000	n.s.
	50 µM/T15%	0.52	0.10	0.50	0.42	0.71		0.042	*
	100 µM/T15%	0.49	0.07	0.51	0.40	0.56		0.042	*
CASP3 (FC)	Ctrl	1.00	0.01	1.00	0.99	1.01	<0.001		***
	T15%	2.86	0.09	2.89	2.69	2.93		<0.001	***
	50 µM/T15%	1.63	0.34	1.69	1.21	2.06		0.326	n.s.
	100 µM/T15%	1.89	0.49	1.96	1.24	2.57		0.075	n.s.
CASP8 (FC)	Ctrl	1.00	0.01	1.00	0.98	1.01	0.008		**
	T15%	1.64	0.33	1.68	1.19	2.00		0.009	**
	50 µM/T15%	1.25	0.36	1.32	0.74	1.78		1.000	n.s.
	100 µM/T15%	1.45	0.17	1.42	1.27	1.72		0.086	n.s.
MAP1LC3A/LC3 (FC)	Ctrl	1.01	0.12	1.00	0.88	1.19	<0.001		***
	T15%	2.14	0.27	2.18	1.80	2.43		<0.001	***
	50 µM/T15%	1.77	0.43	1.63	1.37	2.45		0.033	*
	100 µM/T15%	1.47	0.22	1.45	1.14	1.80		0.345	n.s.
BECN1 (FC)	Ctrl	1.00	0.02	1.00	0.96	1.02	<0.001		***
	T15%	2.98	0.14	2.97	2.80	3.15		<0.001	***
	50 µM/T15%	2.65	0.21	2.64	2.34	2.98		0.037	*
	100 µM/T15%	2.44	0.24	2.44	1.99	2.69		0.396	n.s.
TNFRSF11B/OPG (FC)	Ctrl	1.00	0.02	1.00	0.97	1.03	<0.001		***
	T15%	1.81	0.28	1.77	1.49	2.25		<0.001	***
	50 µM/T15%	1.25	0.12	1.24	1.06	1.39		0.037	*
	100 µM/T15%	0.84	0.16	0.83	0.61	1.11		0.396	n.s.
P2RX7 (FC)	Ctrl	1.00	0.03	1.00	0.96	1.03	<0.001		***
	T15%	1.45	0.12	1.44	1.31	1.66		0.119	n.s.
	50 µM/T15%	1.11	0.20	1.05	0.90	1.35		1.000	n.s.
	100 µM/T15%	0.40	0.06	0.37	0.34	0.51		0.272	n.s.
PGE2 (pg/100,000 cells)	Ctrl	91.91	6.85	93.31	82.88	100.73	<0.001		***
	T15%	139.88	4.20	140.10	135.10	145.15		0.850	n.s.
	50 µM/T15%	169.36	10.80	166.20	157.58	186.22		0.012	*
	100 µM/T15%	185.15	7.16	184.72	177.37	193.31		<0.001	***
IL6 (pg/100,000 cells)	Ctrl	230.68	16.07	236.51	205.93	245.50	<0.001		***
	T15%	281.39	27.81	281.23	253.51	313.45		0.086	n.s.
	50 µM/T15%	301.51	19.78	304.30	270.36	329.25		0.009	**
	100 µM/T15%	226.57	13.24	225.64	207.95	248.14		1.000	n.s.

[a] Sig., significance; *, $p_{adj.} < 0.05$; **, $p_{adj.} < 0.01$; ***, $p_{adj.} < 0.001$; n.s., not significant.

2.3.1. Inflammation

After tension force application, *IL6* expression was significantly more strongly upregulated in cells without prior OS induction than in the groups with OS preinduction,

especially in the experimental group stimulated with 100 µM H_2O_2 ($p_{adj.}$ < 0.001). This was also confirmed by ELISA ($p_{adj.}$ = 0.042). Tension force also increased the expression of the inflammatory gene *PTGS2/COX2* in all groups, especially in the group previously stimulated with 100 µM H_2O_2 concentration ($p_{adj.}$ < 0.001). These results correspond to the measured PGE2 concentrations in supernatants reflecting *PTGS2/COX2* activity. *CXCL8/IL8* was also upregulated in all groups, with the highest upregulation in cells without previous OS induction (Figure 5b–f).

2.3.2. Bone Remodeling

The general stimulatory effect of tension force on genes related to bone formation was observed in groups of cells without H_2O_2 pre-stimulation (Figure 5g–i). This effect was either less pronounced or even caused downregulation in groups previously subjected to H_2O_2 stimulation compared to control.

2.3.3. Apoptosis and Autophagy

Apoptosis- and autophagy-related genes were upregulated in all experimental groups compared to the control; however, this was considerably stronger in cells without previous H_2O_2 stimulation (Figure 6).

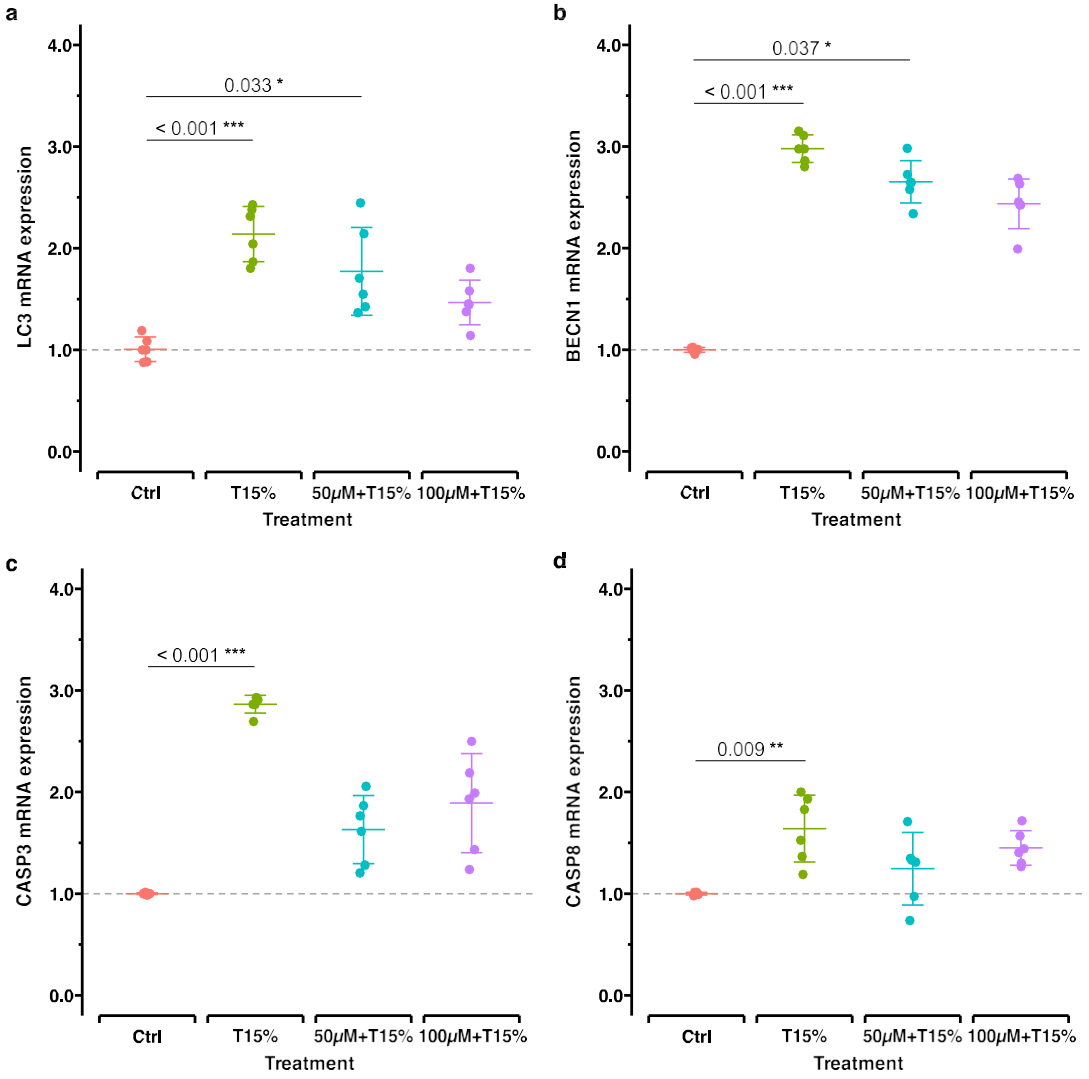

Figure 6. RT-qPCR results for autophagy- (**a**,**b**) and apoptosis (**c**,**d**)-related genes. Shown are the adjusted *p*-values based on multiple comparisons between each experimental treatment. The groups are the same as in Figure 5. *, $p_{adj.}$ < 0.05; **, $p_{adj.}$ < 0.01; ***, $p_{adj.}$ < 0.001.

2.3.4. Effect of Static Tension on Viability and Proliferation

To estimate the cell number, a standard curve was established based on resazurin reduction (Figure 7). Generally, tensile strain seemed to have a positive effect on proliferation; however, the groups previously exposed to H_2O_2 showed a slower proliferation tendency. This is also in line with live/dead staining results (Figure 8).

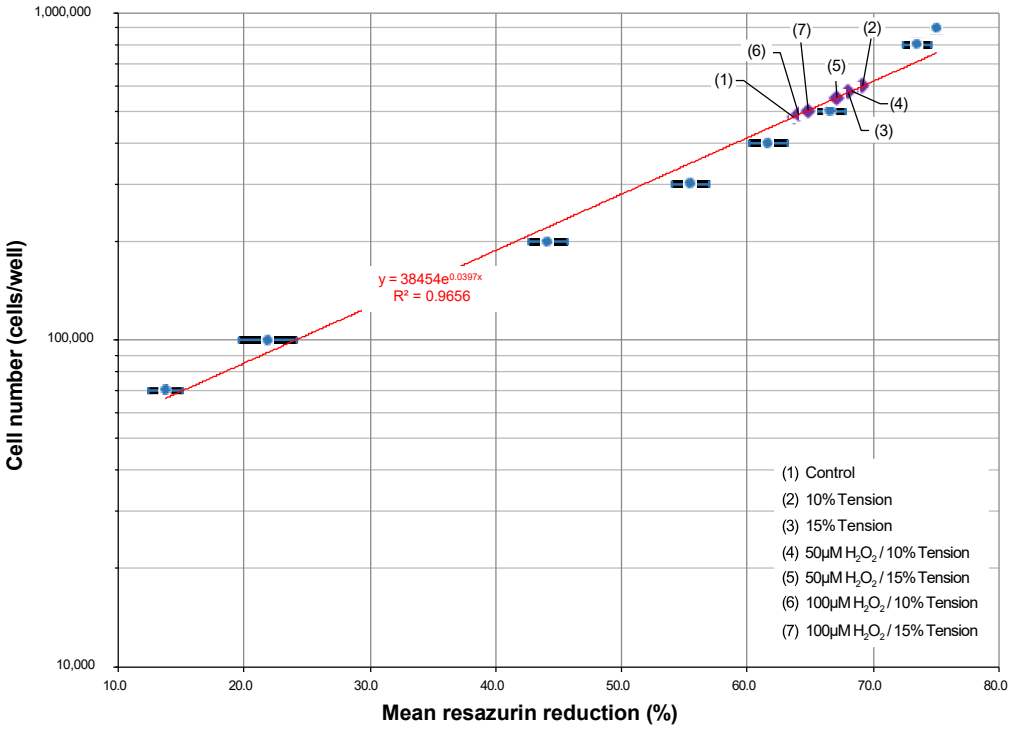

Figure 7. Establishment of a standard curve to assess cell growth of the hOBs used in the experiments. The resazurin standard curve was prepared as described in materials and methods. hOBs of the 5th passage were seeded in triplicate (70,000; 100,000; 200,000; 300,000; 400,000; 500,000) or duplicate (800,000 and 900,000 cells per well). Exponential regression was used to calculate the standard curve (red line) (Microsoft Excel). The cellular growth of hOBs in the different experimental setups (legend: lower right) is shown with violet diamonds (⌥) on the fitted curve.

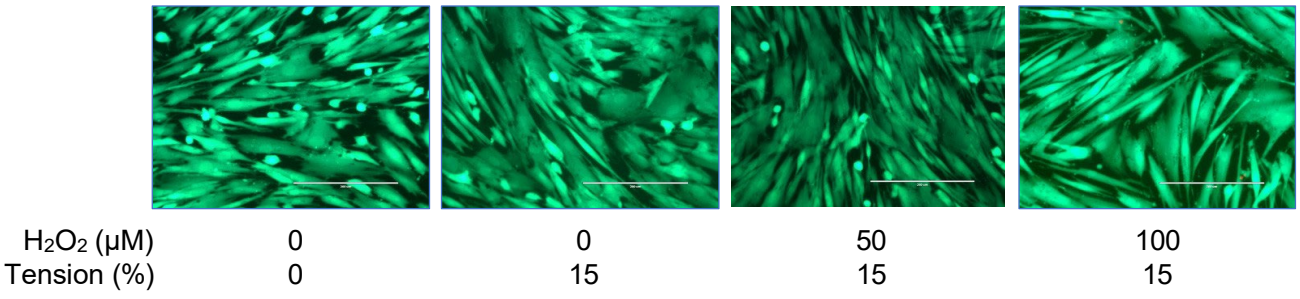

Figure 8. Qualitative assessment of cell viability of cells belonging to the different experimental groups using live/dead cell staining. Independent of the experimental group, cells proved to be viable (green staining). Dead cells were rarely observed (red staining). (Scale bar: 200 µm). (Data from experiments with 10% tension are provided in Supplementary Materials S1.

3. Discussion

With the rising number of adult patients seeking orthodontic treatment in recent years, orthodontists are more frequently encountering individuals with periodontal disease [2]. The dysregulation of redox homeostasis under pathological conditions characterized by chronic inflammation, such as periodontal disease, results in the excessive generation of

reactive oxygen species (ROS), leading to oxidative stress (OS). Although it is known that OS has an important influence on processes that are also affected by mechanical stimulation, such as inflammation, bone metabolism, autophagy and apoptosis, the role of OS in relation to orthodontic tooth movement (OTM) is still largely unknown.

Therefore, this in vitro study aimed to elucidate this topic focusing on cells centrally involved in OTM, human osteoblasts derived from the alveolar bone, and static tension force, as one of the most dominant forces during OTM. For the simulation of oxidative stress, we applied H_2O_2 as an ROS stimulus.

3.1. Experimental Parameters and Viability and Proliferation Assessment in Relation to OS Stimulation

There are several ways to experimentally study OS in cell cultures, where OS is induced by exposure to various chemicals that promote ROS generation, such as menadione, paraquat, and potassium bromate, or by exposure to ROS directly, such as H_2O_2, superoxide anion, hydroxyl radical, and peroxynitrite [23]. Menadione primarily generates superoxide and has been widely used to study ROS-related cell damage and proliferation [23,24]. Potassium bromate induces oxidative stress through distinct pathways, while other oxidants, such as hydroxyl radicals and peroxynitrite, have been employed to study specific cellular effects, including apoptosis and mitochondrial dysfunction [23,25,26]. H_2O_2 is both an ROS and an inducer of further ROS formation, playing a dual role in oxidative stress and cellular signaling. Its use as a stressor is well-established across various cell types, including osteoblasts [27] and periodontal ligament cells [28–31]. The widespread application of H_2O_2 in experimental setups and its reliability as a model for simulating oxidative stress were key factors in our decision to use it in this study.

Although H_2O_2 is widely used in in vitro experiments, its cytotoxicity varies between different cell cultures and thus has to be individually defined for different experimental cell models [32]. Therefore, in all experimental procedures applied in this study, special attention was paid to monitoring cell viability and proliferation. Herein, the experimental parameters were chosen to identify the lowest concentrations of H_2O_2 showing a relevant cytotoxic effect, but without pronounced negative effects on cell viability. H_2O_2 is a non-radical ROS, lacking an unpaired electron, and thus exhibits moderate reactivity [33]. The ability of H_2O_2 to easily penetrate membranes, to migrate significant distances from its production site, and to maintain high stability, enables it to exert its effects at various cellular locations [34]. Physiologically, H_2O_2 demonstrates dual roles in cells, both as a toxic agent and a signaling molecule critical for cellular defense and regulation [34,35]. This dual role is concentration-dependent and exhibits a biphasic effect. At low concentrations, H_2O_2 acts as a signaling molecule that supports cellular proliferation, differentiation, and survival [35]. It achieves this by modulating intracellular redox status, upregulating glutathione, and activating DNA-binding proteins like those targeting the antioxidant response element. These actions contribute to maintaining cellular homeostasis and enhancing adaptive responses to mild oxidative stress [11,35,36]. In contrast, at high concentrations, H_2O_2 is known to have negative effects on cell proliferation, and inflict severe cellular damage through oxidative modifications of proteins and DNA, leading to cell death [33,37].

Clinically, this dual role could have significant implications. Under inflammatory conditions or during aging, where dysregulated ROS levels exacerbate tissue damage, understanding and harnessing the dose-dependent effects of H_2O_2 could guide the development of antioxidant-based treatments to restore redox balance without disrupting essential signaling pathways.

OTM induces differential responses in osteoblast activity, with the stimulation of tissue formation expected on the tension side [38]. According to a recent systematic review [39], tension signals can increase the proliferation in hOBs. In line with these findings, we observed stronger proliferation in cells subjected to tension. However, this was less pronounced if the cells were previously exposed to higher H_2O_2 concentrations, suggesting a potential inhibiting influence of OS on cell proliferation during mechanical

stimulation with tensile strain. These results indicate that oxidative stress may affect orthodontic treatment outcomes in periodontal patients, as an impaired proliferation of osteoblasts could limit the desired response to mechanical forces.

3.2. Gene and Protein Expression Related to Inflammation

Herein, we investigate the expression of three different regulatory genes known to have a critical role in the regulation of inflammation: *IL6*, *CXCL8*/*IL8*, and *PTGS2*/*COX2*. The latter is an enzyme that converts arachidonic acid into prostaglandins, including PGE2. It has been shown that both PGE2 and *PTGS2*/*COX2* regulate inflammation-associated processes by modulating the secretion of cytokines. PGE2 can enhance the synthesis of *IL6*, a pro-inflammatory cytokine, which, if not properly controlled, may result in chronic inflammation and the progression of many inflammatory diseases, including various oral entities, i.e., periodontitis [40,41]. Similarly, PGE2 can also promote the synthesis of *CXCL8/IL8*, which is crucial for attracting neutrophils to sites of infection or inflammation [42]. These cytokines are also essential for coordinating the resorption and formation of bone during OTM, ensuring that the teeth can be moved effectively [43].

It is generally accepted that H_2O_2 at micromolar levels can function as a second messenger, initiating inflammatory responses [44]. Gene expression in hOBs cell culture directly after H_2O_2 incubation showed dose-dependent increases in the proinflammatory gene expressions of all three genes. Although less expressed, this proinflammatory effect was still observable in cells treated with higher H_2O_2 concentrations after 24 h post-incubation. On the contrary, in cells exposed to lower H_2O_2 concentrations, proinflammatory markers were found to be non- or downregulated after 24 h post-incubation. These results suggest a diminishing, but still present, dose-dependent altering effect of OS on cellular function in hOBs. Although these in vitro findings presented here are in line with clinical observations linking oxidative stress marker levels to the severity of periodontal inflammation [15,45–47], they should not be overinterpreted.

Despite being related to anabolic processes during OTM, like OS, tensile strain is also known to induce proinflammatory responses within the surrounding tissues [22]. This is confirmed by many in vitro studies, which were reviewed recently with special focus on human primary PDL cells [22]. However, information derived from studies using hOBs is limited [48,49], and to our knowledge, this is the first study investigating this topic in relation to OS stimulation. Based on our results, the mechanical stimulation of cells previously exposed to oxidative stress (OS) appeared to have a different effect on proinflammatory gene expression. Specifically, for genes like *IL6* and *CXCL8*/*IL8*, tension seems to induce less proinflammatory gene expression in cells previously exposed to OS compared to cells exposed to tension alone. *IL6* and *CXCL8/IL8* are central cytokines in the inflammatory response, and their dysregulation has been strongly implicated in the pathogenesis of periodontal diseases such as gingivitis and periodontitis [50,51]. In periodontitis, the upregulation of *IL6* and *CXCL8/IL8* contributes to tissue destruction and bone resorption, processes that are also regulated during orthodontic tooth movement (OTM) [51–55]. This underscores the importance of understanding how mechanical forces interact with oxidative stress in modulating these cytokines, especially in periodontal tissues, where both factors are at play during inflammation and tissue remodeling [54,56]. Also, contrary to these findings, in the case of *PTRGS2*/*COX2* gene expression and the related PGE2 secretion, tensile strain induced significantly higher gene expression in cells pre-exposed to higher dose of H_2O_2. Nevertheless, the current results indicate that the response towards tensile strains in cells pre-stimulated with H_2O_2 is considerably different to that of unstimulated cells.

3.3. Gene Expression Related to Bone Remodeling

Bone homeostasis involves bone formation and bone resorption, which are processes that maintain skeletal health. Osteoblasts are crucial for bone formation, and the expression of specific genes like *RUNX2*, *P2RX7* and *TNFRSF11B*/*OPG* plays a significant role in

this process. The activation of *RUNX2* and *P2RX7* is known to enhance the expression of osteoblast markers and promote mineralization, while the *TNFRSF11B*/*OPG* protein acts as a decoy receptor for *RANKL*, inhibiting its osteoclast differentiation-inducing effect [57,58].

Oxidative stress is known to cause dysfunctional bone homeostasis, including osteoblast-induced osteogenesis and thus favoring bone resorption [59,60]. According to our results, OS generally had a negative effect on the expression of genes related to bone remodeling with a recovery tendency after 24 h post-incubation.

On the contrary, tensile strain is known to promote bone formation, which was also found herein. However, this stimulatory effect was not observable in groups of cells previously subjected to OS, suggesting and confirming a negative influence of OS on bone remodeling [22,61].

3.4. Apoptosis and Autophagy Related Gene Expression

Herein, we investigated the expressions of genes related to autophagy (*MAP1LC3A*/*LC3* and *BECN1*) and apoptosis (*CASP3* and *CASP8*). Growing evidence suggests that ROS can act as signaling molecules involved in cellular processes that regulate cell destiny, such as autophagy and apoptosis [60,62]. ROS activate autophagy, which helps cellular adaptation and reduces oxidative damage by breaking down and recycling damaged macromolecules and dysfunctional organelles [37,63]. In the same manner, it is also proven to influence apoptosis, maintaining tissue homeostasis by eliminating damaged cells [37]. Our results from the "direct"/"recovery" groups comparison support these findings by showing the upregulation of genes related to autophagy and apoptosis. Nevertheless, to draw more conclusions on how exactly OS triggers the regulation of signaling pathways that culminate in the regulation of autophagy and apoptosis, especially in relation to OTM, more studies are needed.

3.5. Study Limitations

To our knowledge, this is the first study examining the effects of oxidative stress on mechanically stimulated hOBs by combining established experimental setups for OS and mechanical tension application. However, it should be noted that OS and mechanical stimulation are much more complex, and this study is an in vitro simplification of more intricate processes. Our in vitro setup allowed us to break down complex in vivo situations by focusing on a single cell type (hOBs), one type of force (static tension), and one type of ROS, namely, H_2O_2. Nevertheless, this simplification did not consider confounding factors derived from the external environment, including but not limited to interactions with other cell types, the extracellular matrix, and the influence of various signaling molecules, including other reactive oxygen species/molecules and antioxidants [64,65]. Additionally, biological diversity should be considered, including cells from multiple donors of different sex and age groups. To address these complexities, more studies are needed. Nonetheless, this study serves as a valuable milestone for future research in this field.

3.6. Clinical Relevance

For periodontal patients, a distinct approach is imperative due to altered molecular responses. Therefore, studying and understanding molecular events in this population becomes crucial for comprehending therapeutic responses at the cellular and tissue levels. The results of this project can offer a good foundation for future clinical projects, especially in terms of novel methods in periodontal disease treatment combining orthodontic mechanical stimulation as a regenerative stimulus.

4. Materials and Methods

4.1. Primary Cell Culture

This study was conducted in accordance with the Declaration of Helsinki. Approval for the collection and use of human alveolar bone-derived osteoblasts (hOBs) was obtained from the ethics committee of the Ludwig-Maximilians-Universität München (project

number 21-0931). Cells were obtained anonymously from a male donor undergoing orthognathic surgery exclusively for medical indications according to commonly accepted therapeutic standards. Written informed consent was obtained prior to cell sampling. The cells were isolated according to established procedures [66,67] and cultivated in low-glucose DMEM (21885025; Gibco/Life Technologies, Carlsbad, CA, USA) supplemented with 10% FBS (F7524; Sigma-Aldrich, St. Louis, MO, USA), 1 →/ MEM vitamins (M6895; Biochrom, Berlin, Germany) and 1% of antibiotic/antimycotic (15240-062; Life Technologies, Carlsbad, CA, USA). Cells were grown in a humidified atmosphere with 5% CO_2 at 37 °C. Cell passaging was performed in regular intervals of 3 to 4 days using 0.05% trypsin-EDTA solution (59417C; Sigma-Aldrich, St. Louis, MO, USA). In all experiments cells from passages 5 or 6 have been seeded at a density of 2 →/ 10^5 cells/well on 6-well collagen-I coated BioFlex® culture plates (Flexcell Intl. Corp., Hillsborough, NC, USA).

4.2. Selection of H_2O_2 Concentration

To induce an oxidative stress-like environment, H_2O_2 (9681.4; Carl Roth GmbH + Co. KG, Karlsruhe, Germany) was added to the cell culture medium [17,18,28]. A dose–response experiment was carried out to determine the optimal H_2O_2 concentration, defined as the highest H_2O_2 concentration that can be applied in the experiments without affecting cell viability and proliferation [17,18,28]. For this purpose, concentrations ranging from 20 to 500 µM H_2O_2 were tested in hOB cell culture. Cells were seeded as described above and incubated over night to support equilibration. On the next day, the cell culture media was replaced by one containing different concentrations of H_2O_2 (20 µM, 50 µM, 100 µM, 200 µM, 500 µM) and cells were stimulated for an additional 24 h in the CO_2 incubator. Wells with cells containing normal cell culture medium but otherwise treated identically served as controls.

The cytotoxic effect of H_2O_2 on cell viability was assessed as below. Additionally, cell viability was visually assessed using a live/dead viability/cytotoxicity assay as described below.

Cell cytotoxicity/viability assay. Cell culture supernatants were replaced with 2 mL/well of a resazurin-stock solution (alamarBlue™; Bio-Rad AbD Serotec GmbH, Puchheim, Germany) according to a previously published protocol [68]. After 2 h of incubation, cell culture supernatants and medium controls were collected and centrifuged, and the resazurin fluorescence of collected supernatants was determined using a fluorescence microplate reader (Varioscan; Thermo Electron Corporation, Vantaa, Finland) (560 nm excitation, 590 nm emission). For each measurement, "percentage reduction of resazurin" was calculated according to the manufacturer's instructions [68]. Cell viability was calculated as normalized resazurin reduction relative to the control group.

Live/dead and apoptosis staining assays. The viability of hOBs incubated with the different H_2O_2 concentrations was assessed using a live/dead cell staining kit (L3224; ThermoFisher Scientific, Carlsbad, CA) according to the manufacturer's instructions as previously published [20]. For apoptosis detection, one membrane of each experiment group was stained using the CellEvent™ Caspase-3/7 Green ReadyProbes® reagent (R37111; Life Technologies, Carlsbad, CA, USA) according to the manufacturer's instructions. After 30 min of incubation at room temperature in the dark, fluorescence microscopy was performed for all membranes using an EVOS*fl* fluorescence microscope (Invitrogen, Carlsbad, CA, USA) with 10 →/ and 20 →/ objectives.

4.3. Effect of Oxidative Stress Induction on Gene Expression in "Direct" and "Recovery" Setups

To investigate the effects of H_2O_2 treatment directly after 24 h of stimulation ("direct" group) and after additional 24 h post-incubation ("recovery" group), cells were seeded on collagen-I coated BioFlex® plates in two identical setups in triplicates and incubated overnight as described above (Figure 4a). On the next day, cells were treated with cell culture medium containing 0 µM (i.e., control), 50 µM or 100 µM H_2O_2 and incubated in the CO_2 incubator as described above. After 24 h, the cell lysates of the "direct" group

were collected from each well using 750 µL RNA lysis buffer (R0160-1-50; Zymo, Irvine, CA, USA) according to the manufacturer's instructions. Cell lysates were stored at −80 °C for RT-qPCR analysis. For the "recovery" group, fresh normal cell culture medium was added to all wells. After 24 h post-incubation, cell lysates were prepared as described and stored for RT-qPCR analysis.

4.4. Tensile Strain Application During the H_2O_2 "Recovery" Phase

To investigate the effects of H_2O_2 and tension force, for each experimental condition combination (control, 10%/15% tension, 50 µM/100 µM H_2O_2 + 10%/15% tension) two identical setups were used and processed in parallel: one set to assess cell proliferation and cell viability, the other one for gene expression measurement and ELISAs.

4.4.1. Tensile Strain Application

After overnight incubation, cells were stimulated with or without 50/100 µM H_2O_2 and incubated for 24 h. Afterwards, the culture medium was removed, and wells were carefully washed twice with PBS. Fresh cell culture medium was then added as described previously [20]. The static tensile force application of 10% or 15% was conducted for an additional 24 h using a previously published in vitro tension model [20]. Controls were defined as wells without stretching and H_2O_2. For each experimental group, three biological replicates were allocated.

4.4.2. Cell Proliferation and Cell Viability

After completion of the tensile force application, cell growth was assessed in triplicate using resazurin reduction in all experimental samples and their corresponding controls following the disassembly of tension setup as previously described with a shortened incubation time of 2 h [20,68]. For each measurement, the "percentage reduction of resazurin" was calculated.

In parallel with the tensile force application experiments, a resazurin standard curve was prepared as described previously to estimate cell proliferation during this experiment [68]. Briefly, hOBs from the 5th passage were diluted and seeded in triplicate (70,000/100,000/200,000/300,000/400,000/500,000 cells per well), in duplicate (800,000 cells per well) or in a single replication (900,000 cells per well). The cells were allowed to adhere overnight. The resazurin test was performed as described above [68]. For each measurement, the "percentage reduction of resazurin" was calculated. A standard curve (cell number vs. percentage reduction of resazurin) was established utilizing exponential regression (Microsoft Excel for Windows 365 MSO Version 2404, Microsoft Corporation, Redmond, WA, USA) (Figure 7), and the cell number was calculated for each well. The cell viability of hOBs from all experimental groups was then qualitatively assessed using a live/dead cell staining kit as described above.

4.4.3. Sample Preparation

After completion of the experiment, the respective setup was disassembled, and cell culture supernatants were collected from the setup. Next, the adherent cells were washed twice with sterile PBS, and cell lysates were prepared as described in Section 4.3. Meanwhile, ELISA-specific aliquots were prepared from cell culture supernatants as previously published [20].

4.5. Gene Expression Analysis

The analysis of *PTGS2*/*COX2*, *IL6*, *CXCL8*/*IL8*, *RUNX2*, *CASP3*, *MAP1LC3A*/*LC3*, *BECN1*, *TNFRSF11B*/*OPG* and *P2RX7* gene expression following H_2O_2 stimulation and/or tensile strain application was carried out for all experimental groups according to previously described protocols [68]. In the following, a short summary of the sample preparation and quantitative RT-PCR process is given. A checklist based on the "Minimum Information for

Publication of Quantitative Real-Time PCR Experiment" (MIQE) guidelines [69] is provided in Supplementary Materials S2.

Total RNA preparation and cDNA synthesis: RNA isolation and cDNA synthesis were performed as described previously [20,68] using the QuickRNA™ MicroPrep Kit (R1051; Zymo, Irvine, CA, USA) and SuperScript™ IV First-Strand Synthesis System (18091050, Thermo Fisher Scientific, Waltham, MA, USA), respectively.

PCR primer selection: Generally, primer sequences were selected from public sources for both genes of interest and potential reference genes (Supplementary Materials S2). All primer pairs used were tested in silico according to the MIQE guidelines [70] as previously published [68] (Supplementary Materials S2). Unmodified primers were synthesized by TIB Molbiol Syntheselabor GmbH (Berlin, Germany). Optimal annealing temperatures were determined with gradient PCR (TProfessional Gradient; Biometra, Göttingen, Germany) using the qPCR cycling program as specified in the MIQE checklist (Supplementary Materials S2). Primer specificity was confirmed by agarose gel electrophoresis. Primer efficiencies were evaluated using standard curves prepared from serial dilutions of cDNA, as specified in Supplementary Materials S2 and quantified in the LightCycler® 480 (Roche Molecular Diagnostics, Basel, Switzerland) using the primer pairs detailed in Supplementary Materials S2.

Reference gene selection: A set of reference genes (*EEF1A1*, *GAPDH*, *POLR2A*, *PPIB*, *RNA18SN5*, *RPL0*, *RPL22* and *YWHAZ*) was selected from public sources [19,71]. The evaluation of these reference genes was carried out using cDNA sampled from control, tension application (15%), H_2O_2 stimulation for 24 h followed by 24 h recovery (50 µM and 100 µM H_2O_2), and H_2O_2 stimulation for 24 h followed by 24 h tension application (15%/50 µM H_2O_2, and 15%/100 µM H_2O_2). RT-qPCR was performed as described below using gene-specific primers (Supplementary Materials S2). The raw Cq values (Supplementary Materials S3) were analyzed using RefFinder [72,73]. This web-based tool integrates four different algorithms (BestKeeper [74], NormFinder [75], geNorm [76], and comparative DCt method [77]) to compare and rank candidate reference genes. Based on the rankings and the two most stable genes (*PPIB*, *EEF1A1*) were used as reference genes in RT-qPCR (Figure 9).

Quantitative PCR was carried out using the LightCycler® 480 SYBR Green I Master kit (04887352001; Roche Diagnostics GmbH, Mannheim, Germany) as per the manufacturer's protocol, with 5 µL of cDNA (1:10 prediluted) in each PCR reaction. Further details regarding the RT-qPCR reaction conditions are outlined in the MIQE checklist (Supplementary Materials S2). The PCR primer specification is summarized in Table 3.

Table 3. Specification of the PCR primers used for gene quantification.

Gene	GenBank Accession Number	Primer Sequence (f: 5′-Forward Primer-3′; r: 5′-Reverse Primer-3′)	Annealing Temp. (°C)	Amplicon Size (bp)	Reference
PTGS2/COX2	NM_000963.4	f: AAGCCTTCTCTAACCTCTCC r: GCCCTCGCTTATGATCTGTC	58	234	[68,78]
IL6	NM_000600.5	f: TGGCAGAAAACAACCTGAACC r: TGGCTTGTTCCTCACTACTCTC	58	168	[68,78]
CXCL8/IL8	NM_000584.4	f: CAGAGACAGCAGAGCACACAA r: TTAGCACTCCTTGGCAAAAC	55	170	[79]
RUNX2	NM_001015051.4	f: GCGCATTCCTCATCCCAGTA r: GGCTCAGGTAGGAGGGGTAA	58	176	[67,68]
BECN1	NM_003766.5	f: AGGTTGAGAAAGGCGAGACA r: AATTGTGAGGACACCCAAGC	58	196	[80]
MAP1LC3A/LC3	NM_032514.4	f: CGTCCTGGACAAGACCAAGT r: TCCTCGTCTTTCTCCTGCTC	58	183	[80]
CASP3	NM_004346.4	f: TGGAGGCCGACTTCTTGTAT r: ACTGTTTCAGCATGGCACAA	58	111	[81]

Table 3. *Cont.*

Gene	GenBank Accession Number	Primer Sequence (f: 5^{0}-Forward Primer-3^{0}; r: 5^{0}-Reverse Primer-3^{0})	Annealing Temp. (^{o}C)	Amplicon Size (bp)	Reference
CASP8	NM_001228.5	f: GGAGGAGTTGTGTGGGGTAA r: CCTGCATCCAAGTGTGTTCC	58	207	[82]
TNFRSF11B/OPG	NM_002546.4	f: TCAAGCAGGAGTGCAATCG r: AGAATGCCTCCTCACACAGG	64	342	[83]
P2RX7	NM_002562.6	f: AGTGCGAGTCCATTGTGGAG r: CATCGCAGGTCTTGGGACTT	58	143	[67]
EEF1A1	NM_001402.6	f: CCTGCCTCTCCAGGATGTCTAC r: GGAGCAAAGGTGACCACCATAC	61	105	[19,20]
PPIB	NM_000942.5	f: TTCCATCGTGTAATCAAGGACTTC r: GCTCACCGTAGATGCTCTTTC	55	88	[19,20]

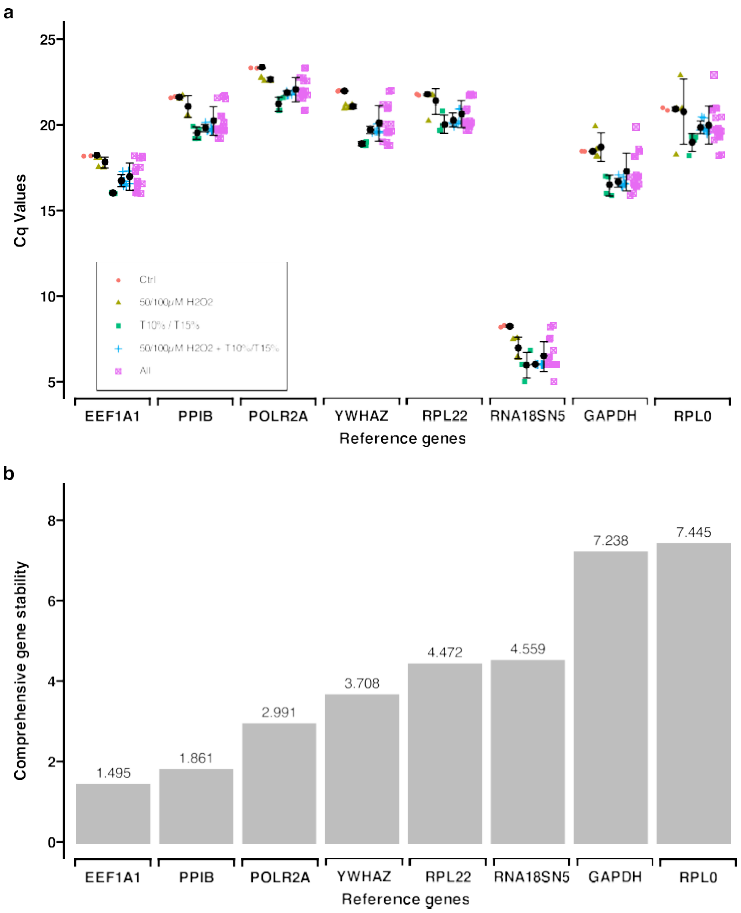

Figure 9. Reference gene selection was obtained with RefFinder. (**a**) Cq values for the panel of reference genes. Six quantitative real-time polymerase chain reaction (qPCR) runs were analyzed representing three biological replicates and two technical replicates each (Supplementary Materials S3). (**b**) Analysis of comprehensive gene stability for the panel of reference genes. Lower values indicate higher gene stability (Supplementary Materials S3).

Gene expression calculation: The expression level of target genes was quantified applying the 2^{-DDCq} method [76,84] using the average (geometric mean) of the selected reference genes (*PPIB* and *EEF1A1*). For each tension/H_2O_2 concentration combination, six RT-qPCR reactions were analyzed, representing three biological replicates with two technical replicates each (n = 3, n = 6).

4.6. Enzyme-Linked Immunosorbent Assay

Cell culture supernatants from all wells were collected for ELISA as described above. IL6 and PGE2 concentrations were determined using specific ELISA systems; for IL6, the DuoSet human IL6 ELISA kit (DY206-05; R&D Systems, Minneapolis, MN, USA) was used, whereas PGE2 was determined using the "PGE2 High Sensitivity ELISA kit" (ADI-931-001; Enzo Life Sciences AG, Lausen, CH). All measurements were conducted using a microplate reader (Varioscan, Thermo Electron Corporation, Vantaa, Finland). For each marker molecule/experimental condition combination, three biological replicates were measured twice. The measurements were reported as "pg per 100,000 cells" using the well-specific cell numbers determined above.

4.7. Statistics

Descriptive statistics of the gene expression and ELISA results are reported as mean and standard deviation (SD), median and minimum/maximum. All calculations were based on three biological replicates with two technical replicates for each gene/experimental condition combination. For each gene locus and marker molecule, differences between the different tensile strain magnitudes and durations were evaluated using the Kruskal–Wallis test followed by multiple comparisons with Bonferroni correction applied ($p_{adj.}$). All statistical procedures were carried out using IBM SPSS Statistics 29 (IBM Corp., Armonk, NY, USA) and were two-tailed considering p_{adj} values < 0.05 as significant.

5. Conclusions

Our results suggest that OS might have a significant impact on OTM through the regulation of bone remodeling-, inflammation-, autophagy-, and apoptosis-related genes. Additionally, this study highlights the necessity of considering the complexity of OS and mechanical stimulation in a more comprehensive manner and environment, accounting for interactions with various cell types, extracellular matrix components, and a range of other signaling molecules, normally present in in vivo situation. Despite its in vitro limitations and the simplified nature of the model, this work provides a valuable milestone for improving our understanding of these complex processes and guiding further clinical studies in the field. Understanding the interplay between OS and mechanical stimulation in these patients is essential for improving clinical outcomes and minimizing risks such as delayed healing, compromised bone remodeling, and exacerbated inflammatory responses.

Supplementary Materials: The following supporting information can be downloaded at: https://www.mdpi.com/article/10.3390/ijms252413525/s1, Supplement 1: Influence of tension during recovery (Table S1 and Graphics) and Live/Dead Cell Staining (Images), Supplement 2: MIQE Reporting (Table S2.1: MIQE Checklist for the RT-qPCR Workflow, Table S2.2: In Silico Analysis of the RT-qPCR Primer, Table S2.3: Primer Validation by RT-qPCR), References [19,20,66–68,71,78–83] are cited here, Supplement 3: RefFinder Results (1: Raw data, Cq Values, 2: RefFinder Summary, 2.1.: Delta CT, 2.2.: BestKeeper, 2.3.: normFinder, 2.4.: Genorm), References [72–77] are cited here.

Author Contributions: Conceptualization, S.H., A.W., U.B. and M.J.R.; methodology, S.H., J.D., M.F., U.B. and M.J.R.; software, U.B.; validation, S.H., M.F., H.S., S.O., A.W., U.B. and M.J.R.; formal Analysis, S.H., U.B. and M.J.R.; investigation, S.H., U.B. and M.J.R.; resources, S.O., T.K.K., A.W., M.F., U.B. and M.J.R.; data curation, S.H., U.B. and M.J.R.; writing—original draft preparation, S.H., U.B. and M.J.R.; writing—review and editing, S.H., J.D., M.F., H.S., S.O., T.K.K., A.W. and U.B.; supervision, A.W., U.B. and M.J.R.; project administration, U.B. and M.J.R.; funding acquisition, M.J.R. All authors have read and agreed to the published version of the manuscript.

Funding: This research was supported by a grant from the Funding Program for Research and Teaching (FöFoLe; LMU Medical Faculty) to M.J.R. (project number 1155).

Institutional Review Board Statement: The study was conducted according to the guidelines of the Declaration of Helsinki. Approval for the collection and use of human alveolar bone-derived osteoblasts was obtained from the ethics committee of the Ludwig-Maximilians-Universität München (project number Nr. 21-0931).

Informed Consent Statement: Informed consent was obtained from all subjects donating bony tissue for cell isolation used in the study.

Data Availability Statement: All authors confirm that all related data supporting the findings of this study are given in the article and its Supplementary Materials.

Acknowledgments: The authors would like to give great thanks to Christine Schreindorfer and Laure Djaleu (both from the Department of Orthodontics, University Hospital, LMU Munich) and Brigitte Hackl (Department of Conservative Dentistry and Periodontology, University Hospital, LMU Munich) for their assistance regarding the lab work.

Conflicts of Interest: The authors declare no conflicts of interest.

Abbreviations

BECN1	Beclin 1
CASP3	Caspase 3
CASP8	Caspase 8
ELISA	Enzyme-linked immunosorbent assay
FC	Fold change
H_2O_2	Hydrogen peroxide
hOBs	Human osteoblasts
IL6	Interleukin 6
CXCL8/IL8	C-X-C Motif Chemokine Ligand 8 (aka: IL8, interleukin-8)
MAP1LC3A/LC3	Microtubule Associated Protein 1 Light Chain 3 Alpha (aka: LC3)
MIQE	Minimum Information for Publication of Quantitative Real-Time PCR Experiment
TNFRSF11B/OPG	TNF Receptor Superfamily Member 11b (aka: OPG, osteoprotegerin)
OS	Oxidative stress
OTM	Orthodontic tooth movement
P2RX7	Purinergic Receptor P2X 7
$p_{adj.}$	Adjusted *p*-value
PGE2	Prostaglandin E2
PTGS2/COX2	Prostaglandin-Endoperoxide Synthase 2 (aka: COX2, cyclooxygenase 2)
ROS	Reactive oxygen species
RT-qPCR	Reverse-transcriptase quantitative polymerase chain reaction
RUNX2	RUNX Family Transcription Factor 2

References

1. Davidovitch, Z. Tooth movement. *Crit. Rev. Oral. Biol. Med.* **1991**, *2*, 411–450. [CrossRef] [PubMed]
2. Christensen, L.; Luther, F. Adults seeking orthodontic treatment: Expectations, periodontal and TMD issues. *Br. Dent. J.* **2015**, *218*, 111–117. [CrossRef] [PubMed]
3. Schröder, A.; Stumpf, J.; Paddenberg, E.; Neubert, P.; Schatz, V.; Köstler, J.; Jantsch, J.; Deschner, J.; Proff, P.; Kirschneck, C. Effects of mechanical strain on periodontal ligament fibroblasts in presence of Aggregatibacter actinomycetemcomitans lysate. *BMC Oral. Health* **2021**, *21*, 405. [CrossRef] [PubMed]
4. Rath-Deschner, B.; Nogueira, A.V.B.; Beisel-Memmert, S.; Nokhbehsaim, M.; Eick, S.; Cirelli, J.A.; Deschner, J.; Jager, A.; Damanaki, A. Interaction of periodontitis and orthodontic tooth movement-an in vitro and in vivo study. *Clin. Oral. Investig.* **2022**, *26*, 171–181. [CrossRef]
5. Nikoletopoulou, V.; Markaki, M.; Palikaras, K.; Tavernarakis, N. Crosstalk between apoptosis, necrosis and autophagy. *Biochim. Biophys. Acta* **2013**, *1833*, 3448–3459. [CrossRef]
6. Juan, C.A.; Perez de la Lastra, J.M.; Plou, F.J.; Perez-Lebena, E. The Chemistry of Reactive Oxygen Species (ROS) Revisited: Outlining Their Role in Biological Macromolecules (DNA, Lipids and Proteins) and Induced Pathologies. *Int. J. Mol. Sci.* **2021**, *22*, 4642. [CrossRef]
7. Bao, J.; Wei, Y.; Chen, L. Research progress on the regulatory cell death of osteoblasts in periodontitis. *J. Zhejiang Univ. (Med. Sci.)* **2024**, *53*, 533–540. [CrossRef]
8. Gölz, L.; Memmert, S.; Rath-Deschner, B.; Jäger, A.; Appel, T.; Baumgarten, G.; Götz, W.; Frede, S. LPS from P. gingivalis and hypoxia increases oxidative stress in periodontal ligament fibroblasts and contributes to periodontitis. *Mediators Inflamm.* **2014**, *2014*, 986264. [CrossRef]
9. Schieber, M.; Chandel, N.S. ROS function in redox signaling and oxidative stress. *Curr. Biol.* **2014**, *24*, R453–R462. [CrossRef]

10. Hong, Y.; Boiti, A.; Vallone, D.; Foulkes, N.S. Reactive Oxygen Species Signaling and Oxidative Stress: Transcriptional Regulation and Evolution. *Antioxidants (Basel)* **2024**, *13*, 312. [CrossRef]
11. Mittal, M.; Siddiqui, M.R.; Tran, K.; Reddy, S.P.; Malik, A.B. Reactive oxygen species in inflammation and tissue injury. *Antioxid. Redox Signal* **2014**, *20*, 1126–1167. [CrossRef] [PubMed]
12. Ranneh, Y.; Ali, F.; Akim, A.M.; Hamid, H.A.; Khazaai, H.; Fadel, A. Crosstalk between reactive oxygen species and pro-inflammatory markers in developing various chronic diseases: A review. *Applied Biological Chemistry* **2017**, *60*, 327–338. [CrossRef]
13. Iantomasi, T.; Romagnoli, C.; Palmini, G.; Donati, S.; Falsetti, I.; Miglietta, F.; Aurilia, C.; Marini, F.; Giusti, F.; Brandi, M.L. Oxidative Stress and Inflammation in Osteoporosis: Molecular Mechanisms Involved and the Relationship with microRNAs. *Int. J. Mol. Sci.* **2023**, *24*, 3772. [CrossRef] [PubMed]
14. Martin, C.; Celis, B.; Ambrosio, N.; Bollain, J.; Antonoglou, G.N.; Figuero, E. Effect of orthodontic therapy in periodontitis and non-periodontitis patients: A systematic review with meta-analysis. *J. Clin. Periodontol.* **2022**, *49* (Suppl. S24), 72–101. [CrossRef]
15. Nibali, L.; Donos, N. Periodontitis and redox status: A review. *Curr. Pharm. Des.* **2013**, *19*, 2687–2697. [CrossRef]
16. Marie, P.J. Osteoblast dysfunctions in bone diseases: From cellular and molecular mechanisms to therapeutic strategies. *Cell Mol. Life Sci.* **2015**, *72*, 1347–1361. [CrossRef]
17. Chen, H.; Huang, X.; Fu, C.; Wu, X.; Peng, Y.; Lin, X.; Wang, Y. Recombinant Klotho Protects Human Periodontal Ligament Stem Cells by Regulating Mitochondrial Function and the Antioxidant System during H_2O_2-Induced Oxidative Stress. *Oxidative Medicine and Cellular Longevity* **2019**, *2019*, 9261565. [CrossRef]
18. Tan, L.; Cao, Z.; Chen, H.; Xie, Y.; Yu, L.; Fu, C.; Zhao, W.; Wang, Y. Curcumin reduces apoptosis and promotes osteogenesis of human periodontal ligament stem cells under oxidative stress in vitro and in vivo. *Life Sci.* **2021**, *270*, 119125. [CrossRef]
19. Nazet, U.; Schröder, A.; Spanier, G.; Wolf, M.; Proff, P.; Kirschneck, C. Simplified method for applying static isotropic tensile strain in cell culture experiments with identification of valid RT-qPCR reference genes for PDL fibroblasts. *Eur. J. Orthod.* **2020**, *42*, 359–370. [CrossRef]
20. Sun, C.; Janjic Rankovic, M.; Folwaczny, M.; Stocker, T.; Otto, S.; Wichelhaus, A.; Baumert, U. Effect of Different Parameters of In Vitro Static Tensile Strain on Human Periodontal Ligament Cells Simulating the Tension Side of Orthodontic Tooth Movement. *Int. J. Mol. Sci.* **2022**, *23*, 1525. [CrossRef]
21. Chen, Z.; Lu, M.; Zhang, Y.; Wang, H.; Zhou, J.; Zhou, M.; Zhang, T.; Song, J. Oxidative stress state inhibits exosome secretion of hPDLCs through a specific mechanism mediated by PRMT1. *J. Periodontal Res.* **2022**, *57*, 1101–1115. [CrossRef] [PubMed]
22. Sun, C.; Janjic Rankovic, M.; Folwaczny, M.; Otto, S.; Wichelhaus, A.; Baumert, U. Effect of Tension on Human Periodontal Ligament Cells: Systematic Review and Network Analysis. *Front. Bioeng. Biotechnol.* **2021**, *9*, 695053. [CrossRef] [PubMed]
23. Goffart, S.; Tikkanen, P.; Michell, C.; Wilson, T.; Pohjoismaki, J. The Type and Source of Reactive Oxygen Species Influences the Outcome of Oxidative Stress in Cultured Cells. *Cells* **2021**, *10*, 1075. [CrossRef] [PubMed]
24. Baran, I.; Ganea, C.; Scordino, A.; Musumeci, F.; Barresi, V.; Tudisco, S.; Privitera, S.; Grasso, R.; Condorelli, D.F.; Ursu, I.; et al. Effects of menadione, hydrogen peroxide, and quercetin on apoptosis and delayed luminescence of human leukemia Jurkat T-cells. *Cell Biochem. Biophys.* **2010**, *58*, 169–179. [CrossRef]
25. Du, J.; Gebicki, J.M. Proteins are major initial cell targets of hydroxyl free radicals. *Int. J. Biochem. Cell Biol.* **2004**, *36*, 2334–2343. [CrossRef]
26. da Rocha, F.A.; de Brum-Fernandes, A.J. Evidence that peroxynitrite affects human osteoblast proliferation and differentiation. *J. Bone Miner. Res.* **2002**, *17*, 434–442. [CrossRef]
27. Fatokun, A.A.; Stone, T.W.; Smith, R.A. Responses of differentiated MC3T3-E1 osteoblast-like cells to reactive oxygen species. *Eur. J. Pharmacol.* **2008**, *587*, 35–41. [CrossRef]
28. Wei, Y.; Fu, J.; Wu, W.; Ma, P.; Ren, L.; Yi, Z.; Wu, J. Quercetin Prevents Oxidative Stress-Induced Injury of Periodontal Ligament Cells and Alveolar Bone Loss in Periodontitis. *Drug Des. Devel Ther.* **2021**, *15*, 3509–3522. [CrossRef]
29. Kuang, Y.; Hu, B.; Feng, G.; Xiang, M.; Deng, Y.; Tan, M.; Li, J.; Song, J. Metformin prevents against oxidative stress-induced senescence in human periodontal ligament cells. *Biogerontology* **2020**, *21*, 13–27. [CrossRef]
30. Costa, F.P.D.; Puty, B.; Nogueira, L.S.; Mitre, G.P.; Santos, S.M.D.; Teixeira, B.J.B.; Kataoka, M.; Martins, M.D.; Barboza, C.A.G.; Monteiro, M.C.; et al. Piceatannol Increases Antioxidant Defense and Reduces Cell Death in Human Periodontal Ligament Fibroblast under Oxidative Stress. *Antioxidants (Basel)* **2019**, *9*, 16. [CrossRef]
31. Cavalla, F.; Osorio, C.; Paredes, R.; Valenzuela, M.A.; Garcia-Sesnich, J.; Sorsa, T.; Tervahartiala, T.; Hernandez, M. Matrix metalloproteinases regulate extracellular levels of SDF-1/CXCL12, IL-6 and VEGF in hydrogen peroxide-stimulated human periodontal ligament fibroblasts. *Cytokine* **2015**, *73*, 114–121. [CrossRef] [PubMed]
32. Chen, J.H.; Ozanne, S.E.; Hales, C.N. Methods of cellular senescence induction using oxidative stress. *Methods Mol. Biol.* **2007**, *371*, 179–189. [PubMed]
33. Sachdev, S.; Ansari, S.A.; Ansari, M.I. Reactive Oxygen Species (ROS): An Introduction. In *Reactive Oxygen Species in Plants*; Sachdev, S., Akthar Ansari, S., Israil Ansari, M., Eds.; Springer Nature Singapore: Singapore, 2023; pp. 1–22.
34. Lennicke, C.; Rahn, J.; Lichtenfels, R.; Wessjohann, L.A.; Seliger, B. Hydrogen peroxide—Production, fate and role in redox signaling of tumor cells. *Cell Commun. Signal* **2015**, *13*, 39. [CrossRef]
35. Day, R.M.; Suzuki, Y.J. Cell proliferation, reactive oxygen and cellular glutathione. *Dose Response* **2006**, *3*, 425–442. [CrossRef]
36. Heo, S.; Kim, S.; Kang, D. The Role of Hydrogen Peroxide and Peroxiredoxins throughout the Cell Cycle. *Antioxidants (Basel)* **2020**, *9*, 280. [CrossRef]

37. Liu, C.; Mo, L.; Niu, Y.; Li, X.; Zhou, X.; Xu, X. The Role of Reactive Oxygen Species and Autophagy in Periodontitis and Their Potential Linkage. *Front. Physiol.* **2017**, *8*, 439. [CrossRef]
38. Sen, S.; Lux, C.J.; Erber, R. A Potential Role of Semaphorin 3A during Orthodontic Tooth Movement. *Int. J. Mol. Sci.* **2021**, *22*, 8297. [CrossRef]
39. Yu, H.S.; Kim, J.J.; Kim, H.W.; Lewis, M.P.; Wall, I. Impact of mechanical stretch on the cell behaviors of bone and surrounding tissues. *J. Tissue Eng.* **2016**, *7*, 2041731415618342. [CrossRef]
40. El-Obeid, A.; Maashi, Y.; AlRoshody, R.; Alatar, G.; Aljudayi, M.; Al-Eidi, H.; AlGaith, N.; Khan, A.H.; Hassib, A.; Matou-Nasri, S. Herbal melanin modulates PGE2 and IL-6 gastroprotective markers through COX-2 and TLR4 signaling in the gastric cancer cell line AGS. *BMC Complement. Med. Ther.* **2023**, *23*, 305. [CrossRef]
41. Yucel-Lindberg, T.; Bage, T. Inflammatory mediators in the pathogenesis of periodontitis. *Expert. Rev. Mol. Med.* **2013**, *15*, e7. [CrossRef]
42. Bickel, M. The role of interleukin-8 in inflammation and mechanisms of regulation. *J. Periodontol.* **1993**, *64*, 456–460. [PubMed]
43. Li, Y.; Zhan, Q.; Bao, M.; Yi, J.; Li, Y. Biomechanical and biological responses of periodontium in orthodontic tooth movement: Up-date in a new decade. *Int. J. Oral. Sci.* **2021**, *13*, 20. [CrossRef] [PubMed]
44. Marinho, H.S.; Real, C.; Cyrne, L.; Soares, H.; Antunes, F. Hydrogen peroxide sensing, signaling and regulation of transcription factors. *Redox Biol.* **2014**, *2*, 535–562. [CrossRef]
45. Shang, J.; Liu, H.; Zheng, Y.; Zhang, Z. Role of oxidative stress in the relationship between periodontitis and systemic diseases. *Front. Physiol.* **2023**, *14*, 1210449. [CrossRef]
46. Bosca, A.B.; Miclaus, V.; Ilea, A.; Campian, R.S.; Rus, V.; Ruxanda, F.; Ratiu, C.; Uifalean, A.; Parvu, A.E. Role of nitro-oxidative stress in the pathogenesis of experimental rat periodontitis. *Clujul Med.* **2016**, *89*, 150–159.
47. Tothova, L.; Celec, P. Oxidative Stress and Antioxidants in the Diagnosis and Therapy of Periodontitis. *Front. Physiol.* **2017**, *8*, 1055. [CrossRef]
48. Zhang, J.; Xu, S.; Zhang, Y.; Zou, S.; Li, X. Effects of equibiaxial mechanical stretch on extracellular matrix-related gene expression in human calvarial osteoblasts. *Eur. J. Oral. Sci.* **2019**, *127*, 10–18. [CrossRef]
49. Motie, P.; Mohaghegh, S.; Kouhestani, F.; Motamedian, S.R. Effect of mechanical forces on the behavior of osteoblasts: A systematic review of in vitro studies. *Dent. Med. Probl.* **2023**, *60*, 673–686. [CrossRef]
50. Mazurek-Mochol, M.; Bonsmann, T.; Mochol, M.; Poniewierska-Baran, A.; Pawlik, A. The Role of Interleukin 6 in Periodontitis and Its Complications. *Int. J. Mol. Sci.* **2024**, *25*, 2146. [CrossRef]
51. Finoti, L.S.; Nepomuceno, R.; Pigossi, S.C.; Corbi, S.C.; Secolin, R.; Scarel-Caminaga, R.M. Association between interleukin-8 levels and chronic periodontal disease: A PRISMA-compliant systematic review and meta-analysis. *Medicine (Baltimore)* **2017**, *96*, e6932. [CrossRef]
52. Graves, D. Cytokines that promote periodontal tissue destruction. *J. Periodontol.* **2008**, *79*, 1585–1591. [CrossRef] [PubMed]
53. Martínez-García, M.; Hernández-Lemus, E. Periodontal Inflammation and Systemic Diseases: An Overview. *Front. Physiol.* **2021**, *12*, 709438. [CrossRef] [PubMed]
54. Nunes, L.; Quintanilha, L.; Perinetti, G.; Capelli, J.J. Effect of orthodontic force on expression levels of ten cytokines in gingival crevicular fluid. *Arch. Oral. Biol.* **2017**, *76*, 70–75. [CrossRef] [PubMed]
55. Bendre, M.S.; Montague, D.C.; Peery, T.; Akel, N.S.; Gaddy, D.; Suva, L.J. Interleukin-8 stimulation of osteoclastogenesis and bone resorption is a mechanism for the increased osteolysis of metastatic bone disease. *Bone* **2003**, *33*, 28–37. [CrossRef]
56. Kapoor, P.; Kharbanda, O.P.; Monga, N.; Miglani, R.; Kapila, S. Effect of orthodontic forces on cytokine and receptor levels in gingival crevicular fluid: A systematic review. *Prog. Orthod.* **2014**, *15*, 65. [CrossRef]
57. Chan, W.C.W.; Tan, Z.; To, M.K.T.; Chan, D. Regulation and Role of Transcription Factors in Osteogenesis. *Int. J. Mol. Sci.* **2021**, *22*, 5445. [CrossRef]
58. Panupinthu, N.; Rogers, J.T.; Zhao, L.; Solano-Flores, L.P.; Possmayer, F.; Sims, S.M.; Dixon, S.J. P2X7 receptors on osteoblasts couple to production of lysophosphatidic acid: A signaling axis promoting osteogenesis. *J. Cell Biol.* **2008**, *181*, 859–871. [CrossRef]
59. Wauquier, F.; Leotoing, L.; Coxam, V.; Guicheux, J.; Wittrant, Y. Oxidative stress in bone remodelling and disease. *Trends Mol. Med.* **2009**, *15*, 468–477. [CrossRef]
60. Zhu, C.; Shen, S.; Zhang, S.; Huang, M.; Zhang, L.; Chen, X. Autophagy in Bone Remodeling: A Regulator of Oxidative Stress. *Front. Endocrinol. (Lausanne)* **2022**, *13*, 898634. [CrossRef]
61. Mao, Y.; Wang, L.; Zhu, Y.; Liu, Y.; Dai, H.; Zhou, J.; Geng, D.; Wang, L.; Ji, Y. Tension force-induced bone formation in orthodontic tooth movement via modulation of the GSK-3beta/beta-catenin signaling pathway. *J. Mol. Histol.* **2018**, *49*, 75–84. [CrossRef]
62. Ornatowski, W.; Lu, Q.; Yegambaram, M.; Garcia, A.E.; Zemskov, E.A.; Maltepe, E.; Fineman, J.R.; Wang, T.; Black, S.M. Complex interplay between autophagy and oxidative stress in the development of pulmonary disease. *Redox Biol.* **2020**, *36*, 101679. [CrossRef] [PubMed]
63. Wang, G.; Zhang, T.; Sun, W.; Wang, H.; Yin, F.; Wang, Z.; Zuo, D.; Sun, M.; Zhou, Z.; Lin, B.; et al. Arsenic sulfide induces apoptosis and autophagy through the activation of ROS/JNK and suppression of Akt/mTOR signaling pathways in osteosarcoma. *Free Radic. Biol. Med.* **2017**, *106*, 24–37. [CrossRef] [PubMed]
64. Kapałczyńska, M.; Kolenda, T.; Przybyła, W.; Zaja¸czkowska, M.; Teresiak, A.; Filas, V.; Ibbs, M.; Bliz´niak, R.; Łuczewski, Ł.; Lamperska, K. 2D and 3D cell cultures – A comparison of different types of cancer cell cultures. *Arch. Med. Sci.* **2018**, *14*, 910–919. [CrossRef]

65. Zhao, C. Cell culture: In vitro model system and a promising path to in vivo applications. *Journal of Histotechnology* **2023**, *46*, 1–4. [CrossRef]
66. Ng, K.W.; Schantz, J.-T. *A Manual for Primary Human Cell Culture*, 2nd ed.; World Scientific: Hackensack, NJ, USA, 2010; pp. 38–47.
67. Shi, J.; Folwaczny, M.; Wichelhaus, A.; Baumert, U. Differences in RUNX2 and P2RX7 gene expression between mono- and coculture of human periodontal ligament cells and human osteoblasts under compressive force application. *Orthod. Craniofac Res.* **2019**, *22*, 168–176. [CrossRef]
68. Janjic Rankovic, M.; Docheva, D.; Wichelhaus, A.; Baumert, U. Effect of static compressive force on in vitro cultured PDL fibroblasts: Monitoring of viability and gene expression over 6 days. *Clin. Oral. Investig.* **2020**, *24*, 2497–2511. [CrossRef]
69. Bustin, S.A.; Beaulieu, J.F.; Huggett, J.; Jaggi, R.; Kibenge, F.S.; Olsvik, P.A.; Penning, L.C.; Toegel, S. MIQE precis: Practical implementation of minimum standard guidelines for fluorescence-based quantitative real-time PCR experiments. *BMC Mol. Biol.* **2010**, *11*, 74. [CrossRef]
70. Bustin, S.A.; Benes, V.; Garson, J.A.; Hellemans, J.; Huggett, J.; Kubista, M.; Mueller, R.; Nolan, T.; Pfaffl, M.W.; Shipley, G.L.; et al. The MIQE guidelines: Minimum information for publication of quantitative real-time PCR experiments. *Clin. Chem.* **2009**, *55*, 611–622. [CrossRef]
71. Chirieleison, S.M.; Marsh, R.A.; Kumar, P.; Rathkey, J.K.; Dubyak, G.R.; Abbott, D.W. Nucleotide-binding oligomerization domain (NOD) signaling defects and cell death susceptibility cannot be uncoupled in X-linked inhibitor of apoptosis (XIAP)-driven inflammatory disease. *J. Biol. Chem.* **2017**, *292*, 9666–9679. [CrossRef]
72. Xie, F.; Xiao, P.; Chen, D.; Xu, L.; Zhang, B. miRDeepFinder: A miRNA analysis tool for deep sequencing of plant small RNAs. *Plant Mol. Biol.* **2012**, *80*, 75–84. [CrossRef]
73. RefFinder. Available online: https://www.ciidirsinaloa.com.mx/RefFinder-master/ (accessed on 11 July 2024).
74. Pfaffl, M.W.; Tichopad, A.; Prgomet, C.; Neuvians, T.P. Determination of stable housekeeping genes, differentially regulated target genes and sample integrity: BestKeeper--Excel-based tool using pair-wise correlations. *Biotechnol. Lett.* **2004**, *26*, 509–515. [CrossRef] [PubMed]
75. Andersen, C.L.; Jensen, J.L.; Orntoft, T.F. Normalization of real-time quantitative reverse transcription-PCR data: A model-based variance estimation approach to identify genes suited for normalization, applied to bladder and colon cancer data sets. *Cancer Res.* **2004**, *64*, 5245–5250. [CrossRef]
76. Vandesompele, J.; De Preter, K.; Pattyn, F.; Poppe, B.; Van Roy, N.; De Paepe, A.; Speleman, F. Accurate normalization of real-time quantitative RT-PCR data by geometric averaging of multiple internal control genes. *Genome Biol.* **2002**, *3*, research0034.0031. [CrossRef]
77. Silver, N.; Best, S.; Jiang, J.; Thein, S.L. Selection of housekeeping genes for gene expression studies in human reticulocytes using real-time PCR. *BMC Mol. Biol.* **2006**, *7*, 33. [CrossRef]
78. Shi, J.; Baumert, U.; Folwaczny, M.; Wichelhaus, A. Influence of static forces on the expression of selected parameters of inflammation in periodontal ligament cells and alveolar bone cells in a co-culture in vitro model. *Clin. Oral. Investig.* **2019**, *23*, 2617–2628. [CrossRef]
79. Jones, R.L.; Hannan, N.J.; Kaitu'u, T.J.; Zhang, J.; Salamonsen, L.A. Identification of chemokines important for leukocyte recruitment to the human endometrium at the times of embryo implantation and menstruation. *J. Clin. Endocrinol. Metab.* **2004**, *89*, 6155–6167. [CrossRef]
80. Zhuang, H.; Hu, D.; Singer, D.; Walker, J.V.; Nisr, R.B.; Tieu, K.; Ali, K.; Tredwin, C.; Luo, S.; Ardu, S.; et al. Local anesthetics induce autophagy in young permanent tooth pulp cells. *Cell Death Discov.* **2015**, *1*, 15024. [CrossRef]
81. Wang, Y.; Du, C.; Wan, W.; He, C.; Wu, S.; Wang, T.; Wang, F.; Zou, R. shRNA knockdown of integrin-linked kinase on hPDLCs migration, proliferation, and apoptosis under cyclic tensile stress. *Oral. Dis.* **2020**, *26*, 1747–1754. [CrossRef]
82. Cao, Z.; Zhang, H.; Cai, X.; Fang, W.; Chai, D.; Wen, Y.; Chen, H.; Chu, F.; Zhang, Y. Luteolin Promotes Cell Apoptosis by Inducing Autophagy in Hepatocellular Carcinoma. *Cell Physiol. Biochem.* **2017**, *43*, 1803–1812. [CrossRef]
83. Yang, Y.; Yang, Y.; Li, X.; Cui, L.; Fu, M.; Rabie, A.B.; Zhang, D. Functional analysis of core binding factor a1 and its relationship with related genes expressed by human periodontal ligament cells exposed to mechanical stress. *Eur. J. Orthod.* **2010**, *32*, 698–705. [CrossRef]
84. Livak, K.J.; Schmittgen, T.D. Analysis of relative gene expression data using real-time quantitative PCR and the 2^{-DDC}T Method. *Methods* **2001**, *25*, 402–408. [CrossRef] [PubMed]

Supplement 1 to manuscript

“Investigation of Oxidative-Stress Impact on Orthodontic Tooth Movement Using an In Vitro Tension Model”

Content

Influence of tension during recovery

Results from RT-qPCR

The adjusted *p*-values are reported.

Analyte	Treatment	N	Mean	SD	Median	Min	Max	K-W	Vs. ctrl.		Adj. multiple comparisons
IL8_dCq	Ctrl	6	8.56	0.04	8.56	8.48	8.61	0.003		**	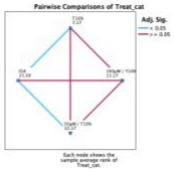
	T10%	6	7.28	0.42	7.29	6.75	7.74		0.003	**	
	50µM / T10%	6	7.68	0.52	7.56	6.98	8.47		0.033	*	
	100µM / T10%	6	7.71	0.38	7.68	7.22	8.38		0.068	n.s.	
IL8_FC	Ctrl	6	1.00	0.03	1.00	0.96	1.05				
	T10%	6	2.52	0.73	2.40	1.76	3.49				
	50µM / T10%	6	1.93	0.67	2.00	1.06	2.98				
	100µM / T10%	6	1.84	0.44	1.83	1.13	2.52				
IL6_dCq	Ctrl	6	10.43	0.07	10.43	10.33	10.55	<0.001		***	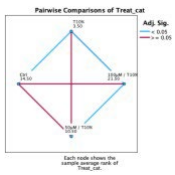
	T10%	6	9.15	0.12	9.15	9.00	9.31		0.042	*	
	50µM / T10%	6	10.26	0.17	10.32	10.03	10.43		1.000	n.s.	
	100µM / T10%	6	11.21	0.16	11.13	11.09	11.42		0.516	n.s.	
IL6_FC	Ctrl	6	1.00	0.05	1.00	0.92	1.07				
	T10%	6	2.44	0.21	2.43	2.17	2.69				
	50µM / T10%	6	1.13	0.14	1.08	1.00	1.32				
	100µM / T10%	6	0.59	0.06	0.62	0.50	0.63				
COX2_dCq	Ctrl	6	6.64	0.06	6.64	6.54	6.74	<0.001		***	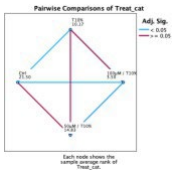
	T10%	6	5.89	0.12	5.89	5.73	6.03		0.033	*	
	50µM / T10%	6	6.07	0.10	6.06	5.95	6.24		0.613	n.s.	
	100µM / T10%	6	4.66	0.11	4.66	4.52	4.81		<0.001	***	
COX2_FC	Ctrl	6	1.00	0.04	1.00	0.93	1.07				
	T10%	6	1.69	0.14	1.68	1.53	1.88				
	50µM / T10%	6	1.49	0.10	1.50	1.32	1.62				
	100µM / T10%	6	3.98	0.30	3.97	3.56	4.35				
RUNX2_dCq	Ctrl	6	6.72	0.13	6.71	6.61	6.97	<0.001		***	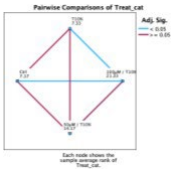
	T10%	6	6.64	0.43	6.60	6.04	7.20		1.000	n.s.	
	50µM / T10%	6	7.23	0.41	7.12	6.71	7.89		0.518	n.s.	
	100µM / T10%	6	8.05	0.12	8.05	7.86	8.20		0.003	**	
RUNX2_FC	Ctrl	6	1.00	0.09	1.01	0.84	1.08				
	T10%	6	1.10	0.33	1.10	0.72	1.60				
	50µM / T10%	6	0.73	0.20	0.76	0.45	1.01				
	100µM / T10%	6	0.40	0.03	0.40	0.36	0.45				

Analyte	Treatment	N	Mean	SD	Median	Min	Max	K-W	Vs. ctrl.		Adj. multiple comparisons
CASP3_dCq	Ctrl	6	6.41	0.01	6.41	6.39	6.43	<0.001		***	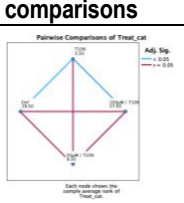
	T10%	6	4.72	0.09	4.72	4.59	4.85		0.001	**	
	50µM / T10%	6	5.07	0.04	5.07	5.03	5.14		0.084	n.s.	
	100µM / T10%	6	6.22	0.54	6.22	5.58	6.88		1.000	n.s.	
CASP3_FC	Ctrl	6	1.00	0.01	1.00	0.99	1.01				
	T10%	6	3.24	0.20	3.24	2.95	3.53				
	50µM / T10%	6	2.53	0.07	2.53	2.41	2.60				
	100µM / T10%	6	1.21	0.44	1.14	0.72	1.78				
CASP8_dCq	Ctrl	6	7.61	0.02	7.61	7.59	7.64	0.001		**	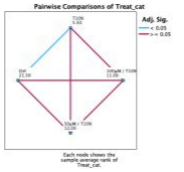
	T10%	6	6.71	0.33	6.53	6.43	7.17		0.001	**	
	50µM / T10%	6	7.20	0.32	7.24	6.68	7.56		0.119	n.s.	
	100µM / T10%	6	7.05	0.33	7.15	6.61	7.49		0.060	n.s.	
CASP8_FC	Ctrl	6	1.00	0.01	1.00	0.98	1.01				
	T10%	6	1.91	0.40	2.11	1.36	2.27				
	50µM / T10%	6	1.35	0.32	1.30	1.04	1.91				
	100µM / T10%	6	1.51	0.36	1.38	1.09	2.00				
LC3_dCq	Ctrl	6	7.88	0.17	7.88	7.63	8.07	<0.001		***	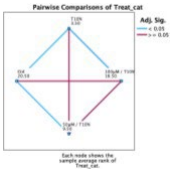
	T10%	6	6.63	0.15	6.63	6.46	6.84		<0.001	***	
	50µM / T10%	6	7.12	0.12	7.12	6.96	7.27		0.042	*	
	100µM / T10%	6	7.66	0.18	7.64	7.44	7.98		1.000	n.s.	
LC3_FC	Ctrl	6	1.01	0.12	1.00	0.88	1.19				
	T10%	6	2.39	0.24	2.38	2.06	2.68				
	50µM / T10%	6	1.70	0.14	1.69	1.53	1.89				
	100µM / T10%	6	1.17	0.14	1.18	0.93	1.36				
BECN1_dCq	Ctrl	6	6.80	0.03	6.79	6.76	6.86	<0.001		***	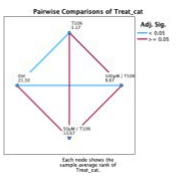
	T10%	6	5.12	0.06	5.12	5.04	5.20		<0.001	***	
	50µM / T10%	6	5.52	0.28	5.60	5.12	5.83		0.328	n.s.	
	100µM / T10%	6	5.27	0.21	5.27	5.07	5.65		0.022	*	
BECN1_FC	Ctrl	6	1.00	0.02	1.00	0.96	1.02				
	T10%	6	3.21	0.13	3.20	3.02	3.38				
	50µM / T10%	6	2.46	0.49	2.30	1.95	3.19				
	100µM / T10%	6	2.90	0.39	2.88	2.21	3.31				
OPG_dCq	Ctrl	6	3.13	0.03	3.13	3.09	3.17	<0.001		***	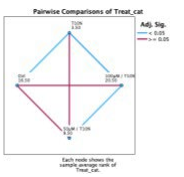
	T10%	6	2.16	0.23	2.12	1.84	2.50		0.009	**	
	50µM / T10%	6	2.70	0.12	2.67	2.57	2.87		0.518	n.s.	
	100µM / T10%	6	3.29	0.14	3.32	3.04	3.46		1.000	n.s.	
OPG_FC	Ctrl	6	1.00	0.02	1.00	0.97	1.03				
	T10%	6	1.98	0.31	2.02	1.54	2.44				
	50µM / T10%	6	1.35	0.11	1.37	1.20	1.47				

Analyte	Treatment	N	Mean	SD	Median	Min	Max	K-W	Vs. ctrl.		Adj. multiple comparisons
	100µM / T10%	6	0.90	0.09	0.88	0.79	1.06				
P2RX7_dCq	Ctrl	6	10.19	0.04	10.19	10.14	10.25	<0.001		***	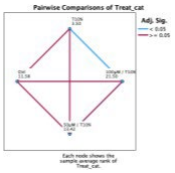
	T10%	6	9.15	0.12	9.15	9.00	9.31		0.285	n.s.	
	50µM / T10%	6	10.23	0.16	10.27	10.03	10.43		1.000	n.s.	
	100µM / T10%	6	11.19	0.13	11.13	11.09	11.41		0.090	n.s.	
P2RX7_FC	Ctrl	6	1.00	0.03	1.00	0.96	1.03				
	T10%	6	2.05	0.18	2.05	1.83	2.27				
	50µM / T10%	6	0.97	0.11	0.95	0.84	1.11				
	100µM / T10%	6	0.50	0.04	0.52	0.43	0.53				
PGE2ELISA	Ctrl	6	91.91	6.85	93.31	82.88	100.73	<0.001		***	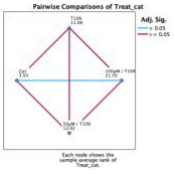
	T10%	6	130.92	3.85	130.97	125.15	135.78		0.379	n.s.	
	50µM / T10%	6	135.73	6.51	136.09	125.15	143.78		0.064	n.s.	
	100µM / T10%	6	200.03	13.56	202.74	182.44	219.06		<0.001	***	
IL6ELISA	Ctrl	6	230.68	16.07	236.51	205.93	245.50	0.006		**	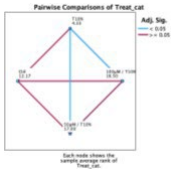
	T10%	6	208.60	2.83	208.24	205.04	213.70		0.330	n.s.	
	50µM / T10%	6	242.60	14.94	243.72	225.49	262.82		1.000	n.s.	
	100µM / T10%	6	241.29	6.99	243.25	232.04	248.81		1.000	n.s.	

Graphic - Inflammation

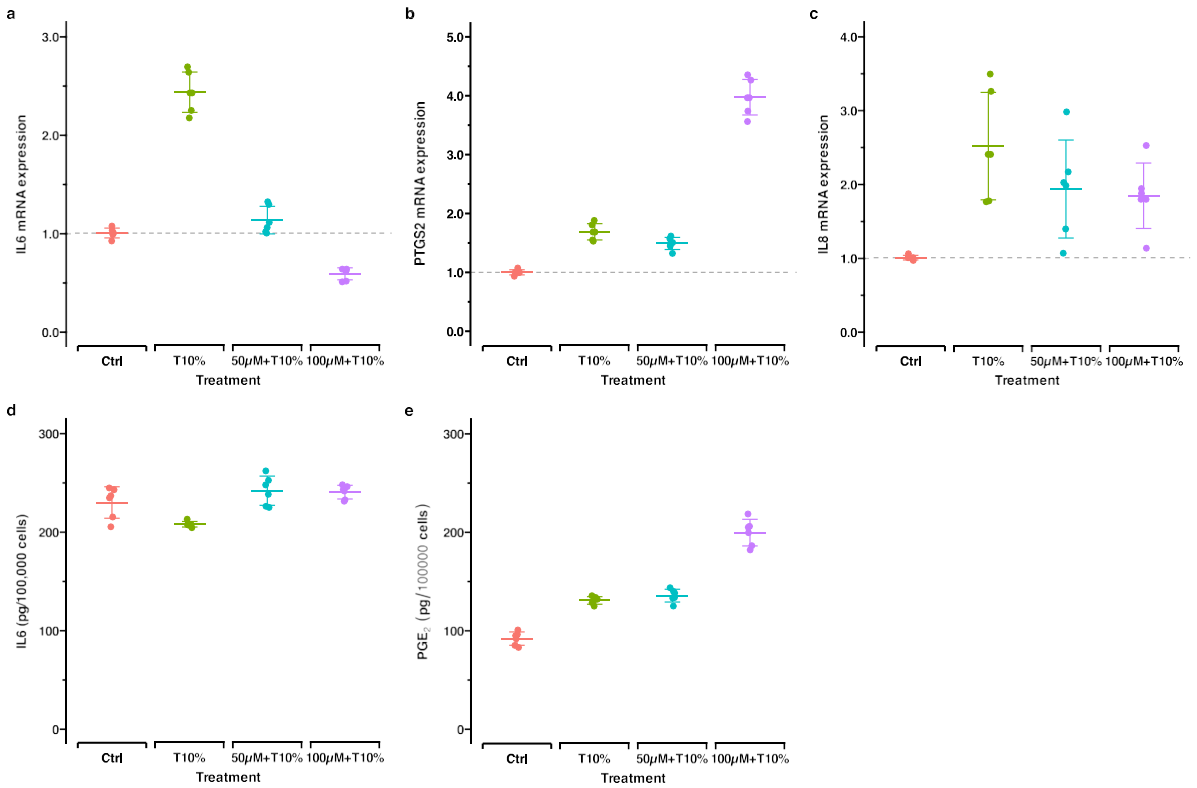

Graphic - Bone remodeling

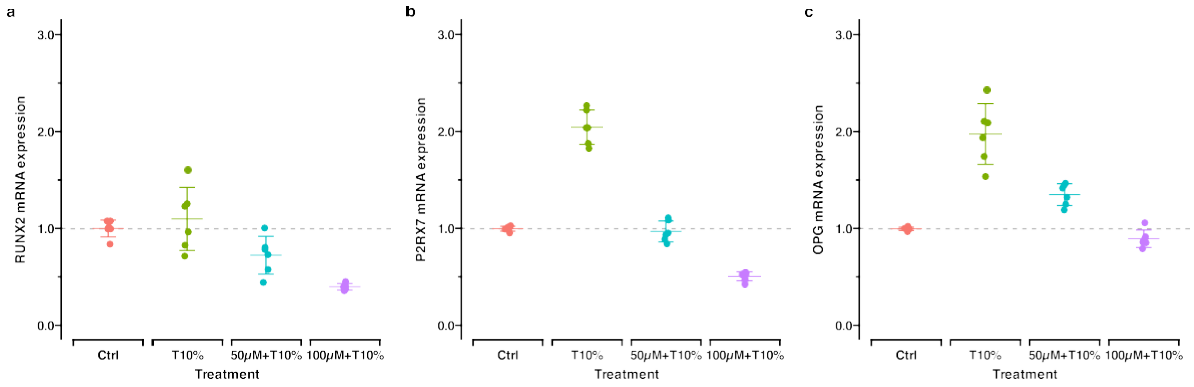

Graphic - Autophagy and apoptosis

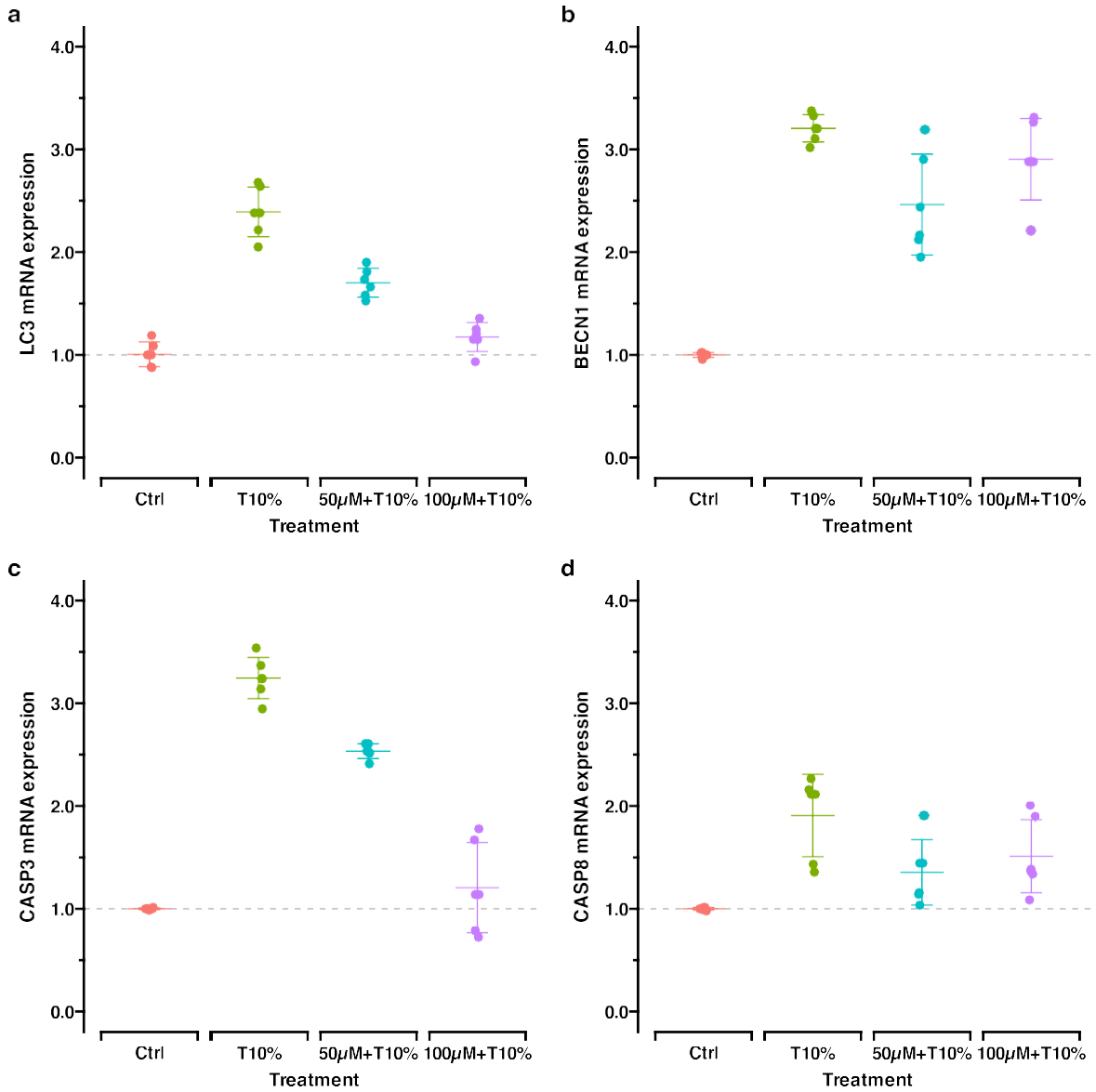

Live/Dead cell staining

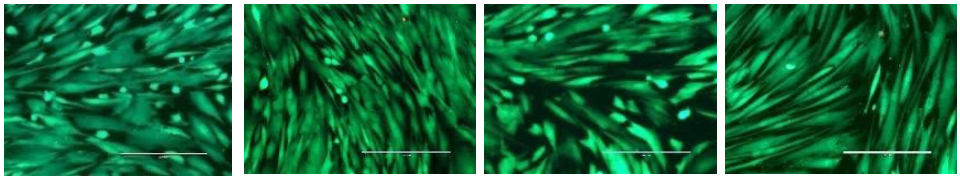

H_2O_2 (µM)	0	0	50	100
Tension (%)	0	10	10	10

Supplement 2 to manuscript

"Investigation of Oxidative-Stress Impact on Orthodontic Tooth Movement Using an In Vitro Tension Model"

Contents

Supplementary Table S2.1: MIQE checklist for the RT-qPCR workflow

	Details	Checklist
Sample/Template		
Source	If cancer, was biopsy screened for adjacent normal tissue?	Human alveolar-bone derived osteoblasts (hOBs) were obtained anonymously from a male donor undergoing a surgical procedure based orthodontic treatment and isolated according to established procedures [1,2].
Method of preservation	Liquid N2/RNAlater/formalin	Cell lysates were snap frozen in liquid N2 and stored at -80°C until all samples were collected.
Storage time (if appropriate)	If using samples >6 months old	Not applicable.
Handling	Fresh/frozen/formalin	Cell lysates were prepared using RNA lysis buffer from Quick-RNA™ MicroPrep kit (R1051; Zymo). They were snap-frozen in liquid nitrogen, and then stored at -80°C until further use for RNA extraction.
Extraction method	TriZol/columns	Defrosted cells lysates were passed through QIAshredder™ columns (Qiagen) to shear genomic DNA. The Quick-RNA™ Miniprep Kit (Zymo) was used for further RNA purification. After primary column purification, DNase I digestion was applied to reduce genomic DNA contamination as described by the manufacturer (Zymo). Finally, DNase/RNase-free water was used to elute the RNA from the columns. Before storage in the -80°C, RNase inhibitor RNasin® (Promega) was added to each preparation.
RNA:DNA-free	Intron-spanning primers/no RT control	Most primers were intron-spanning (Supplementary Table 2.2). Treatment with QIAshredder™ columns (Qiagen) and DNase I digestion were applied to reduce genomic DNA contamination according to the manufacturer's instructions (Zymo).
Concentration	Nanodrop/ribogreen/microfluidics	Purity and concentration of extracted RNA were detected photometrically (Nanodrop ND-1000; PeqLab). Ratio of $A_{260/280}$>1.8 was found, indicating free of protein contamination during RNA preparations.
RNA: integrity	Microfluidics/3':5' assay	No.
Inhibition-free	Method of testing	Serial dilution of cDNA as shown in “Primer efficiency” in Supplementary Table S2.3 below.
Assay optimisation/validation		
Accession number	RefSeq XX_1234567	Table 1 in the manuscript and Supplementary Table S2.2.

	Details	Checklist
Amplicon details	Exon location, amplicon size	Supplementary Table S2.2
Primer sequence	Even if previously published	Table 3 in the manuscript; Supplementary Tables S2.2 and S2.3.
*Probe sequence**	Identify LNA or other substitutions	No probes were used.
In silico	BLAST/Primer-BLAST/m-fold	Primer-BLAST, UCSC In-Silico PCR, and ENSEMBL were used for *in silico* testing.
empirical	Primer concentration/annealing temperature	The optimal annealing temperatures were first identified by gradient PCR (TProfessional Gradient; Biometra, Goettingen, Germany) and then were finalized by qPCR on Roche LightCycler® 480 (LC480). Optimal annealing temperatures are recorded in Supplementary Table S2.3 below.
Priming conditions	Oligo-dT/random/combination/target-specific	The SuperScript® IV First Strand Synthesis System (Invitrogen) was used for cDNA synthesis with random hexamers provided. For each cDNA synthesis reaction, 600 ng total RNA was used. Target-specific primers for qPCR were used after assessment (Table 1 of the manuscript; Supplementary Table S2.3).
PCR efficiency	Dilution curve	Information on serial dilutions and primer efficiency was summarized in Supplementary Table S2.3. For each gene, two technical replicates were used for each dilution for qPCR. For analysis of qPCR including the standard curves, LC480 software version 1.5.0.39 was used.
Linear dynamic range	Spanning unknown targets	The analyzing software for qPCR appointed the linear dynamic range automatically.
Limits of detection	LOD detection/accurate quantification	The analyzing software for qPCR appointed the LOD automatically.
Intra-assay variation	Copy numbers not Cq	Each gene was detected on one individual plate.
RT/PCR		
Protocols	Detailed description, concentrations, volumes	For real-time PCR, LightCycler® 480 SYBR Green I Master kit (04887352001; Roche Diagnostics GmbH, Mannheim, Germany) was used to detect gene expression of PTGS2/COX2, IL6, CXCL8/IL8, RUNX2, CASP3, CASP8, MAP1LC3A/LC3, BECN1, TNFRSF11B/OPG and P2RX7 using the LightCycler® 480 with LC480 software version 1.5.0.39 (both from Roche Molecular Diagnostics, Basel, Switzerland). According to the manufacturer' protocol, 5 µl diluted cDNA (1:10 with double distilled, sterile water), 1 µl gene-specific forward primer, 1 µl gene-specific reverse primers, 3 µl PCR water and 10 µl qPCR mastermix were added for reaction. PCR reactions proceeded as follows: 10 min of initial denaturation at 95 °C and 45 cycles of amplifications. Each amplification consisted of three steps: 15 s of denaturation at 95 °C, 15 s of specific annealing temperature for each primer pair and 15 s of elongation at 72 °C.

	Details	Checklist
Reagents	Supplier, Lot number	Primers for genes were synthesized using sequences from related literatures. The primers were verified by *in silico* tests using related bioinformatic tools given in **Supplementary Table S2.2**. All primers were synthesized by TIB Molbiol Syntheselabor GmbH (Berlin, Germany). Information on the kits used (Quick-RNA™ MicroPrep kit; SuperScript® IV First Strand Synthesis kit, Invitrogen; LightCycler® 480 SYBR Green I Master kit, Roche) were all given in the manuscript.
Duplicate RT	ΔCq	No, but two technical replicates were repeated for each biological replicate at minimum.
NTC	Cq & melt curves	Yes
NAC	ΔCq beginning:end of qPCR	No, as no probes were used.
Positive control	Inter-run calibrators	No, each gene was tested on one plate with all samples included.
Data analysis		
Specialist software	e.g., QBAsePlus	IBM SPSS Statistics 29 (IBM Corp., Armonk, NY, USA)
Statistical justification	e.g., biological replicates	For each force magnitude for every force duration, three biological replicates were used. Each biological replicate was repeated with two technical replicates, giving a total of 6 amplifications of qPCR.
Transparent, validated normalization	e.g., GeNorm summary	After testing with RT-qPCR using cDNA from some samples and assessment with RefFinder, *EEF1A1* and *PPIB* were proved to be most stable in this experiment among the panel of reference genes. Therefore, *EEF1A1* and *PPIB* were used as reference genes for following analysis.

Supplementary Table S2.2: *In-silico* analysis of the RT-qPCR primer

Official gene symbol	**Reference sequence** (NCBI GenBank)	**5'-forward primer-3'** (length / T_m / %GC / Self-comp./Self-3'-comp.)	**5'-reverse primer-3'** (length / T_m / %GC / Self-comp./Self-3'-comp.)	**Amplicon length (bp)**	**Amplicon location** (bp of Start/Stop)	**Intron spanning** (length, bp)	**In silico qPCR specificity**	**Variants targeted** (Transcript/ Splice)	**Reference**
Genes of interest									
PTGS2	NM_000963.4	AAGCCTTCTCTAACCTCTCC (20 / 55.9°C / 50% / 5/0)	GCCCTCGCTTATGATCTGTC (20 / 58.2°C / 55% / 4/1)	234	510 / 743	Yes (430)	Yes (BLAST, UCSC)	Yes	[3], [4]
IL6	NM_000600.5	TGGCAGAAAACAACCTGAACC (21 / 56.5°C / 48% / 3/0)	TGGCTTGTTCCTCACTACTCTC (22 / 56.9°C / 50% / 2/0)	168	317 / 484	Yes (707)	Yes (BLAST, UCSC)	Yes	[3], [4]
CXCL8 / IL8	NM_000584.4	CAGAGACAGCAGAGCACACAA (21 / 60.5°C / 52% / 2/0)	TTAGCACTCCTTGGCAAAAC (20 / 56.5°C / 45% / 5/0)	170	10 / 179	Yes (819)	Yes (BLAST)	Yes	[5]
RUNX2	NM_001015051.4	GCGCATTCCTCATCCCAGTA (20 / 56.9°C / 55% / 4/2)	GGCTCAGGTAGGAGGGGTAA (20 / 56.9°C / 60% / 3/1)	176	947 / 1122	Yes (20131)	Yes (BLAST, UCSC)	Yes	[1], [3]
BECN1	NM_003766.5	AGGTTGAGAAAGGCGAGACA (20 / 58.9°C / 50% / 2/0)	AATTGTGAGGACACCCAAGC (20 / 58.3°C / 50% / 4/2)	196	1297 / 1492	Yes (726)	Yes (BLAST)	Yes	[6]
MAP1LC3A/LC3	NM_032514.4	CGTCCTGGACAAGACCAAGT (20 / 59.6°C / 55% / 7/2)	TCCTCGTCTTTCTCCTGCTC (20 / 58.8°C / 55% / 2/0)	183	286 / 468	Yes (179)	Yes (BLAST)	Yes	[6]
CASP3	NM_004346.4	TGGAGGCCGACTTCTTGTAT (20 / 58.4°C / 50% / 4/2)	ACTGTTTCAGCATGGCACAA (20 / 58.6°C / 45% / 4/2)	111	801 / 911	Yes (1535)	Yes (BLAST)	Yes	[7]
CASP8	NM_001228.5	GGAGGAGTTGTGTGGGGTAA (20 / 58.9°C / 55% / 2/1)	CCTGCATCCAAGTGTGTTCC (20 / 59.1°C / 55% / 4/0)	207	931 / 1137	Yes (1873)	Yes (BLAST)	Yes	[8]
TNFRSF11B	NM_002546.4	TCAAGCAGGAGTGCAATCG (19 / 54.9°C / 53% / 6/4)	AGAATGCCTCCTCACACAGG (20 / 56.3°C / 55% / 4/1)	342	342 / 683	Yes (6020)	Yes (BLAST, UCSC)	Yes	[9]
P2RX7	NM_002562.6	AGTGCGAGTCCATTGTGGAG (20 / 57.0°C / 55% / 5/3)	CATCGCAGGTCTTGGGACTT (20 / 57.0°C / 55% / 5/2)	143	1303 / 1445	Intron- and exon-spanning	Yes (BLAST, UCSC)	Yes	[1]
Reference genes									
RPL0	NM_001002.4	GAAACTCTGCATTCTCGCTTCC (22 / 57.4°C / 50% / 4/0)	GACTCGTTTGTACCCGTTGATG (22 / 57.1°C / 50% / 4/0)	120	702 / 821	Yes (1091)	Yes (BLAST/UCSC)	Yes	[10], [11]
RPL22	NM_000983.4	TGATTGCACCCACCCTGTAG (20 / 56.6°C / 55% / 4/2)	GGTTCCCAGCTTTTCCGTTC (20 / 56.4°C / 55% / 4/0)	98	91 / 188	Yes (4597)	Yes (BLAST/UCSC)	Yes	[10], [11]
GAPDH	NM_002046.7	CTCCTGTTCGACAGTCAGCC (20 / 57.4°C / 60% / 6/1)	CGACCAAATCCGTTGACTCC (20 / 55.9°C/ 55%/ 3/1)	103	12 / 114	Yes, rev. primer on exon junction	Yes (BLAST/UCSC)	Yes	[10], [12]
EEF1A1	NM_001402.6	CCTGCCTCTCCAGGATGTCTAC (22 / 59.0°C / 59% / 5/2)	GGAGCAAAGGTGACCACCATAC (22 / 58.7°C / 55% / 6/2)	105	804 / 908	Yes (87)	Yes (BLAST/UCSC)	Yes	[10], [11]
PPIB	NM_000942.5	TTCCATCGTGTAATCAAGGACTTC (24 / 56.7°C / 42% / 4/2)	GCTCACCGTAGATGCTCTTTC (21 / 56.1°C / 52% / 4/0)	88	313 / 400	Yes (3194)	Yes (BLAST/UCSC)	Yes	[10], [11]
YWHAZ	NM_003406.4	AGGAGATTACTACCGTTACTTGGC (24 / 57.8°C / 46% / 4/2)	AGCTTCTTGGTATGCTTGTTGTG (23 / 57.4°C / 43% / 4/0)	91	491 / 581	Yes (617)	Yes (BLAST/UCSC)	Yes	[10], [11]
RNA18SN5	NR_003286.4	AACTGCGAATGGCTCATTAAATC (23 / 55.8°C / 39% / 6/3)	GCCCGTCGGCATGTATTAG (19 / 55.2°C / 58% / 5/1)	103	84 / 186	No (rRNA)	No (RNA45S5 also targeted)	-	[10], [11]
POLR2A	NM_000937.5	TCGCTTACTGTCTTCCTGTTGG (22 / 57.8°C / 50% / 3/0)	TGTGTTGGCAGTCACCTTCC (20 / 57.4°C / 55% / 3/3)	108	3811 / 3918	Yes (468)	Yes (BLAST/UCSC)	Yes	[10], [11]

T_m, melting temperature of primer or qPCR product (amplicon); %GC, percent of guanin/cytosine content; bp, base pairs; Self-comp., self-complementary; Self-3'-comp., self 3' complementary.

To perform silico analysis of RT-qPCR primers, their targets and corresponding amplification products, the following programs and online resources were used. All URLs were valid on 02-12-2020.

a. Primer-BLAST (URL: https://www.ncbi.nlm.nih.gov/tools/primer-blast/) was used to check the melting temperature (T_m) and the "length" of each primer, their "in silico qPCR specificity", possible co-amplification of genomic DNA, "Self-comp." and "Self-3'-comp".
    i. Settings for "Refseq mRNA": max primer annealing: 65; intron length range: 100 – 100000, max. target amplicon size: 40000
    ii. Settings for "Refseq representative genomes": max primer annealing: 65; intron length range: 100 – 100000, max. target amplicon size: 40000
b. UCSC In-Silico PCR (URL: https://genome.ucsc.edu/cgi-bin/hgPcr) was used to check "In silico qPCR specificity" and RT-qPCR in genomic context.
c. "Amplicon (length)", "Amplicon location (bp of Start/Stop)", "Intron-spanning (length)" was identified or calculated by either Primer-BLAST or UCSC In-Silico PCR
d. ENSEMBL (URL: https://www.ensembl.org) was used to check "Variants targeted (Transcript/Splice)".

Supplementary Table S2.3: Primer validation by RT-qPCR

Gene symbol	Primer sequence (f: 5'-forward primer-3'; r: 5'-reverse primer-3')	Reference	Specificity by melting curve / T_m (°C)	Specificity by agarose gel / amplicon size (bp)	Annealing temp. (°C)	Dilution series used for efficiency testing – starting from 1:10 prediluted cDNA	Primer efficiency			
							Efficiency	Error	Slope	Y intercept
Genes of interest										
PTGS2	f: AAGCCTTCTCTAACCTCTCC r: GCCCTCGCTTATGATCTGTC	[3], [4]	Yes / 81.7	234	58	1:1, 1:10, 1:100, 1:1000	2.028	0.0768	-3.257	35.67
IL6	f: TGGCAGAAAACAACCTGAACC r: TGGCTTGTTCCTCACTACTCTC	[3], [4]	Yes / 80.3	168	58	1:1, 1:10, 1:100, 1:1000	1.999	0.0277	-3.325	39.05
CXCL8	f: CAGAGACAGCAGAGCACACAA r: TTAGCACTCCTTGGCAAAAC	[5]	Yes/ 84.5	170	55	1:1, 1:4, 1:16, 1:64, 1:256	2.082	0.025	-3.141	34.17
RUNX2	f: GCGCATTCCTCATCCCAGTA r: GGCTCAGGTAGGAGGGGTAA	[1], [3]	Yes / 85.3	176	58	1:1, 1:10, 1:100, 1:1000	1.94	0.00746	-3.475	39.04
BCN1	f: AGGTTGAGAAAGGCGAGACA r: AATTGTGAGGACACCCAAGC	[6]	Yes/ 82.7	196	58	1:1, 1:10, 1:100, 1:1000	2.037	0.0676	-3.237	33.41
MAP1LC3A	f: CGTCCTGGACAAGACCAAGT r: TCCTCGTCTTTCTCCTGCTC	[6]	Yes/ 87.8	183	58	1:1, 1:10, 1:100, 1:1000	1.951	0.0674	-3.445	34.7
CASP3	f: TGGAGGCCGACTTCTTGTAT r: ACTGTTTCAGCATGGCACAA	[7]	Yes/ 81.7	111	58	1:1, 1:10, 1:100, 1:1000	1.984	0.01	-3.362	37.23
CASP8	f: GGAGGAGTTGTGTGGGGTAA r: CCTGCATCCAAGTGTGTTCC	[8]	Yes/ 81.0	207	58	1:1, 1:10, 1:100, 1:1000	2.033	0.0614	-3.245	35.23
TNFRSF11B	f: TCAAGCAGGAGTGCAATCG r: AGAATGCCTCCTCACACAGG	[9]	Yes / 84.8	342	64	1:1, 1:10, 1:100, 1:1000, 1:10000	1.915	0.0164	-3.545	37.27
P2RX7	f: AGT GCG AGT CCA TTG TGG AG r: CAT CGC AGG TCT TGG GAC TT	[1]	Yes/ 82.5	143	58	undiluted, 1:2, 1:4, 1:8	2.048	0.0298	-3.211	35.24
Reference genes										
RPL0	f: GAAACTCTGCATTCTCGCTTCC r: GACTCGTTTGTACCCGTTGATG	[10], [11]	Yes / 83.8	120	64	1:1, 1:10, 1:100, 1:1000, 1:10000	1.947	0.027	-3.455	32.54
RPL22	f: TGATTGCACCCACCCTGTAG r: GGTTCCCAGCTTTTCCGTTC	[10], [11]	Yes / 80.1	98	61	1:1, 1:10, 1:100, 1:1000, 1:10000	2.004	0.007	-3.313	33.4
GAPDH	f: CAACTACATGGTTTACATGTTC r: GCCAGTGGACTCCACGAC	[10], [12]	Yes / 84.4	103	52	1:1, 1:10, 1:100, 1:1000, 1:10000	1.968	0.002	-3.4	30.4
EEF1A1	f: CCTGCCTCTCCAGGATGTCTAC r: GGAGCAAAGGTGACCACCATAC	[10], [11]	Yes / 82.4	105	61	1:1, 1:10, 1:100, 1:1000, 1:10000	2.038	0.002	-3.235	29.41
PPIB	f: TTCCATCGTGTAATCAAGGACTTC r: GCTCACCGTAGATGCTCTTTC	[10], [11]	Yes / 82.4	88	55	1:1, 1:10, 1:100, 1:1000, 1:10000	1.992	0.007	-3.341	33.77
YWHAZ	f: AGGAGATTACTACCGTTACTTGGC r: AGCTTCTTGGTATGCTTGTTGTG	[10], [11]	Yes / 81.3	91	55	1:1, 1:10, 1:100, 1:1000, 1:10000	2.019	0.012	-3.276	33.48
RNA18SN5	f: AACTGCGAATGGCTCATTAAATC r: GCCCGTCGGCATGTATTAG	[10], [11]	Yes / 80.4	103	55	1:1, 1:10, 1:100, 1:1000, 1:10000	2.022	0.021	-3.271	19.26
POLR2A	f: TCGCTTACTGTCTTCCTGTTGG r: TGTGTTGGCAGTCACCTTCC	[10], [11]	Yes / 83.7	108	58	1:1, 1:10, 1:100, 1:1000, 1:10000	2.046	0.016	-3.216	34.72

References

1. Shi, J.; Folwaczny, M.; Wichelhaus, A.; Baumert, U. Differences in *RUNX2* and *P2RX7* gene expression between mono- and coculture of human periodontal ligament cells and human osteoblasts under compressive force application. *Orthod. Craniofac. Res.* **2019**, *22*, 168-176.
2. Ng, K.W.; Schantz, J.-T. *A Manual for Primary Human Cell Culture*, 2nd ed.; World Scientific: Hackensack, NJ, USA, 2010; pp. 38-47.
3. Janjic Rankovic, M.; Docheva, D.; Wichelhaus, A.; Baumert, U. Effect of static compressive force on in vitro cultured PDL fibroblasts: monitoring of viability and gene expression over 6 days. *Clin. Oral Investig.* **2020**, *24*, 2497-2511.
4. Shi, J.; Baumert, U.; Folwaczny, M.; Wichelhaus, A. Influence of static forces on the expression of selected parameters of inflammation in periodontal ligament cells and alveolar bone cells in a co-culture in vitro model. *Clin. Oral Investig.* **2019**, *23*, 2617-2628.
5. Jones, R.L.; Hannan, N.J.; Kaitu'u, T.J.; Zhang, J.; Salamonsen, L.A. Identification of chemokines important for leukocyte recruitment to the human endometrium at the times of embryo implantation and menstruation. *J. Clin. Endocrinol. Metab.* **2004**, *89*, 6155-6167.
6. Zhuang, H.; Hu, D.; Singer, D.; Walker, J.V.; Nisr, R.B.; Tieu, K.; Ali, K.; Tredwin, C.; Luo, S.; Ardu, S.; et al. Local anesthetics induce autophagy in young permanent tooth pulp cells. *Cell Death Discov.* **2015**, *1*, 15024.
7. Wang, Y.; Du, C.; Wan, W.; He, C.; Wu, S.; Wang, T.; Wang, F.; Zou, R. shRNA knockdown of integrin-linked kinase on hPDLCs migration, proliferation, and apoptosis under cyclic tensile stress. *Oral Dis.* **2020**, *26*, 1747-1754.
8. Cao, Z.; Zhang, H.; Cai, X.; Fang, W.; Chai, D.; Wen, Y.; Chen, H.; Chu, F.; Zhang, Y. Luteolin Promotes Cell Apoptosis by Inducing Autophagy in Hepatocellular Carcinoma. *Cell. Physiol. Biochem.* **2017**, *43*, 1803-1812.
9. Yang, Y.; Yang, Y.; Li, X.; Cui, L.; Fu, M.; Rabie, A.B.; Zhang, D. Functional analysis of core binding factor a1 and its relationship with related genes expressed by human periodontal ligament cells exposed to mechanical stress. *Eur. J. Orthod.* **2010**, *32*, 698-705.
10. Sun, C.; Janjic Rankovic, M.; Folwaczny, M.; Stocker, T.; Otto, S.; Wichelhaus, A.; Baumert, U. Effect of Different Parameters of In Vitro Static Tensile Strain on Human Periodontal Ligament Cells Simulating the Tension Side of Orthodontic Tooth Movement. *Int. J. Mol. Sci.* **2022**, *23*, 1525.
11. Nazet, U.; Schröder, A.; Spanier, G.; Wolf, M.; Proff, P.; Kirschneck, C. Simplified method for applying static isotropic tensile strain in cell culture experiments with identification of valid RT-qPCR reference genes for PDL fibroblasts. *Eur. J. Orthod.* **2020**, *42*, 359-370.
12. Chirieleison, S.M.; Marsh, R.A.; Kumar, P.; Rathkey, J.K.; Dubyak, G.R.; Abbott, D.W. Nucleotide-binding oligomerization domain (NOD) signaling defects and cell death susceptibility cannot be uncoupled in X-linked inhibitor of apoptosis (XIAP)-driven inflammatory disease. *J. Biol. Chem.* **2017**, *292*, 9666-9679.

Supplement 3 to manuscript

"Investigation of Oxidative-Stress Impact on Orthodontic Tooth Movement Using an In Vitro Tension Model"

URL: https://www.ciidirsinaloa.com.mx/RefFinder-master/ (2024-04-26)

RefFinder is a user-friendly web-based comprehensive tool developed for evaluating and screening reference genes from extensive experimental datasets. It integrates the currently available major computational programs (geNorm, Normfinder, BestKeeper, and the comparative ΔCt method) to compare and rank the tested candidate reference genes. Based on the rankings from each program, it assigns an appropriate weight to an individual gene and calculated the geometric mean of their weights for the overall final ranking.

Citation: F Xie, P Xiao, D Chen, L Xu, B Zhang. 2012. miRDeepFinder: a miRNA analysis tool for deep sequencing of plant small RNAs. Plant Mol Biol 80 (1), 75-84.

References

1. BestKeeper: Pfaffl MW, Tichopad A, Prgomet C, Neuvians TP. 2004. Determination of stable housekeeping genes, differentially regulated target genes and sample integrity: BestKeeper--Excel-based tool using pair-wise correlations. Biotechnology Lett 26:509-515.
2. NormFinder: Andersen CL, Jensen JL, Orntoft TF. 2004. Normalization of real-time quantitative reverse transcription-PCR data: a model-based variance estimation approach to identify genes suited for normalization, applied to bladder and colon cancer data sets. Cancer Res 64:5245-5250.
3. Genorm: Vandesompele J, De Preter K, Pattyn F, Poppe B, Van Roy N, De Paepe A, Speleman F. 2002. Accurate normalization of real-time quantitative RT-PCR data by geometric averaging of multiple internal control genes. Genome Biol 3:RESEARCH0034.
4. The comparative delta-Ct method: Silver N, Best S, Jiang J, Thein SL. 2006. Selection of housekeeping genes for gene expression studies in human reticulocytes using real-time PCR. BMC Mol Biol 7:33.

Contents

1 Raw data (Cq values)

Condition	Group	GAPDH	RPL22	RPL0	RNA18SN5	PPIB	YWHAZ	EEF1A1	POLR2A
Control	0	18.43	21.75	21.01	8.17	21.62	22.00	18.17	23.28
Control	0	18.44	21.68	20.86	8.27	21.55	21.96	18.15	23.26
H_2O_2 100µM	1	18.56	21.69	22.89	6.40	20.51	21.00	17.50	22.53
H_2O_2 100µM	1	19.86	20.24	18.30	6.44	20.52	20.97	17.52	22.52
H_2O_2 50µM	1	18.14	21.67	20.97	7.53	21.49	21.21	18.04	22.71
H_2O_2 50µM	1	18.14	21.71	20.97	7.47	21.69	21.19	18.06	22.73
H_2O_2 100µM + T10%	3	16.97	20.91	20.42	6.00	20.15	20.09	17.26	21.73
H_2O_2 100µM + T10%	3	17.09	20.91	20.48	6.00	20.17	20.10	17.29	21.74
H_2O_2 50µM + T10%	3	16.42	20.05	19.65	6.00	19.80	19.59	16.42	21.73
H_2O_2 50µM + T10%	3	16.43	19.91	19.49	6.00	19.69	19.60	16.44	21.73
T10%	2	16.97	20.80	19.33	6.82	19.23	18.86	15.99	20.83
T10%	2	17.01	19.98	18.24	6.00	19.22	18.87	16.04	20.87
H_2O_2 100µM + T15%	3	16.61	20.21	19.83	6.00	19.65	19.67	16.69	21.95
H_2O_2 100µM + T15%	3	16.55	20.14	19.77	6.00	19.66	19.68	16.71	21.97
H_2O_2 50µM + T15%	3	16.56	20.10	19.69	6.00	19.72	19.67	16.53	21.96
H_2O_2 50µM + T15%	3	16.50	20.09	19.72	6.00	19.73	19.66	16.56	21.99
T15%	2	16.03	19.71	19.31	5.00	19.92	19.05	16.02	21.52
T15%	2	15.91	19.70	19.15	6.00	19.75	19.08	16.05	21.58

	Ctrl (N= 2)	H_2O_2 100µM, H_2O_2 50µM (N= 4)	T10%, T15% (N= 4)	H_2O_2 50/100µM + T10%, H_2O_2 50/100µM + T15% (N= 8)	All (N= 18)
Group	0	1	2	3	5
GAPDH					
Mean (SD)	18 (0.0071)	19 (0.81)	16 (0.59)	17 (0.25)	17 (1.1)
Median [Min, Max]	18 [18, 18]	18 [18, 20]	17 [16, 17]	17 [16, 17]	17 [16, 20]
RPL22					
Mean (SD)	22 (0.049)	21 (0.73)	20 (0.52)	20 (0.39)	21 (0.77)
Median [Min, Max]	22 [22, 22]	22 [20, 22]	20 [20, 21]	20 [20, 21]	20 [20, 22]
RPL0					
Mean (SD)	21 (0.11)	21 (1.9)	19 (0.52)	20 (0.37)	20 (1.1)
Median [Min, Max]	21 [21, 21]	21 [18, 23]	19 [18, 19]	20 [19, 20]	20 [18, 23]
RNA18SN5					
Mean (SD)	8.2 (0.071)	7.0 (0.62)	6.0 (0.74)	6.0 (0)	6.5 (0.87)
Median [Min, Max]	8.2 [8.2, 8.3]	7.0 [6.4, 7.5]	6.0 [5.0, 6.8]	6.0 [6.0, 6.0]	6.0 [5.0, 8.3]
PPIB					
Mean (SD)	22 (0.049)	21 (0.63)	20 (0.36)	20 (0.21)	20 (0.82)
Median [Min, Max]	22 [22, 22]	21 [21, 22]	19 [19, 20]	20 [20, 20]	20 [19, 22]
YWHAZ					
Mean (SD)	22 (0.028)	21 (0.13)	19 (0.12)	20 (0.21)	20 (1.0)
Median [Min, Max]	22 [22, 22]	21 [21, 21]	19 [19, 19]	20 [20, 20]	20 [19, 22]
EEF1A1					
Mean (SD)	18 (0.014)	18 (0.31)	16 (0.026)	17 (0.35)	17 (0.79)
Median [Min, Max]	18 [18, 18]	18 [18, 18]	16 [16, 16]	17 [16, 17]	17 [16, 18]
POLR2A					
Mean (SD)	23 (0.014)	23 (0.11)	21 (0.41)	22 (0.13)	22 (0.69)
Median [Min, Max]	23 [23, 23]	23 [23, 23]	21 [21, 22]	22 [22, 22]	22 [21, 23]

2 RefFinder – Summary

Ranking Order (Better--Good--Average)

Method	1	2	3	4	5	6	7	8
Delta CT	EEF1A1	PPIB	YWHAZ	POLR2A	RPL22	RNA18SN5	GAPDH	RPL0
BestKeeper	POLR2A	RNA18SN5	PPIB	RPL22	EEF1A1	RPL0	YWHAZ	GAPDH
Normfinder	EEF1A1	PPIB	YWHAZ	RPL22	POLR2A	RNA18SN5	GAPDH	RPL0
Genorm	PPIB | EEF1A1		YWHAZ	POLR2A	RPL22	RNA18SN5	GAPDH	RPL0
Recommended comprehensive ranking	**EEF1A1**	**PPIB**	**POLR2A**	**YWHAZ**	**RPL22**	**RNA18SN5**	**GAPDH**	**RPL0**

Comprehensive Ranking:

Genes	Geomean of ranking values
EEF1A1	1.50
PPIB	1.86
POLR2A	2.99
YWHAZ	3.71
RPL22	4.47
RNA18SN5	4.56
GAPDH	7.24
RPL0	7.44

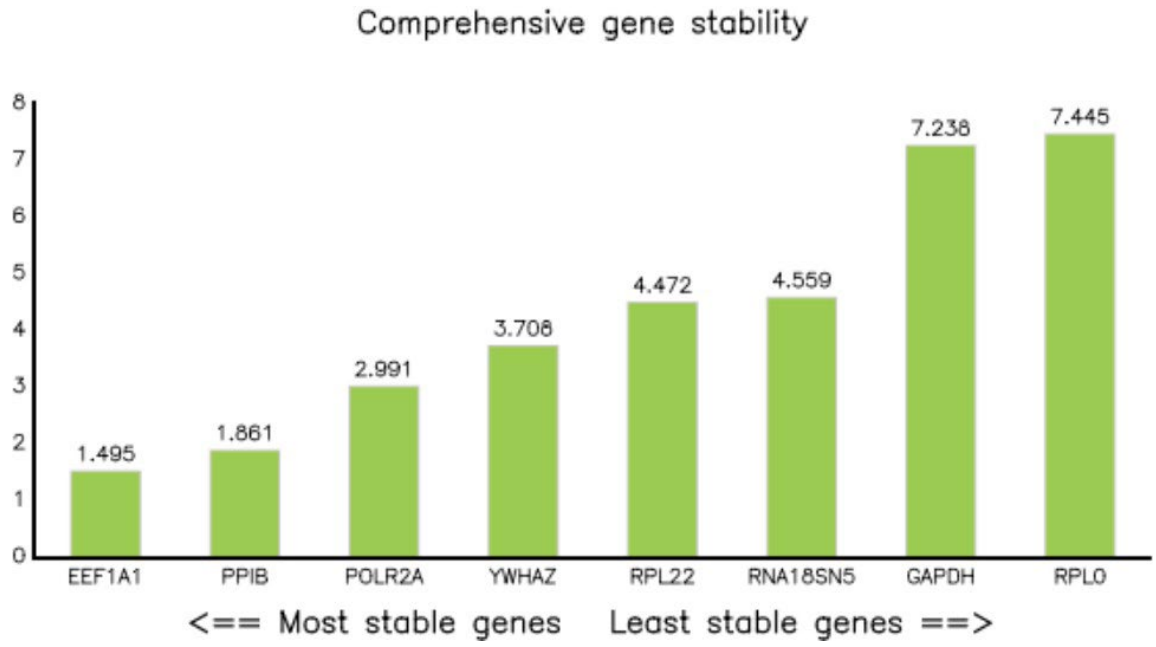

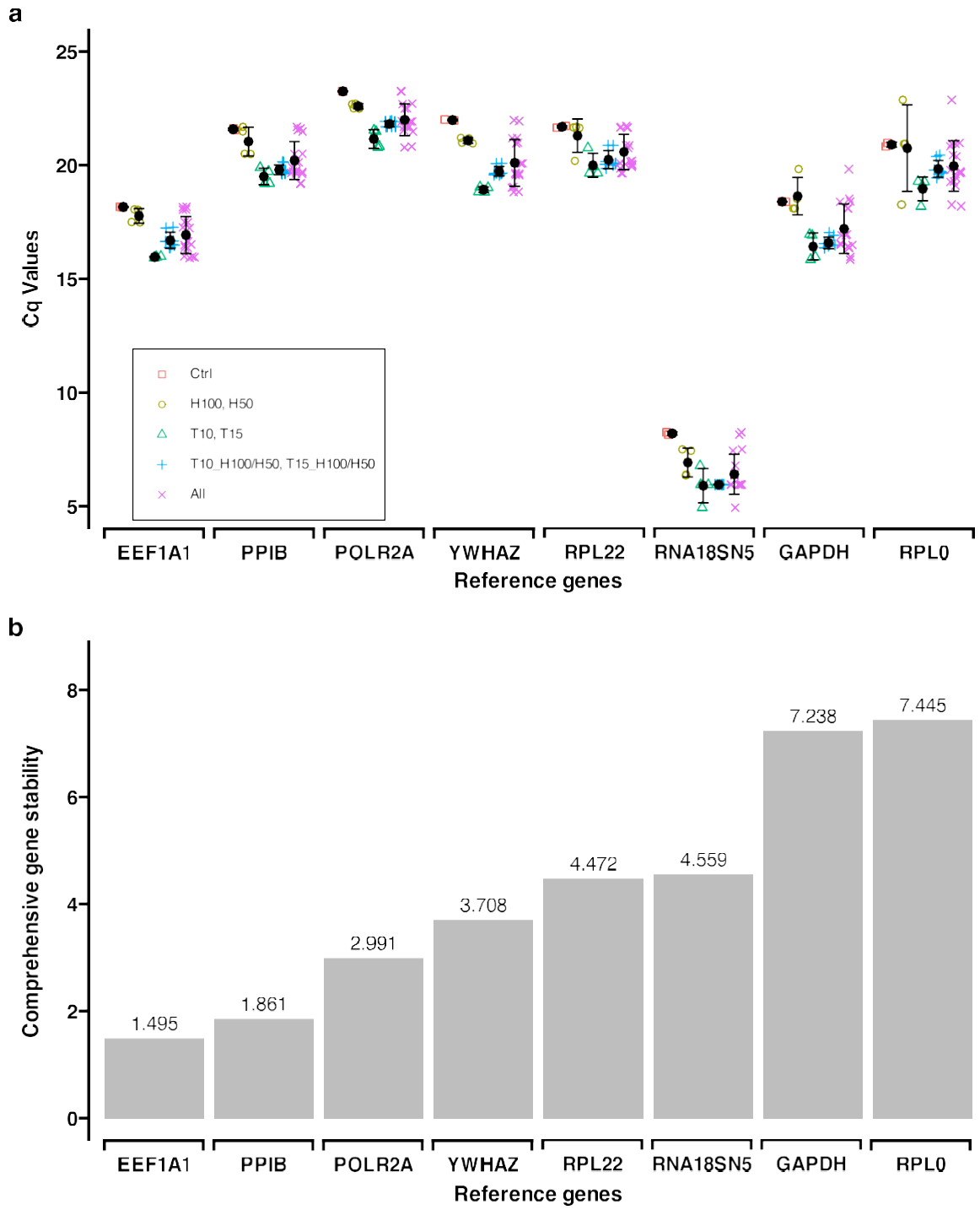

Summary figure. Reference gene stability - comparison between qPCR raw data (see section 1) RefFinder results. (a) Cq values for the panel of reference genes, using samples exposed to different experimental conditions (Ctrl, control; H100/H50, 50 µM or 100 µM H_2O_2 incubation for 24 h and 24 h recovery; T10 / T15, 10 % or 15 % static stretching applied for 24 h; T10_H100/H50 resp. T15_H100/H50, 50 µM or 100 µM H_2O_2 incubation for 24 h followed by 24 h static stretching at 10 % or 15 %; All, average expression for all four experimental regimes). Two qPCR runs of each combination were analyzed representing one biological sample with two technical replicates each. (b) Comprehensive gene stability analysis for the panel of reference genes. Lower values indicate higher gene stability.

2.1 Delta CT

Genes	Average of STDEV
EEF1A1	0.48
PPIB	0.53
YWHAZ	0.54
POLR2A	0.56
RPL22	0.57
RNA18SN5	0.66
GAPDH	0.81
RPL0	0.92

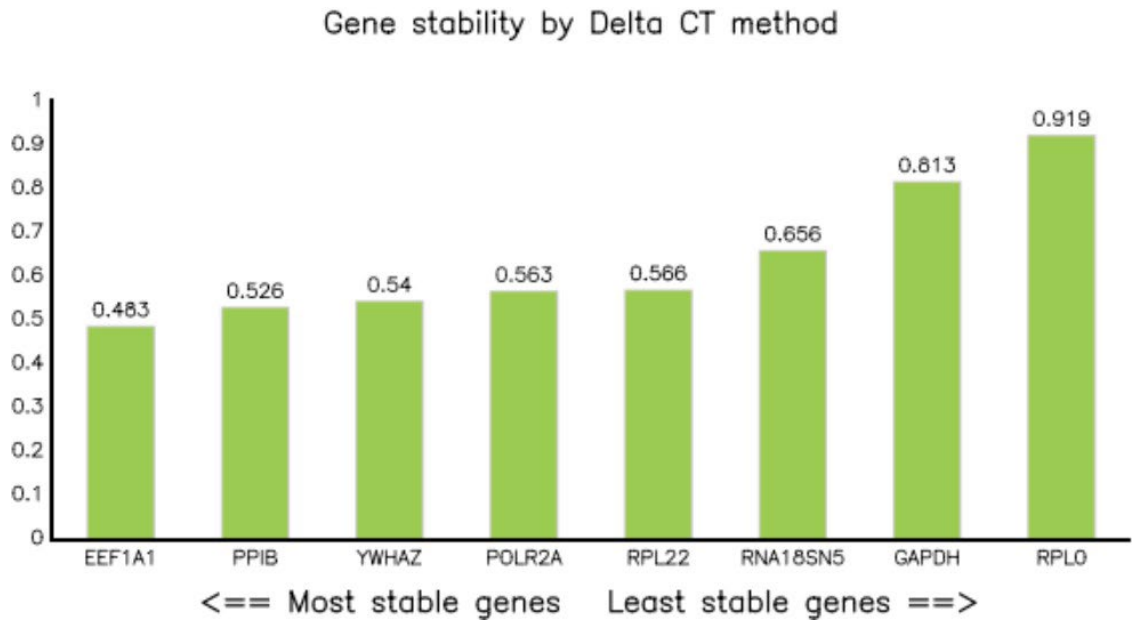

2.2 BestKeeper

CP data of housekeeping Genes by BEST KEEPER

	GAPDH	RPL22	RPL0	RNA18SN5	PPIB	YWHAZ	EEF1A1	POLR2A
n	18	18	18	18	18	18	18	18
geo Mean [CP]	17.23	20.61	19.98	6.40	20.21	20.10	16.95	22.02
AR Mean [CP]	17.26	20.63	20.00	6.45	20.23	20.13	16.97	22.04
min [CP]	15.91	19.70	18.24	5.00	19.22	18.86	15.99	20.83
max [CP]	19.86	21.75	22.89	8.27	21.69	22.00	18.17	23.28
std dev [+/- CP]	0.89	0.68	0.84	0.67	0.67	0.84	0.69	0.54
CV [% CP]	5.17	3.30	4.20	10.35	3.31	4.18	4.09	2.43
min [x-fold]	-2.49	-1.88	-3.33	-2.64	-1.99	-2.36	-1.95	-2.29
max [x-fold]	6.21	2.20	7.54	3.66	2.79	3.73	2.33	2.39
std dev [+/- x-fold]	1.86	1.60	1.79	1.59	1.59	1.79	1.62	1.45

Pearson correlation coefficient (r) by BEST KEEPER

	GAPDH	RPL22	RPL0	RNA18SN5	PPIB	YWHAZ	EEF1A1	POLR2A
RPL22	0.684	-	-	-	-	-	-	-
p-value	0.002	-	-	-	-	-	-	-
RPL0	0.351	0.805	-	-	-	-	-	-
p-value	0.153	0.001	-	-	-	-	-	-
RNA18SN5	0.664	0.826	0.466	-	-	-	-	-
p-value	0.003	0.001	0.051	-	-	-	-	-
PPIB	0.704	0.825	0.612	0.811	-	-	-	-
p-value	0.001	0.001	0.007	0.001	-	-	-	-
YWHAZ	0.817	0.833	0.642	0.818	0.936	-	-	-
p-value	0.001	0.001	0.004	0.001	0.001	-	-	-
EEF1A1	0.794	0.868	0.658	0.786	0.935	0.973	-	-
p-value	0.001	0.001	0.003	0.001	0.001	0.001	-	-
POLR2A	0.689	0.695	0.609	0.734	0.901	0.954	0.900	-
p-value	0.002	0.001	0.007	0.001	0.001	0.001	0.001	-

Pearson correlation coefficient (r)

BestKeeper vs.	GAPDH	RPL22	RPL0	RNA18SN5	PPIB	YWHAZ	EEF1A1	POLR2A
coeff. of corr. [r]	0.803	0.926	0.689	0.907	0.933	0.968	0.956	0.889
p-value	0.001	0.001	0.002	0.001	0.001	0.001	0.001	0.001

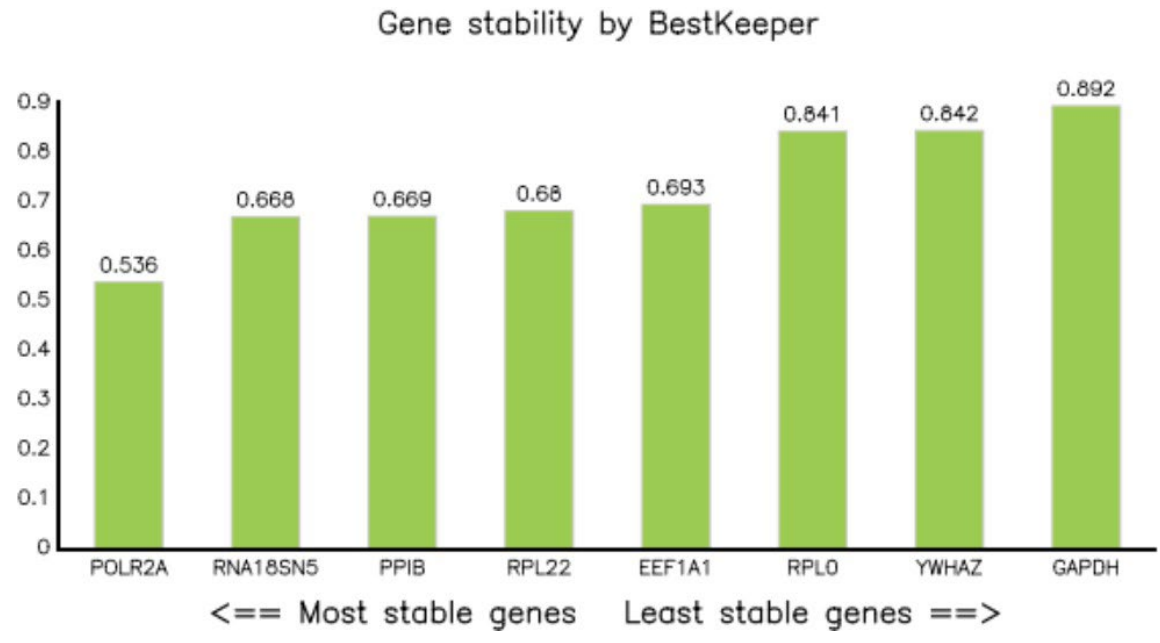

2.3 normFinder

Gene name	Stability value
EEF1A1	0.106
PPIB	0.262
YWHAZ	0.278
RPL22	0.295
POLR2A	0.331
RNA18SN5	0.488
GAPDH	0.714
RPL0	0.846

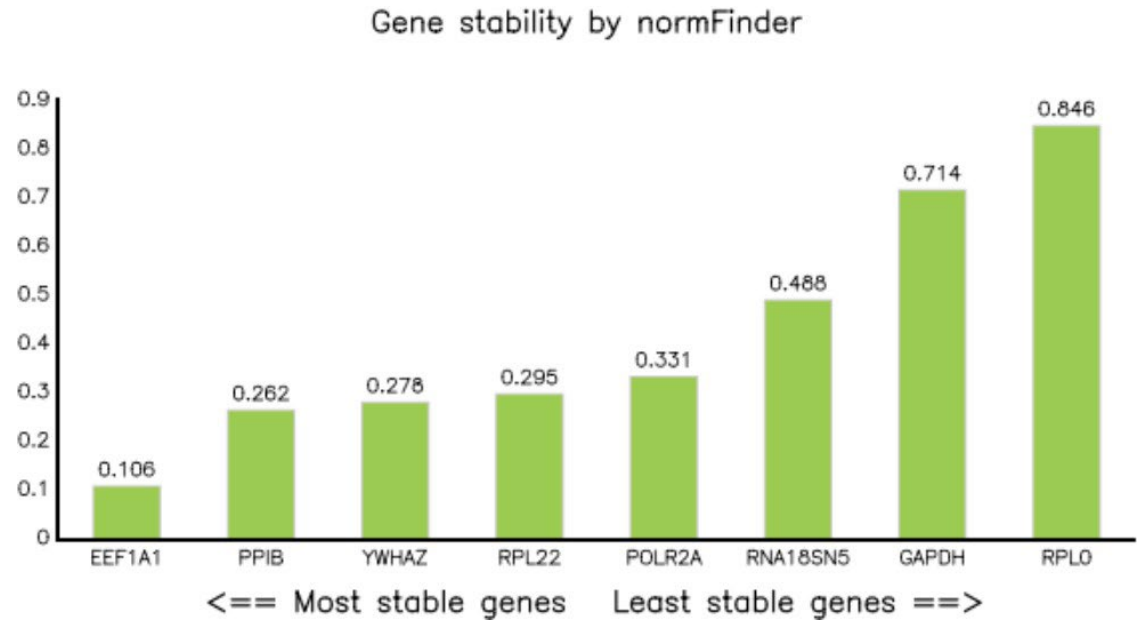

2.4 Genorm

Gene name	Stability value
PPIB | EEF1A1	0.293
YWHAZ	0.326
POLR2A	0.349
RPL22	0.411
RNA18SN5	0.456
GAPDH	0.538
RPL0	0.633

References

Almerich-Silla JM, Montiel-Company JM, Pastor S, Serrano F, Puig-Silla M, Dasi F (2015). Oxidative Stress Parameters in Saliva and Its Association with Periodontal Disease and Types of Bacteria. Dis Markers; 2015:653537.

Chen H, Huang X, Fu C, Wu X, Peng Y, Lin X, Wang Y (2019a). Recombinant Klotho Protects Human Periodontal Ligament Stem Cells by Regulating Mitochondrial Function and the Antioxidant System during H_2O_2-Induced Oxidative Stress. Oxid Med Cell Longev; 2019:9261565.

Chen M, Cai W, Zhao S, Shi L, Chen Y, Li X, Sun X, Mao Y, He B, Hou Y, Zhou Y, Zhou Q, Ma J, Huang S (2019b). Oxidative stress-related biomarkers in saliva and gingival crevicular fluid associated with chronic periodontitis: A systematic review and meta-analysis. J Clin Periodontol; 46(6):608-622.

Chen Z, Lu M, Zhang Y, Wang H, Zhou J, Zhou M, Zhang T, Song J (2022). Oxidative stress state inhibits exosome secretion of hPDLCs through a specific mechanism mediated by PRMT1. J Periodontal Res; 57(6):1101-1115.

Christensen L, Luther F (2015). Adults seeking orthodontic treatment: expectations, periodontal and TMD issues. Br Dent J; 218(3):111-7.

Davidovitch Z (1991). Tooth movement. Crit Rev Oral Biol Med; 2(4):411-50.

Durham J, Fraser HM, McCracken GI, Stone KM, John MT, Preshaw PM (2013). Impact of periodontitis on oral health-related quality of life. J Dent; 41(4):370-6.

Hosseini S, Diegelmann J, Folwaczny M, Frasheri I, Wichelhaus A, Sabbagh H, Seidel C, Baumert U, Janjic Rankovic M (2024a). Investigation of Impact of Oxidative Stress on Human Periodontal Ligament Cells Exposed to Static Compression. Int J Mol Sci; 25(24):13513.

Hosseini S, Diegelmann J, Folwaczny M, Sabbagh H, Otto S, Kakoschke TK, Wichelhaus A, Baumert U, Janjic Rankovic M (2024b). Investigation of Oxidative-Stress Impact on Human Osteoblasts During Orthodontic Tooth Movement Using an In Vitro Tension Model. Int J Mol Sci; 25(24):13525.

Janjic M, Docheva D, Trickovic Janjic O, Wichelhaus A, Baumert U (2018). In Vitro Weight-Loaded Cell Models for Understanding Mechanodependent Molecular Pathways Involved in Orthodontic Tooth Movement: A Systematic Review. Stem Cells Int; 2018:3208285.

Kanai K (1992). Initial effects of continuously applied compressive stress to human periodontal ligament fibroblasts. J Jpn Orthod Soc; 51:153-163.

Kanzaki H, Chiba M, Shimizu Y, Mitani H (2002). Periodontal ligament cells under mechanical stress induce osteoclastogenesis by receptor activator of nuclear factor kappaB ligand up-regulation via prostaglandin E2 synthesis. J Bone Miner Res; 17(2):210-20.

Mittal M, Siddiqui MR, Tran K, Reddy SP, Malik AB (2014). Reactive oxygen species in inflammation and tissue injury. Antioxid Redox Signal; 20(7):1126-67.

Pizzino G, Irrera N, Cucinotta M, Pallio G, Mannino F, Arcoraci V, Squadrito F, Altavilla D, Bitto A (2017). Oxidative Stress: Harms and Benefits for Human Health. Oxid Med Cell Longev; 2017:8416763.

Schröder A, Stumpf J, Paddenberg E, Neubert P, Schatz V, Köstler J, Jantsch J, Deschner J, Proff P, Kirschneck C (2021). Effects of mechanical strain on periodontal ligament fibroblasts in presence of Aggregatibacter actinomycetemcomitans lysate. BMC Oral Health; 21(1):405.

Sokos D, Everts V, de Vries TJ (2015). Role of periodontal ligament fibroblasts in osteoclastogenesis: a review. J Periodontal Res; 50(2):152-9.

Šromová V, Sobola D, Kaspar P (2023). A Brief Review of Bone Cell Function and Importance. Cells; 12(21):2576.

Sun C, Janjic Rankovic M, Folwaczny M, Otto S, Wichelhaus A, Baumert U (2021). Effect of Tension on Human Periodontal Ligament Cells: Systematic Review and Network Analysis. Front Bioeng Biotechnol; 9:695053.

Sun C, Janjic Rankovic M, Folwaczny M, Stocker T, Otto S, Wichelhaus A, Baumert U (2022). Effect of Different Parameters of In Vitro Static Tensile Strain on Human Periodontal Ligament Cells Simulating the Tension Side of Orthodontic Tooth Movement. Int J Mol Sci; 23(3):1525.

Tan L, Cao Z, Chen H, Xie Y, Yu L, Fu C, Zhao W, Wang Y (2021). Curcumin reduces apoptosis and promotes osteogenesis of human periodontal ligament stem cells under oxidative stress in vitro and in vivo. Life Sci; 270:119125.

Tonetti MS, Jepsen S, Jin L, Otomo-Corgel J (2017). Impact of the global burden of periodontal diseases on health, nutrition and wellbeing of mankind: A call for global action. J Clin Periodontol; 44(5):456-462.

Vansant L, Cadenas De Llano-Pérula M, Verdonck A, Willems G (2018). Expression of biological mediators during orthodontic tooth movement: A systematic review. Arch Oral Biol; 95:170-186.

Wang Y, Andrukhov O, Rausch-Fan X (2017). Oxidative Stress and Antioxidant System in Periodontitis. Front Physiol; 8:910.

Wei Y, Fu J, Wu W, Ma P, Ren L, Yi Z, Wu J (2021). Quercetin Prevents Oxidative Stress-Induced Injury of Periodontal Ligament Cells and Alveolar Bone Loss in Periodontitis. Drug Des Devel Ther; 15:3509-3522.

Wichelhaus A (2018). Orthodontic Therapy : Fundamental Treatment Concepts. Stuttgart: Thieme.

Xiao X, Zou S, Chen J (2023). Cyclic tensile force modifies calvarial osteoblast function via the interplay between ERK1/2 and STAT3. BMC Mol Cell Biol; 24(1):9.

Yang L, Yang Y, Wang S, Li Y, Zhao Z (2015). In vitro mechanical loading models for periodontal ligament cells: from two-dimensional to three-dimensional models. Arch Oral Biol; 60(3):416-24.

Zhu C, Shen S, Zhang S, Huang M, Zhang L, Chen X (2022). Autophagy in Bone Remodeling: A Regulator of Oxidative Stress. Front Endocrinol (Lausanne); 13:898634.

Zhu L, Xie H, Liu Q, Ma F, Wu H (2021). Klotho inhibits H_2O_2-induced oxidative stress and apoptosis in periodontal ligament stem cells by regulating UCP2 expression. Clin Exp Pharmacol Physiol; 48(10):1412-1420.

Acknowledgements

I would like to express my deepest gratitude to all those who have supported me throughout my Ph.D. journey, both academically and personally. It has been an incredible privilege to work with such a talented and supportive team. This accomplishment would not have been possible without the efforts of many individuals and organizations.

First and foremost, I would like to extend my sincere thanks to my supervisors and thesis committee members Prof. Dr. Wichelhaus, PD Dr. Baumert, and Prof. Dr. Dr. Folwaczny, without whom this work would not have been possible:

- I am deeply grateful to **Prof. Dr. Wichelhaus** for providing me with the opportunity to study in her esteemed department. Her generous support, both academically and administratively, has been invaluable, and I greatly appreciate her insightful feedback and suggestions as well as her pivotal role in securing and facilitating my research contract.
- I am very much thankful to my main supervisor **PD Dr. Baumert** for his constant guidance, encouragement, and patience as well as for always challenging me to think critically. His expertise and thoughtful advice have been always a great source of inspiration. I feel very fortunate to have had the opportunity of learning from him, and I deeply appreciate the time and care he devoted to my development.
- I would also like to thank **Prof. Dr. Dr. Folwaczny** for his significant contributions to the development of this research proposal and his continuous support throughout my Ph.D. journey. Not only I learnt academic skills from him, but also, I gained invaluable lessons in professionalism and ethics.

My heartfelt thanks go to **Dr. Mila Janjic Rankovic**, who has been much more than just a colleague for me. I cannot express how grateful I am for her constant support, patience, and mentorship. Her guidance, from the very basics to the more complex aspects of this research journey, has greatly contributed to the success of my Ph.D. Her advice has shaped both my research and personal growth, and I believe without her, I would not have been able to achieve all these milestones, as I have reached.

Special thanks go to my wonderful lab colleagues, **Christine Schreindorfer** and **Laure Djaleu** for their collaborative spirit and technical assistance. Working with them has made the research process both productive and enjoyable.

I would also like to thank **Brigitte Hackl** and **Dr. Julia Diegelmann** from the “Department of Conservative Dentistry and Periodontology-Research Laboratory” for their continuous willingness to answer my questions. Their helpful suggestions and insights have been essential in improving the quality of this research.

In addition, I gratefully acknowledge the financial support provided by the “Funding Program for Research and Teaching (FöFoLe; LMU Medical Faculty) to M.J.R. (project number 1155)” which made this research possible.

Finally, I wish to express my deepest gratitude to my beloved family and friends. Specially to my lovely parents, siblings, nieces, nephews, and to my adored second family here in Germany. Their support has been my constant source of motivation, and I couldn't have completed this journey without them. I would also like to specially and deeply thank my dearest and beloved partner for his instant love, support and encouragement which have been always my greatest strength.

This journey has gifted me not only academic achievements of my Ph.D. but also countless lovely memories, thanks to the support, wisdom, and kindness of all these incredible individuals.